UNIVERSITY OF THE
WITWATERSRAND,
JOHANNESBURG

Synthesis and Evaluation of Silica Sodalite/PSF/PVA Membrane for Removal of Phenol from Industrial Wastewater

Rivoningo Ngobeni
(573321)

School of Chemical and Metallurgical Engineering, Faculty of Engineering and the Built Environment, University of the Witwatersrand, Johannesburg, South Africa for the Degree of MSc Chemical Engineering

Supervisor: Prof M.O. Daramola

September 2020

DECLARATION

I, Rivoningo Ngobeni, declare that this dissertation is my unaided work. It is being submitted for the degree of Master of Science in Engineering at the University of the Witwatersrand Johannesburg, South Africa. It has not been submitted before for any other degree or examination at any other university.

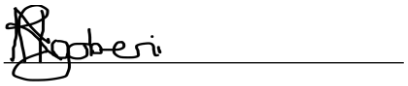

Date: 17/09/2020

Abstract

Human activities such as industrial developments are polluting and compromising the safety and quality of water resources available for human consumption and domestic purposes. Phenol is one of the major pollutants produced by industrial processes and it has high toxicity levels even at low. United States Environmental Protection Agency (EPA) and the National Pollutant Release Inventory (NPRI) of Canada have designated phenol as one of the priority pollutants. Recently researchers have focused attention towards the utilization of membrane technology for removal of phenol from industrial wastewater due to its cost effectiveness as compared to other technologies. In this study, a novel mixed matrix composite membranewas developed for removal of phenol from a synthetic wastewater consisting of phenol. Organic- free silica sodalite (SSOD) nano-particles were synthesized via topotactic conversion and embedded in polysulfone (PSF) matrix for enhancement of mechanical strength and separation performance of the polymer membrane. As comparison, a similar membrane was prepared using hydroxy sodalite (HSOD) nano-particles obtained via hydrothermal synthesis method. The composite membranes were synthesized via phase inversion and coated with polyvinyl alcohol (PVA) for improving anti-fouling property. Different characterization techniques such as; Scanning Electron Microscope (SEM) to examine the surface morphology, Brunauer Emmett–Teller (BET) for evaluating textural properties of the nanoparticles. Contact angle measurements to check the surface hydrophilicity; nanotensile tests to measure the mechanical properties; and Atomic Force Microscopy (AFM) to study the surface roughness of the membrane. The results obtained show that pure PSF has highest contact angle of 83.81° while composite membrane coated with PVA showed significantly lower contact angle of 57.47°, indicating enhanced hydrophilicity of the PSF membranes. The composite membrane displayed 56.14% increase in young's modulus and 81.53% increase in ultimate tensile strength when compared to that of the pure PSF, indicating an enhancement in the mechanical strength of the PSF AFM results showed that surface roughness reduces with increasing nano-particles loading and PVA coating of PSF membranes. Separation performance of the fabricated membranes was carried out using a dead-end filtration cell at varied feed pressure with a synthetic phenol-containing wastewater of 20 mg/L of phenol. Results showed that, 10 wt.% SSOD/PSF/PVA displayed the highest flux; 0.835 $Lm^{-2}h^{-1}$ for pure water and 0.625 $Lm^{-2}h^{-1}$ phenol-containing water, attributable to the enhanced hydrophilicity as seen bylower contact angle. Furthermore, results showed that phenol rejection decreased with increasing pressure. Pure PSF membrane performed well rejecting 93.55% phenol at 4 Bar. However, the 10 wt.% SSOD/PSF/PVA, 0% wt.%SSOD/PSF/PVA, and 10 wt.% HSOD/PSF/PVA all coated with PVA displayed lower

rejection of 27.9%, 40.65% and 35.6%, respectively. Nonetheless, 10 wt.% SSOD/PSF membrane performed relatively well with 64.75% rejection compared to 27.9% achieved with 10 wt.% SSOD/PSF/PVA. Therefore, a novel mixed matrix membrane with enhanced mechanical properties and selectivity was successfully developed for removal of phenol from industrial wastewater.

Acknowledgments

I will like to express my sincere appreciation to my supervisor Prof M.O. Daramola for his guidance and providing research insights.

I will also like to thank Dr O.O Sadare for being there for me as my daily supervisor every time I needed her research insights, guidance and emotional encouragement.

I would like to appreciate the assistance with lab work and analytical machines I received from CHMT staff: Mr Phali, Mrs Smith, Mr B Mothibeli, Lettie, Hopewell, Petra and Bernnet.

I would like to thank the assistance I have received from my research colleagues in Sustainable Energy and Environment Research Unit (SEERU), Thomas Aniokete, Orevaoghene Eterigho-Ikelegbe, Sharon Mabusha Rameetse, Nobuhle Ntshangase, Christin Eden

I would also like to appreciate the support I received from my parents and siblings

Dedication

This dissertation work is dedicated to my Lord and savior Jesus Christ, who gives peace which surpasses all understanding, guard my heart and mind.

This work is also dedicated to my family for all their undying love and support throughout the project

Contents

Table of Contents

List of Figures

List of Tables

Nomenclature

A	Effective area
AFM	Atomic Force Microscope
BET	Brunauer–Emmett–Teller
BIS	Bureau of Indian Standards
C_b	Concentration of the solution in the bulk
Cm	Concentration of the membrane surface
CNT	Carbon nanotubes
C_p	Concentration of the solution in the permeate
FTIR	Fourier Transform Infrared spectroscope
HSOD	Hydroxy sodalite
J	Permeate flux
HPLC	High Performance Liquid Chromatography
MMM	Mixed Matrix Membrane
MOEF	Ministry of Environment and forest
PSF	Polysulfone
PVA	Polyvinylalcohol
R	Rejection
SEM	Scanning Electron Microscope
SOD	Sodalite
SSOD	Silica sodalite
UN	United Nations
USEPA	United States Environmental Protection Agency
V	Volumetric flow
WHO	World Health Organization
Wt.%	Weight percentage
XRD	X-ray Diffraction

Chapter One

1. Introduction

This chapter describes the background, the problem statement, aim and objectives of the study and the significance of the research.

1.1. Background and motivation

Over 1.1 billion people do not have adequate drinking water supply, this is caused by the high costs of potable water, exponential population growth and climatic and environmental factors (WHO, 2015). The World Health Organization has predicted that the number of people affected by water shortages may reach up to 4 billion by 2050 (WHO-UNICEF, 2018). Water constitutes more than 70% of the earth's surface. However, 96% of it contains too much salt for human consumption, and the remaining 3% is trapped beneath the ground, glaciers and ice caps. This leaves only less than 1% of world water supply available for human use (Shirazi et al., 2012). Furthermore, human activities such as industrial developments are endangering the safety of the water resources available for human consumption and domestic purposes (Unesco.org, 2019). There are several organic pollutants that play a major role in water pollution. Phenols, aliphatic, heterocyclic compounds and polycyclic aromatic hydrocarbons, and are prevalent in industrial wastewater (Choi and Spengler, 2014)

Phenols and other phenolic compounds are present in various industrial effluents such as resin manufacturing, plastics, paper, paint, wood oil, petroleum refining, coal processing, petrochemicals, pharmaceuticals, and coking operations (Ahmaruzzaman and Sharma, 2005). Discharging phenolic compounds without proper treatment poses a serious health hazard to animals, humans and aquatic life. United States Environmental Protection Agency (EPA) and the National Pollutant Release Inventory (NPRI) of Canada have designated phenol as a priority pollutant. International regulatory bodies have put stringent discharge limits for phenols (Mohammadi et al., 2014). EPA has regulated water purity standards for less than 1 ppb for phenol in surface water. The phenol toxicity levels is in the range 9–25 mg/L for aquatic life and humans (U.S EPA, 1998). Exposure to phenol for a longer period can lead to irregular breathing, respiratory arrest, and tremor and muscle weakness in humans. Chronic effects due to long-term phenol exposure include weight loss, diarrhea, anorexia, vertigo, salivation, vertigo, salivation and dark colorations of the urine (Bergeson, 2016: U.S EPA, 1998). There are several processes that have been proposed for phenol treatment in wastewater.

Traditional methods used for removal of phenol such as steam distillation, wet air oxidation, adsorption, electrochemical oxidation, solid-phase extraction, liquid-liquid extraction, and catalytic wet air oxidation, show high phenol removal efficiency. However, they use excessive chemicals (Sun et al., 2015). Advanced technologies used for phenolic treatment which include photo-oxidation, ozonation, UV/H_2O_2 and Fenton reaction are costly (Kulkarni and Kaware, 2015). Membrane technology is also classified among the advanced technologies for phenol treatment, which is eco-friendly and relatively cheaper (Kulkarni and Kaware, 2015: Mohammadi, et al., 2014).

The obvious advantages for application of membrane treatment processes are cost-effectiveness and the absence of chemical additives. However, the main drawback is the flux decline caused by membrane fouling (Mohammadi et al., 2014). Membrane fouling is the phenomenon caused by the accumulation of biological species, inorganic, organic and colloidal on the membrane surface or within its pores. It results in flux decline and a rapidly increasing transmembrane pressure during operation, and the possible deterioration of mechanical strength (Wang et al, 2017: Sioutopoulos and Karabelas, 2012). In order to minimize fouling, various techniques are continuously being developed by researchers which include; altering feed solution properties, surface modification and changing the operational conditions (Altaee et al., 2010). Amongst these, researchers have shifted the focus to the modification of membranes by coating with a hydrophilic polymer layer such as polyvinyl alcohol and chitosan (Jie et al., 2015). Polyvinyl alcohol and chitosan are biodegradable polymers which can be used to enhance hydrophilicity, mechanical and chemical properties of the membranes (Jayakumar et al., 2011)

Polymers and ceramics are commonly used in the fabrication of membranes which are used for filtration purposes. Polymer membranes are relatively cheap but have lower tolerance to harsh conditions, whereas ceramic membranes have higher mechanical strength which results in greater resistance to harsh environments and longer lifespan (Atadashi, 2015; Kumar et al., 2015). The wastewater industries have been extensively using polymeric and ceramic membranes for wastewater treatment, hence the pros and cons of the two membranes are clearly understood (Abadi et al., 2010). Researchers are exploring effective ways of combining the advantageous features of the two membranes; polymeric and ceramic membrane to produce a composite material called mixed matrix membrane (MMM) (Kumar, et al, 2015). The purpose

of developing this membrane is to enhance the overall performance of the membrane which would not otherwise be achieved by just using one of the two membranes (Qadiret al., 2016).

MMMs are prepared through dispersion of porous particles, such as silica, carbon molecular sieves, carbon nanotubes (CNTs) and zeolites within a continuous polymer matrix such as polyethersulfone, polysulfone, and polyamide (Aroon et al., 2010; Damjanovica et al., 2010). This has proven to enhance mechanical properties, selectivity and permeability of the polymeric membranes as compared to the equivalent pure polymeric membranes (Chung et al., 2007). The synthetic hydroxy sodalite zeolites have high adsorption capacity. Hence, several researchers propose them as potential fillers in MMM for wastewater treatment (Xue et al., 2014).

Hydroxy sodalite zeolite, has attractive features for application of selective wastewater treatment such as its high adsorption capacity and very small pores such that only tiny molecules; water (2.65 Å), helium (2.6 Å) and ammonia (2.5 Å), can access and pass through the hydroxy sodalite pores making it a good candidate for wastewater treatment (Khajavi et al., 2007). However, occluded organic matter present in the cages of hydroxy sodalite could result in lower membrane permeation. The attempt to get rid of organic matter through dehydration of the sodalite results in the destabilization and partial collapse of framework that makes sodalite structure (Khajavi et al., 2010).

Silica sodalite synthesized via topotactic conversion of a silicate layer as a precursor is formed without organic matter, therefore has accessible micropores (Moteki et al., 2011). Silica sodalite as a filler in the polymeric matrix could be the candidate that might out-perform the hydroxy sodalite in terms of membrane flux since it has more accessible pore space for permeation (Daramola., et al 2016). Therefore, there is a need for a cheap and reliable treatment method that could be used to safely remove hazardous contaminants such as phenols to a permissible level. This study seeks to fabricate fouling resistant MMM for treatment of phenol-containing wastewater consisting of; polysulfone as the matrix base, silica sodalite as a filler and polyvinyl alcohol as a coating agent used to increase the hydrophilicity of the membrane in order to address membrane fouling.

1.2. Problem Statement

Phenol is very toxic to humans and highly irritating to eyes, mucous membranes and skin even for a short-period dermal exposures and inhalation (U.S EPA, 1998). Phenol oral exposure to animals' offspring cause growth retardation, abnormal growth and reduced fetal body weight (EPA, 1998). There are several methods available for treatment of industrial phenolic effluents such as steam distillation, liquid-liquid extraction, electrochemical oxidation, solid-phase extraction, catalytic wet air oxidation, wet air oxidation and adsorption. These methods suffer from high capital cost, operating cost and residual disposal challenge (Salame and Bandosz, 2003). Membrane processes are highly reliable and cost effective to treat phenol and have many benefits such as low energy consumption, high-quality effluent, small footprint, and can be easily scaled up with membrane modules (Qu et al., 2012). Typical polymers used for membrane processes include polysulfone, poly (vinylidene fluoride), poly (acrylonitrile), and poly (acrylonitrile) and poly (vinyl chloride) copolymers (Goosen et l., 2005). In this study, polysulfone was used as a continuous matrix base due to its strong chemical and thermal stability. However, polysulfone material is hydrophobic in nature which is the main drawback of this material since several studies concluded that hydrophobicity results in high concentration polarization and membrane fouling (Ngo and Guo, 2009). Concentration polarization (CP) is when a solution meets the surface of the membrane and the solute builds upon the on the membrane surface and if left in contact with the membrane long enough it leads to fouling. Fouling is defined as the adhesion (adsorption) of particles on the surface or within the membrane pores (Van der Bruggen, 2009). The two phenomena (concentration polarisation and fouling) result in flux decline reduction, rapidly increasing transmembrane pressure, and the possible deterioration of mechanical strength (Van der Bruggen, 2009).

1.3. Research aim, questions and objectives

1.3.1. Research aim

This study aims to synthesize and study the performance of silica sodalite/PSF/PVA membrane and evaluate the effect of silica sodalite (SSOD) loading on the PSF based membrane for phenolic wastewater treatment.

1.3.2. Research questions

i. Can embedding silica sodalite particles into Psf membrane enhance separation performance of Psf membrane?
ii. What will be the effect of silica sodalite loading on the performance of the membrane in (i) for the separation of industrial waste water?
iii. Can coating the membrane in (i) with PVA improve its anti-fouling property?
iv. What will be the effect of feed pressure on the separation performance of membranes during the treatment of wastewater?

1.3.3. Research Objectives

To proffer solution to the above research questions, the following research objectives were considered:

i. To fabricate polysulfone membranes with silica sodalite filler dispersed in the polymer and evaluate it for treatment of phenolic wastewater.
ii. To investigate the effect of different silica sodalite loadings in the polysulfone membrane during the treatment of phenol-containing wastewater.
iii. To ascertain whether coating the surface layer of the membrane with polyvinyl alcohol will improve membrane anti-fouling property.
iv. To investigate the effect of varying pressure on the separation performance of silica sodalite/PSF/PVA membranes during phenol-containing wastewater treatment.

1.4. Scope of Study

In order to develop mixed matrix membrane with anti-fouling property, this project was completed in five stages

i. Synthesis of nanoparticles via hydrothermal synthesis and topotactic conversion
ii. Embedment of nanoparticles in 20 wt. % polysulfone to develop composite membranes.
iii. Performance evaluation of the synthesized composite membranes in (ii) then compare their performance with one another and literature.

iv. Addition of hydrophilic layer (PVA) on the surface of pure polysulfone and composite membranes.

v. Performance evaluation of composite membranes coated with PVA.

1.5. Dissertation outline

Chapter 1

Background and motivation, problem statement, aim, objectives, research question, of this study are described in this chapter.

Chapter 2

This chapter focuses on the literature review whereby previous studies on the removal of phenol are discussed. The literature review discussed in detail membrane technology for wastewater treatment and the advantages of incorporating fillers in a polymer matrix for the treatment of wastewater.

Chapter 3

This chapter describes the material and experimental procedures employed for the synthesis and characterization for nanoparticles and fabricated pure and composite membranes. The chapter also gives description for preparation of synthetic phenol-containing wastewater and performance evaluation of membranes.

Chapter 4

The fabrication of composite membranes whereby sodalite crystals (hydroxy sodalite and silica sodalite) have been embedded into a polymer matrix (polysulfone), separately. The chapter gives comparison of the performance of PSF infused with HSOD and SSOD crystals.

Chapter 5

This chapter focuses on the effect of silica sodalite loading in polysulfone matrix, silica sodalite has been varied to give 5 % wt. and 10% wt. loadings. The characterization and performance evaluation of the two membranes were compared in this chapter.

Chapter 6

The chapter studies the effect of coating pure polysulfone and composite membranes with PVA during treatment of phenol-containing wastewater.

Chapter 7

This chapter gives a brief summary of the findings in this study with general conclusion and recommendation for future research work.

Chapter two

2. Literature Review

In this chapter, related literature emphasizing the present trends in the synthesis and evaluation of silica sodalite/PSF/PVA membrane for removal of phenol from industrial wastewater are critically discussed.

2.1. Phenol properties, phenolic compounds and maximum permissible limit

Phenol is the common name for hydroxybenzene, it is an aromatic compound with a molecular formula C_6H_5OH. Phenol is the simplest member of the family having a phenyl group ($-C_6H_5$) that is bonded to an -OH group. It is naturally mild acidic and has to be handled with extra care due to its toxic nature and can cause severe chemical burns (Verma, 2008).

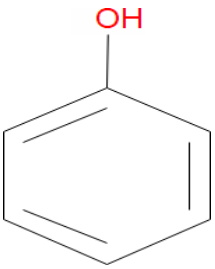

Figure 2.1: Chemical structure of phenol (Sobiesiak, 2017)

Phenol is soluble and stable in water making it difficult to decompose. It has half-life time that ranges between 2 to 72 days and very strong unpleasant smell making contaminated water unusable without treatment (Vazquez et al., 2007). Phenol is commonly used to produce commercial resins, epoxy resins and resins used in the manufacturing of automobiles and appliances, adhesives, and polyamide used various applications (Cheng et al., 2013). However, phenol gets disposed into the environment mainly as the industrial waste and is present in high quantity in several industrial effluents (Mohammadi et al., 2014).

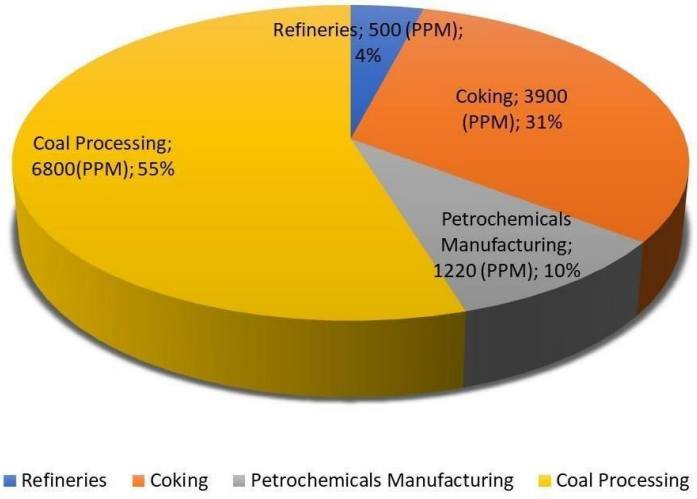

Figure 2.2: Phenol present in various industrial effluents adapted from (Mohammadi et al., 2014)

Pollution of natural water caused by phenol can lead to the formation of chlorophenols, which are carcinogenic compounds. Phenol and its derivative compounds (figure. 2.3) are common organic water contaminants caused by industrial processes due to its importance as a raw material for various chemical, petrochemical and pharmaceutical processes (Conidi and Cassano, 2014). Phenolic compounds have negative impacts in ecosystems due to the high toxicity levels at low concentrations (Bruce, et al., 1987). Phenolic compounds do not only get produced and discharged through human activities, but they are also naturally formed hence they are found in soil and sediments as the result they contaminate groundwater (Nafees and Waseem, 2014).

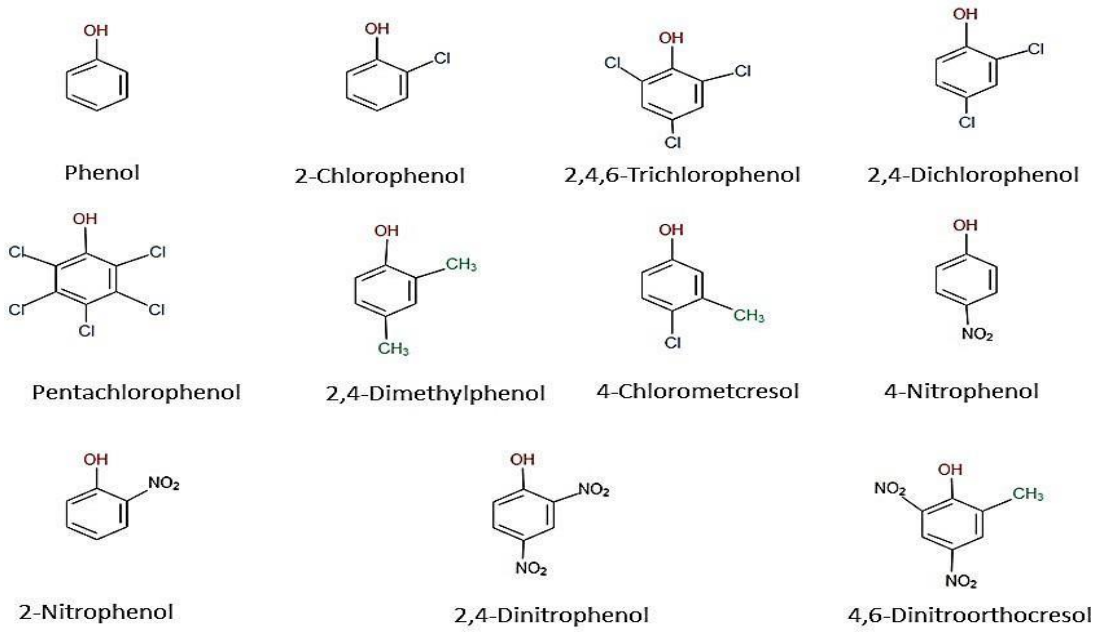

Figure 2.3: Phenolic compounds adapted from (Adapted from Baransi et al., 2012)

The regulatory bodies around the world such as Ministry of Environment and forest (MOEF), Government of India, WHO, EPA, and USEPA have designated phenol and phenolic compounds as the priority pollutants this is due to their toxic nature and high stability that make them difficult to degrade biologically (Murray and Sasnett, 2000). Phenol is responsible for chronic toxic effect reported in humans such as difficulty in swallowing, vomiting, fainting, anorexia, liver damage and kidney failure, headaches and mental disturbances (Bruce et al., 1987). The regulatory bodies have set the maximum permissible limit of phenol in different water categories as presented in the Table 2.1 (Murray and Sasnett, 2000).

Table 2.1: Maximum permissible limit

Agency	Type of Water	Maximum permissible Limit	Ref
USEPA	Waste Water	0.1 PPM	Salame and Bandosz, 2003)
BIS	Drinking Water	1 PPB	Salame and Bandosz, (2003)
WHO	Drinking Water	1 PPB	Suresh et al. (2011)
MOEF	Industrial Effluent	1 PPM	Suresh et al. (2011)

2.2. Methods for treatment of phenol-containing wastewater

2.2.1. Adsorption

Adsorption is the most commonly used treatment method for phenol removal from wastewater and it effectively removes phenol at either low or high concentrations. Activated carbon is the widely used adsorbent due to its high removal efficiency (Villegas et al., 2016). It is a capital-intensive method but is very effective in the removal of trace organic compounds (Villegas et al., 2016: Park et al., 2015). Therefore, new adsorbent materials are continuously being developed including impregnation with nano- particles, carbon nanotubes (CNTs), different activation methods and graphene-based materials (Tran et al., 2005). In recent studies, researchers are working on the replacement of expensive adsorbent with low cost biosorbent, such as chitosan/chitin for removal of phenolic compounds (Villegas et al., 2016; Masomi et al., 2014).

2.2.2. Electrochemical oxidation

This method can oxidize different organic contaminants effectively using high chloride concentrations that are greater than 3 g/L. The electrochemical oxidation is an alternative destructive of phenols and operates without addition of reagents, but requires equipment and energy cost (Villegas et al., 2016). There are two ways in which this method oxidizes organic contaminants: direct and indirect oxidation. Direct oxidation is also referred to as anodic treatment takes place during the adsorption of contaminants on the anode surface (Martinez-Huitle and Ferro, 2006). Researchers have focused their attention on the investigation of anode

materials such as; Pt, SnO_2, PbO_2, IrO_2 and BDD (boron-doped diamond). The efficiency of this process is determined by the parameters such as current density, pH, and electrolyte and anode materials used. Indirect oxidation uses intermediary redox reagents to make electron transfer between electrode and contaminant therefore, fouling of the electrode by contaminants is prevented (boron-doped diamond). When the reaction takes place in the presence of chloride ions the removal of phenols or phenolic compounds is improved through the formation of Cl_2 or ClO^- the process is known as electrochemical oxidation of active chlorine (Tasic and Antonijevic, 2014).

2.2.3. Advanced oxidation processes (AOP)

These are treatment techniques that usually form hydroxyl radical ($OH^{\bullet}$) in situ. The radical can mineralize most organic compounds including phenolic compounds (Villegas et al., 2016). AOP is commonly used in the treatment of water contaminated with recalcitrant organics such as surfactants, pharmaceuticals, pesticides and coloring matters. Fenton and fenton-like treatment are an examples AOP which are capable of oxidizing aromatic compounds (Villegas et al., 2016).

2.2.4. Distillation

This technique applies variants of steam distillation causing high energy demand, thus the technique requires careful economic consideration. The technologies are classified as destructive or non-destructive, the latter allows recovery of phenolic compounds (El-Ashtoukhy et al., 2013). Steam or azeotropic distillation takes advantage of relatively volatile phenol to remove phenol impurities from water (Mohammadi et al., 2014). During the phenol removal, aqueous phenol solution is added into a steam plasma torch (steam plasma jet treatment), phenol decomposes rapidly in the thermal plasma jet through the production of hydroxyl radicals which caused oxidative degradation of organic contaminants in aqueous solutions (Ni et al., 2013). The primary intermediates such as hydroquinone, maleic acid, pyrocatechol, butanedioic acid and muconic acid are formed in liquid phase whereas in gaseous phase products such as CO, CO_2 and H_2 are formed. Steam thermal plasmas techniques have high enthalpy values and activity (Villegas et al., 2016).

2.2.5. Membrane treatment

Membrane technology is economically feasible for removal of phenol from aqueous effluents and have manybenefits such as small footprint, high-quality effluent, low power consumption and can be easily scaled up (Khazaali et al., 2014). There are different types of membranes used for phenol removal in wastewater such as photocatalytic membrane, hollow fiber membranes, extractive membrane bioreactors, and pressure driven membrane processes such as pervaporation, membrane distillation, nanofiltration and reverse osmosis (Mohammadi et al., 2014; Loh et al., 2016).

2.3. Membrane-based treatment technologies

Membrane technology began in the 1960s due to the successful development of high-performance reverse osmosis membrane (Loeb and Sourirajan, 1961), this has led to development of large desalination plants in arid parts of the world. Thereafter, the membrane technology experienced exponential growth where large quantity of membranes were sold for water treatment, this has been highly influenced by the growth of microfiltration and ultrafiltration membranes towards the end of the twentieth century (White, 2016). Since then membrane technology has been applied extensively across the manufacturing industries such as gas separation, ultrapure water production, water desalination, production of beverages, emission control and product recycling and pollution abatement (Kim, Park and Kim, 2005).

2.3.1. Microfiltration

Microfiltration is a separation technique that removes particles of the microscopic size which includes yeast cells, bacteria, colloids and gases. The membrane has filtration pores of the size ranging between 0.1 to 10 μm, which permeate fluid but rejects particles, this results in separation. Microfiltration membranes were commercialized as early as the 1920s and were used mainly for removal of bacteria in water (Ruutenhuch, 1992). The technique experienced rapid growth in the 1960s following the successful applications in a variety of fields such as automobile, biotechnological, bacterial, food industry and electronics (Tang and Goldman, 2002). Examples of microfiltration application are purification of the electronics industry, recovery of latex pigments from paints and bacterial harvest and yeast. In the food technology microfiltration is applied in the purification processes of the fruit juices, beer and wine and removal bacteria (Baumgartinger et al., 2009).

2.3.1. Ultrafiltration

Ultrafiltration is a separation method that uses finely porous membranes with pore sizes ranging from 0.1 to 0.001 μm in which hydrostatic pressure pressurizes a liquid against a semi-permeable membrane (Tay et al., 2018; Baker, 2012). Ultrafiltration works as a molecular sieve where larger molecular-weight substances, viruses, colloidal materials, organic and inorganic molecules are retained while water, other low molecular weight organic and ions such as sodium, magnesium chloride and calcium can pass through the membrane pores (Zhang and Minear, 2006; Tsapuik and Bryk, 1993). Since only larger molecular weight species get rejected, the osmotic pressure differential on the surface of the membrane is negligible. High fluxes can be achieved at a low pressure operation from an ultrafiltration membrane (Tsapuik and Bryk, 1993).

2.3.2. Nanofiltration

Nanofiltration (NF) is most recently developed high pressure-driven membrane process, it is characterized by a membrane with pores between 0.001 to 0.01 μm. The membrane lies between ultrafiltration (UF) and reverse osmosis (RO) with regards to the pore sizes and separation level. A typical NF membrane lies in a separation range of 150–500 Da molecular weight and is characterized by its ability to retain charged and neutral particles (Bowen et al., 2002: Shon et al., 2013). NF removes most organic molecules, harmful microorganisms (e.g., algae, protozoa, bacteria, viruses, and fungi), the natural organic matter and dissolved matter as well as a range of salts. NF membrane can be used as ion-selective barrier, since it separates different ions as it collects charged groups, electrostatic repulsion or attraction forces take place between the liquid and the membrane surface (Bowen and Welfoot, 2002). Pore size is not the property determining the diffusion of ions, however, the charge of the ion is also very important. For that reason, the rejection of sulfates (being larger in size than chlorides, i.e. 0.23 nm vs. 0.12 nm) is above 90% while the rejection of chlorides is at maximum 90%. Nanofiltration has replaced reverse osmosis in a few applications due to its high flux while operating at lower energy (Cadotte et al, 1988; GozaIvez et al, 2002).

2.3.3. Reverse osmosis

Reverse osmosis (RO) applies high pressure on the feed stream as it flows through a semipermeable membrane. Water permeate through the membrane, when the pressure applied

is higher than the osmotic pressure, while salt is retained (Mathioulakis et al., 2007). RO membranes do not have distinct pores that traverse the membrane because it has very small.pores at the size ranging from 0.0001 to 0.001µm. The polymer material of membranes forms a layered, web-like structure, and water must follow a tortuous pathway through the membrane to reach the permeate side (Greenlee et al., 2007). Reverse osmosis is applied extensively in the removal of single charge ions, including Na+ and Cl- mainly from brackish or seawater (Chun et al., 2017). The main attractive feature of the reverse osmosis desalination process is the simplicity of its layout in comparison with the large-scale thermal desalination processes. However, RO requires high energy consumption during operation which is one of the main draw backs of this separation process (GozaIvez et al, 2002).

Table 2.2: Difference between membrane processes (Ruutenhuch, 1992: Bowen et al., 2002: Greenlee et al., 2009: Tay et al., 2018)

	Microfiltration	**Ultrafiltration**	**Nanofiltration**	**Reverse osmosis**
Membrane structure	Porous	Porous	Porous	Dense
Pore size (µm)	0.1 to 10	0.1 to 0.001	0.001 to 0.01	0.0001 to 0.001
Pressure (Bar)	below 1	1–6	4–20	40–60
Transport mechanism	Sieving and adsorptive mechanisms	Sieving and preferential adsorption	Sieving/electrostatic hydration/diffusive	Solutes migrate by diffusion mechanism

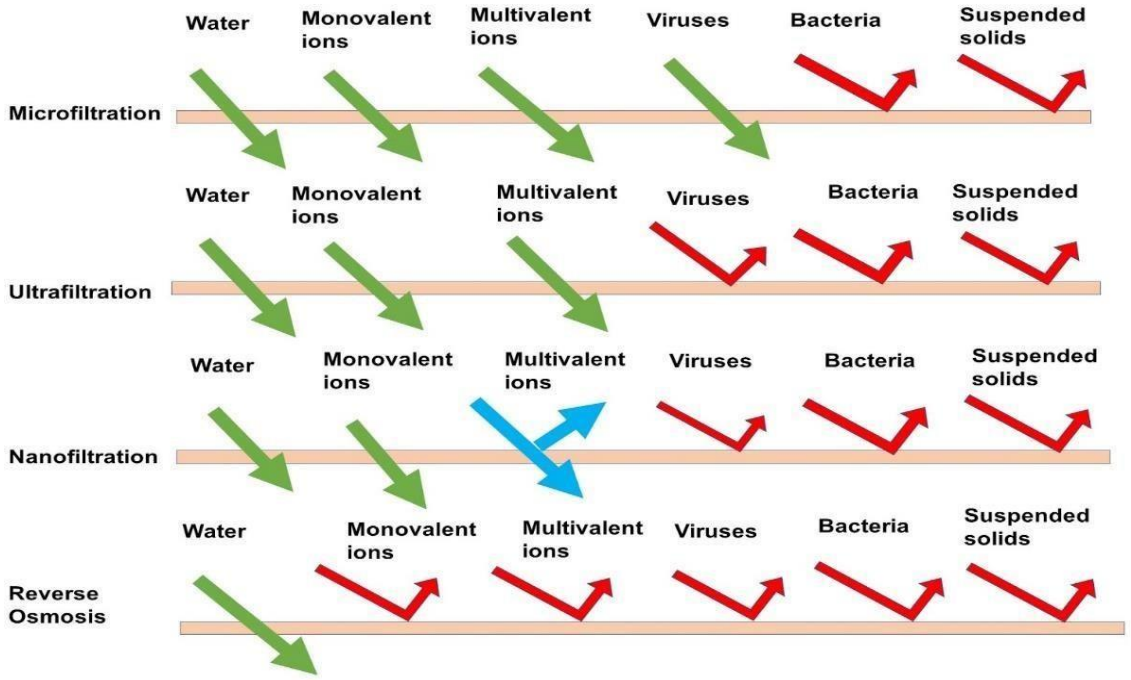

Figure 2.4: Range of membrane process rejections adapted from (Adapted from Maphutha et al, 2013)

2.4. Types of membrane-based methods and treatment mechanism

2.4.1. Polymer membranes

Polymeric membranes can be made from different types of polymers. Polymers with linear-chain become softer and lose structural integrity when subjected to high temperature, and are soluble in organic solvents. These types of polymers are called thermoplastics. The polymers that have highly cross-linked chained decompose at a higher temperature compared to the linear-chain polymers and are not soluble in water. These polymers are called thermosetting polymers (Seader et al., 2013). Furthermore, polymers can be classified as either amorphous or crystalline. Glassy polymers become rubbery when temperature is increased to a glass transition temperature (Tg). On the other hand, the crystalline polymers are opaque with a crystalline structure. Melting temperature (Tm) is reached when increasing the temperature of the crystalline polymer until the point of melting (melting point). Most polymers have both amorphous and crystalline regions so they have both the Tg and Tm (Seader et al., 2013). Table 2.3 show list of types of polymers, their repeat units, values of glass transition temperature (*Tg*) and/or melting temperature (*Tm*) for various polymers.

Table 2.3: The summary of polymer properties adapted from (Seader et al., 2013)

Polymer	Type	Representative repeating units	*Tg*, °C	*Tm* °C
Polysulfone	Glassy	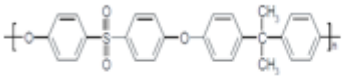	190	
Polyethersulfone	Glassy	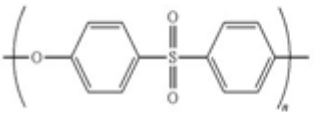	224	
Cellulose acetate	Crystalline	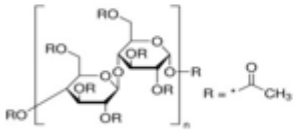		300
Polyimide	Glassy	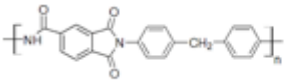	310-365	
Polytetrafluoroethylene (Teflon)	Crystalline	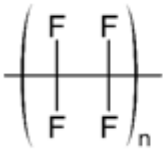		327

In this study polysulfone is used due to attractive material that possesses excellent film and membrane forming properties, it has a good chemical and thermal stability and flexibility. It is made of thermoplastic resin with high mechanical properties and one of the highest operating temperatures (190°C) of any melt-processible thermoplastic (Seader et al., 2013). It can be easily manufactured with good resistance to harsh conditions such as exposure to solutions, mineral acids, alkalis, detergent, oils, salts, and alcohol (Ebnesajjad, 2011) making it suitable for this study.

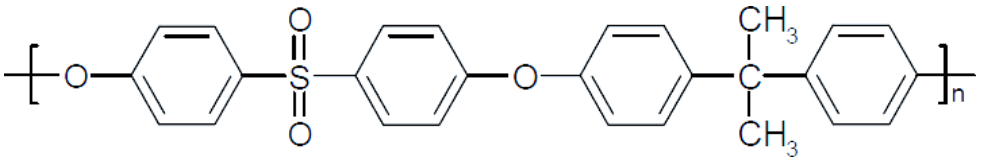

Figure 2.5: Polysulsone chemical structure (https://en.wikipedia.org/wiki/Polysulfone)

Important properties summarized:

- ✓ Good thermal stability
- ✓ Good resistance to environmental stress crack
- ✓ Good resistance to forming fire
- ✓ Good toughness and strength

However, polysulfone material is highly hydrophobic in nature which is the main drawback of this material. Several studies have reached the conclusion that hydrophobicity is directly linked to membrane fouling during membrane filtration (Ngo and Guo, 2009). The performance of the polysulfone membrane for wastewater separation can be improved by tuning the hydrophilicity, pore size and mechanical stability of the membrane. Yurekli, (2016) coupled the filtration (size exclusion) and adsorption process by impregnating polysulfone with zeolite nano-particle membrane for the removal of lead and nickel from wastewater. They observed that the hydraulic permeability and adsorption of the membrane have significantly improved by simply changing conditions during membrane fabrication that include NaX loading andthe evaporation period of the casting film. The impregnated membrane depicted good efficiency in absorption capacity of nickel and lead ions during the 60 min of filtration period at a transmembrane pressure of one bar.

Membrane filtration is a physical separation method which applies a thin barrier (<1 mm), the barrier is primarily a synthetic polymer that is semi-permeable. Water is pressurized against the membrane surface resulting in two products water that could not pass through the membrane containing the rejected particles (retentate) and cleaner water which is filtered (Kumar et al., 2011). While conventional filtration processes can only remove particles larger than 10^{-2} mm, membrane filtration can remove particles of any size down to 10^{-7} mm depending on the membrane process used. Permeation

is the penetration substances such as gas, liquid or vapour through a porous or permeable solid. It has a direct relationship with a concentration gradient of permeate, material's intrinsic permeability and material's mass diffusivity (Donald, 1980). Permeation works by diffusion as permeate from higher concentration move to the lower concentration across interface. The molecular size of the permeating liquid plays a very important role in permeation. Liquid permeation is a function of the molecular size of the liquid, this means that smaller molecules permeate faster than larger molecules (Donald, 1980). The polarity of the liquid is also an important factor in permeation. Non polar liquids such toluene permeates faster than polar aniline in membranes such as polyethylene (Suda et al., 2000).

There are two types of filtration mode used for transportation particles during performance evaluation of membranes: Cross-flow and dead-end filtration.

- Dead end filtration: The filtrate (permeate together with retentate) flows away from and at 90^{o} to the surface in the same direction as the flow of feed (Iritani et al., 1995). The advantage of dead-end filtration is that it is cost effective and easy to operate (Rossignol et al., 1999). The major drawback of the dead-end filtration is its susceptibility to fouling and concentration polarization (Sun et al., 2012). The figure 2.6 below illustrate the dead-end filtration mechanism in dead-end filtration.

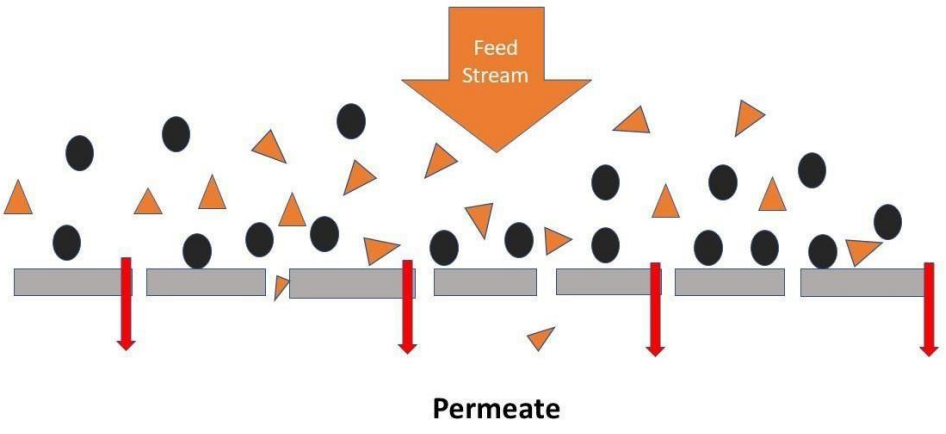

Figure 2.6: Schematic diagram of dead-end filtration mode adapted from (Lee et al., 2016)

- Cross flow filtration: The permeate flows away from the surface, perpendicular to the flow of feed where it is to be collected; while the retentate (the rejected component) flows in the same direction as and away from the flow of feed (Gohil and Ray, 2009).

  The advantages of cross flow filtration are less fouling due to hydrophilicity and shear rates of the passing flow (Haldenwang et al., 2019). The disadvantage of cross flow filtration is relatively expensive compared to the dead end filtration. Cross-flow filtration also has many advantages over conventional filtration, flocculation-flotation sedimentation processes and centrifugation (Laval, 2007). Particularly, when appropriate membranes are used, good filtration rates can be achieved, and the debris, colloidal and cells are completely removed (Rushton and Matsis, 1994). The figure below (Figure 2.7) illustrate the tangential flow mechanism in cross-flow.

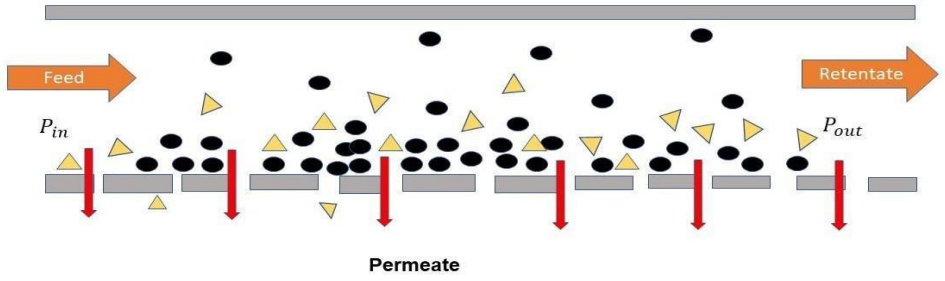

Figure 2.7: Schematic diagram of cross-flow filtration mode (Adapted from Lee et al., 2020)

2.4.2. Inorganic membranes

Inorganic membranes are made up metal oxides, glass, metals or ceramics, and can be prepared in multi-layer supporting structures, or as self-supporting structures with materials including aluminium carbon, silica, zirconia and zeolites particles (Wang and Peng, 2010). In comparison with polymeric membranes, inorganic membranes are highly selective and permeable and can operate at extreme conditions such as, very high temperature and acidic environment. Hence, they are well-defined with stable pore structure, high chemical stability and extended lifespan (Ismail and David, 2001). Ceramic membranes are most widely used inorganic membranes due very high melting point and can operate at any pH level making it easier for chemical cleaning especially in microfiltration and ultrafiltration. These properties are very important for gas

separation that uses very high temperature. The major draw backs associated with inorganic membrane include high cost and reproducibility (Kayvani Fard et al., 2018).

Table 2.4: Summary comparison between polymeric and inorganic membranes (Kayvani Fard et al., 2018: Ismail and David, 2001)

Properties	Polymeric	Inorganic
Material	Glassy, rubbery	Inorganic material: silica, zirconia and zeolites particles
Characteristics	Rigid in glassy and flexible in rubbery	Thermal, chemical and mechanical stability
Advantages	Cheaper, easy scale up, high selectivity	Withstand harsh conditions
Disadvantages	Fouling, short life-span, limited operating pressure, and temperature	High cost, rigid, fragile

2.4.3. Mixed-matrix membranes

Researchers are currently exploring effective ways of combining the advantageous features of the polymeric and inorganic membranes into single membrane. This type of membrane is referred to as a mixed matrix membrane (MMM) (Chinh et al., 2018). Inorganic materials play a very important role in improving the physicochemical, separation performances and antifouling properties of polymer membranes. Introducing nanoparticles into a polymeric membrane effectively enhance the hydrophilicity of the membrane. The commonly used nanoparticles include Mg $(OH)_2$, TiO_2, SiO_2, ZnO, carbon nanotubes, and zeolites (Alavi and Thompson, 2004). The nanoparticles are blended into polymeric membranes either in polymer solution or coagulation bath during preparation process in order to make the overall membrane fouling resistant. Inorganic materials have proven to be an efficient way to fill the membrane pores and reduce pore size distributions, highly increases permeability and or selectivity (Bachman et al., 2016). The mixed matrix membrane combines adsorption and filtration to enhance the performance of the membrane. The adsorption uses inorganic materials to capture wastewater contaminants removing them from water by binding liquid molecules to their surface (Yi, 2015). Figure 2.5 below illustrates mixed matrix membrane.

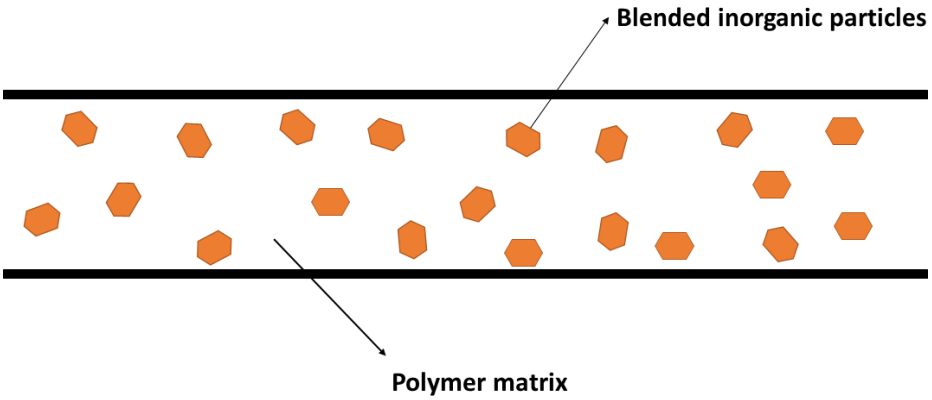

Figure 2.8: Mixed matrix membrane (Adapted from Khulbe and Matsuura, 2018)

Ahmadiannamini et al., (2017) effectively incorporated zeolite 13X into polysulfone polymer matrices. They have reported that these composite materials remove ammonium without leaching zeolite materials. This mixed matrix membrane demonstrated high water flux and over 90% of total ammonia nitrogen was removed from relatively low total ammonia nitrogen aquaculture wastewaters. In another study, Kumar and colleagues incorporated bentonite (8% wt) into polysulfone and reported a 50% increase in water flux while maintaining more than 90% oil rejection in comparison with the control membrane (Kumar et al., 2016). Daramola et al., (2015), blended hydroxy sodalite in polyethersulfone (PES-SOD) to form a mixed matrix membrane for AMD treatment, the membrane increased the rejection of Mg^{2+} to 50% from 20% of non-blended PES.

2.4.4. Methods of preparation of mixed-matrix membranes

There are several methods used in preparation of MMM including dip-coating, interfacial polymerization and phase inversion. Porous support layers which are used for the preparation of MMM, include PSF, PES, PAN, PI and CA (Fauzan et al., 2019)

2.4.4.1. Dip-Coating Method

During dip-coating process for preparation of MMM membranes, a selective layer is coated on a porous membrane support by dipping the membrane into the polymer solution, thereafter liftinging at a fixed speed. Concentration of the polymer solution, drenched time rate of the support removal and the temperature of the surrounding are the conditions that are controlled (Yanagishita et al., 2001: Fauzan et al., 2019). However, the most preferred membrane is the

one that has high solvent resistance since coating solution needs to be cast without destructing the membrane support (Dai et al., 2016: Armanet and Hunkeler, 2006).

2.4.4.2. Interfacial polymerization

Interfacial polymerization (IP) is used for preparation of thin-film composite membranes for reversed osmosis and nanofiltration. The polymerization take place at the interface between two immiscible phases (Kumar et al., 2017). The polymeric amine in aqueous solution is allowed to soak the microporous support such as polysulfone. The amine-impregnated membrane is immersed in a solution of a diisocyanate in hexane. Thereafter, the membrane is cross-linked by performance heat treatment at 110°C. The main advantage of the membrane fabricated using this method is that its polyamide selective layer and porosity can be optimized independently to obtain the best results (Jeong et al., 2007). Ma et al. (2012) successfully prepared a zeolite-incorporated polyamide layer on the surface of polysulfone substrate.

2.4.4.3. Phase Inversion

Phase inversion is a process whereby a thermodynamically stable liquid polymer transforms into solid state in a manageable manner (Wang et al., 2013). The liquid polymer solution is precipitated into two phases, the high polymer concentration phase and the lower polymer concentration phase. The higher polymer concentration solidifies shortly after phase inversion to form the membrane, the low concentration phase forms the pores (Yu et al., 2017). This method is used to fabricate asymmetric membrane and most of the polymeric membranes (Gordano and Buonomenna, 2012)

- Dry phase inversion method involves casting a prepared solution onto the glass plate using casting blade and the solvent and non-solvent are left to vaporize at the same time.
- Wet phase inversion method occurs when a membrane is soaked into the non-solvent bath after casting. The phase separation take place due to the reaction between solvent and nonsolvent mixture. The process is commonly used for fabrication of asymmetric membrane for MF and UF

- Dry/wet inversion method after casting, the membranes are left for a moment to vaporize before immersion into non-solvent medium (Unuigbe et al., 2019; Mazinani et al., 2017).

2.4.5. Characterization techniques for mixed-matrix membranes

The thermomechanical properties of the membranes are studied using analytical techniques to provide information on the morphology, topology, roughness, wettability, chemical composition and mechanical properties (Adamsons, 2000; Bubert and Jenett, 2002). The analysis techniques listed below are very important in characterizing pure and MMM

- Scanning Electron Microscopy (SEM) is used to study the morphological properties of the membranes. The surface and cross-sectional morphologies of pure and mixed matrix membranes are explored by SEM photographs of the micro or nano scale. The images are used to study the distribution and size of the pores of the membranes.
- Fourier Transform Infrared (FT-IR) is a very important technique to examine the functional groups molecular structure for polymer characterization. The surface chemistry of the membranes was checked with FT-IR spectroscopy.
- Contact angle measurement is the method used to evaluate the hydrophilicity or hydrophobic of the membrane and gives the wettability of the membrane. The fillers in MMM enhances the hydrophilicity making membranes fouling resistant. The contact angle value made by a liquid droplet deposited on the membrane surface is greater than 90° if the affinity is low.
- Atomic force microscope is used for measuring surface roughness of the membrane. Roughness in membranes is defined as the deviation of the actual membrane surface from the ideally atomic smooth surface. Roughness determines how the membrane surface interacts with the environment. It evaluates the performance of the membranes as it influences the fouling potential of the membranes (Hobbs et al., 2006). The surface may also be influenced by other material characteristics such as the molecular weight cutoff pore-size (Bowen and Deneva, 2000)
- Tensile strength, of the membrane can be measured by a tensile tester to evaluate the mechanical properties. Ultimate tensile strength is the maximum stress that a material in this case a membrane can withstand while under tension before breaking (Kuilla et al., 2010). MMM generally have higher mechanical strength in comparison with pure

polysulfone. Maputha et al (2013), reported 119% increase in tensile strength for polysulfone infused with 7.5 wt. % CNTs relative to the pure polysulfone membrane.

2.4.6. Performance evaluation of mixed-matrix membranes during wastewater treatment

Mixed matrix membranes achieve higher performance compared to the conventional polymeric membranes during wastewater treatment. The higher performance such as higher selectivity and permeability with desirable mechanical properties is achieved due to the incorporation of fillers in the pure polymer matrix. Zhao et al., (2011) incorporated PANI nanosphere and PANI oligomers into polysulfone matrix. The fillers increased the pure water flux up to four times higher than a pure polysulfone membranes. The PANI produced interconnected pores in membrane structure leading to enhanced pure water permeation. The introduction of PANI into polysulfone also improved membrane rejection rate significantly by creating smaller pores. Zhao et al., (2011) in another study have also obtained the results with the same trend for PANI-based nanocomposite membranes with added polyvinylpyrrolidone, whereby they successfully enhanced antifouling separation efficiency, the pure water flux, and showed good mechanical properties. However, the rejection did no show significant improvement.

2.4.7. Factors affecting separation performance of mixed-matrix membranes during wastewater treatment

Mixed matrix membranes have excellent advantages compared to the conventional polymeric membranes such as enhanced selectivity, permeability, mechanical strength and thermal stability. However, MMM suffer from poor polymer-filler interaction leading to the leaching out of filler from polymer and generation of microbial colonies on the membrane surface during wastewater treatment (Qadir et al., 2016). The other issues concerned with fillers in MMM are stability, agglomeration, homogenous distribution and relation with water chemistry. Some fillers are of toxic nature, hence their use in wastewater treatment may pose risk to humans and environment (Ridzuan and Musa, 2012)

2.5. Concentration polarization and fouling phenomena in membranes

The performance of the membrane may change over time due to decrease in transmembrane flux. This occurs due to concentration polarization and fouling and causing a operating

efficiency, premature membrane replacement, down time and thus higher operating cost. Concentration polarization and fouling are two main phenomena causing flux decline in membranes. However, they may be dependent on each other as concentration polarization lead to fouling if no mitigation is put in place (Kim et al., 2009).

2.5.1. Concentration Polarization

Concentration polarization is when rejected solute from the feed accumulates on the membrane surface, this process is reversible (Figure 2.9). The solvent passes through the membrane freely. The concentration of the solute in the permeate (C_p) is lower than the concentration in the bulk (C_b). (Mulder, 1996). The concentration of the solute increases on the membrane surface due to the accumulation of solute from the convective flow. At the steady-state, the convective solute flow to the membrane surface will be balanced by the solute flux through the membrane and diffusive flow from the surface of the membrane to the bulk (Seader et al., 2013: Mulder, 1996) Concentration polarization profile will be established whereby the concentration at the membrane surface (Cm) will be greater than the (C_b). Concentration polarization causes a decline in the transmembrane flux, and it may be severe in membranes such as microfiltration or ultrafiltration (Mulder, 1996).

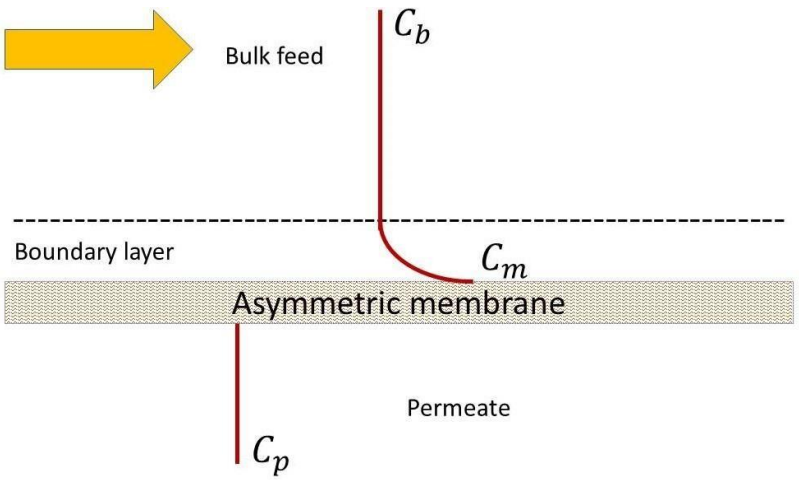

Figure 2.9: Concentration polarization profile (Adapted from Mulder, 1996)

2.5.2. Membrane fouling

Membrane fouling is caused by deposition of colloids, emulsions, suspensions, macromolecules, salts, and so on the membrane surface or within the pores of the membrane, the process could either be reversible or irreversible (Lin, Lee and Huang, 2010). The main difference between concentration polarization and fouling is that in the case of concentration polarization steady state is reached. Whereas, membrane fouling leads to a non-steady decrease of flux over time (Kwon et al., 2008). Figure 2.10 shows the variation of transmembrane flux as a function of time when concentration polarization and fouling occur.

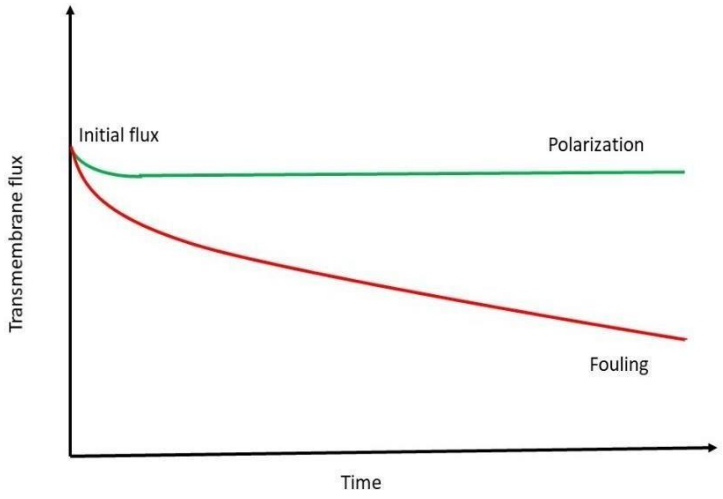

Figure 2.10: Membrane fouling and concentration polarization as function of time (Adapted from Mulder, 1996)

Fouling could be severe in pressure-driven processes such as microfiltration andultrafiltration due to utilization of fouling susceptible porous membrane. In order to mitigate the effect of fouling, it is required to constantly clean the membrane mechanically (e.g., using oversized sponge balls) or chemically and even the complete replacement of the membrane after some time is required (Lin et al., 2010; Sioutopoulos et al., 2019). Further minimization of membrane fouling is achieved by applying different types of techniques that have been developed in recent years like membrane modification, changing feed solution properties and operational conditions (Boributh et al., 2009). Among all these techniques, the main focus has been on the membrane modification by coating with a hydrophilic polymer layer such as chitosan and polyvinyl alcohol and inorganic modification (Liu et al., 2019).

2.5.3. Types of fouling and its minimization methods for polymeric membranes

Membrane fouling is classified by formation mechanisms in which particles are deposited on the pores. There are different mechanisms that contribute to the structure and composition of the fouling. Judd (2006) classified the main mechanisms that are common in polymeric membranes as shown in Figure 2.11. Pore blocking and cake formation occur when the molecules in the solute are large enough and gets retained by the membrane through size exclusion. When molecules deposit on those that have already adhered to membrane surface, intermediate blocking predominates, this is followed by cake formation (Bowen et al., 1995). The standard blocking occurs when the solute made up of small molecules that can access the membrane pores and are adsorbed on the walls (Ouma et al., 2016).

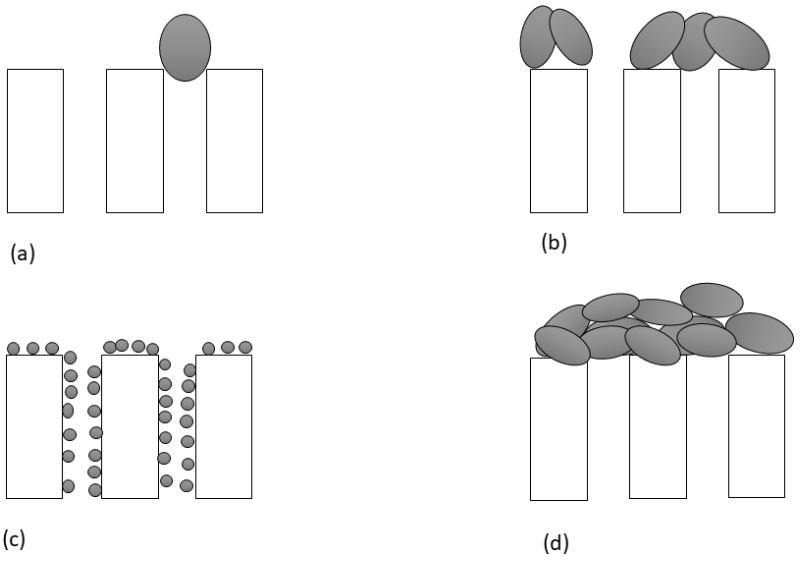

Figure 2.11: *(a) Complete pore blocking, (b) intermediate blocking, (c) standard blocking (adsorption) and (d) cake formation (Adapted from Ouma et al., 2016).*

2.5.3.1. Chemical Modification

Chemical treatment modifies the polymeric membrane surface through covalent bonding. The polymer base chain gets activated by chemical reaction or high-energy radiation, this is followed by grafting of hydrophilic modifiers (Mofradi, et al, 2019). This enhances the

membrane surface properties without significantly affecting the membrane bulk. In addition, covalent bonding of the modifiers on the membrane surface offers long-term chemical stability (Mofradi et al, 2019). As far as the chemical modification is concerned, exploration in this area has focused mostly on pegylation, sulfonation, preactivation, electron beam radiation, O_3/O_2 and plasma treatment (Takewaki, 2019).

2.5.3.2. Pretreatment of the feed solution

Pretreatment methods include thermal treatment, pH adjustment, addition of complexing agent such as EDTA, chlorination and chemical clarification. Sieving membranes such as MF and UF may be used as pretreatment for membranes with smaller pores such as nano-filtration or reverse osmosis (Shugman, Aldrich, Sanderson and Mclachlan, 2013)

2.5.3.3. Physical Modification

This method involves hydrophilic modification on the polymeric membrane surface using physical interaction but not covalent bonding. The modification doesn't alter the chemical composition of the polymeric membrane. However, a chemical reaction may be required for a successful modification (Sun et al., 2013). There are two approaches in which physical modification could be achieved. In the first approach, the surface of the polymeric membrane is directly coated with a hydrophilic polymer. The second approach involves immersing polymeric membrane in a solution of chemically active monomers (Rana et al., 2005). Thereafter, the monomers are immobilized onto the surface of the membrane via cross-linking or polymerization reaction that does not involve chemical participation of the basemembrane. Commercially available materials such as polyether block amide, chitosan and polyvinyl alcohol are used for surface modification in polymeric membranes (Hoffmann et al., 2018; Mehrparvar). Polyvinyl alcohol is a biodegradable water-soluble material that is environmentally friendly, and it has been successfully used in numerous studies of membrane fabrication (Cadotte, et al., 1988). It consists of OH groups which make it a good candidate for

insertion of hydrophilic groups into a polymeric structure so that the overall material becomes more hydrophilic and thus less prone to organic fouling (Ngo and Guo, 2009). It is chemical resistant with good film-forming abilities and must be cross-linked by another material such as glutaraldehyde or maleic acid to stabilize it in the aqueous phase. Cross-linking PVA with glutaraldehyde reduces PVA water solubility and increases the mechanical strength of polymeric membranes (Rudra et al., 2015; Kasongo et al., 2019)

2.6. Zeolites materials as a filler in mixed-matrix membranes

Zeolites are microporous natural occurring crystalline aluminosilicates consisting of a framework of SiO_4 and AlO_4 tetrahedral molecules, linked with each other by shared oxygen atoms to form cavities or cages, which are connected by ring or pore openings, with defined size and shape (Sano et al., 1994). They have ion-exchange properties which improve their adsorption capabilities. Zeolites can be synthesized from various raw materials such as natural kaolinite or metakaolinite with NaOH and colloidal silica. Commercially synthesized zeolites are the most commonly used since they can be made with fixed composition and uniform characteristics such as pore sizes and surface morphology (Wang et al., 2013). Zeolites can be modified by adding functional groups through several processes in order to improve their activity and selectivity for certain substances. The industrial application of zeolites includes; catalyst, adsorbent and ion exchangers (Oliveira and Rubio 2007). The incorporation of zeolite fillers into polymer matrix has gained attention of researchers in membrane technology, this is due the advantages such as high permeability and good selectivity that exceed Robeson upper bound (Sano et al., 1994). In addition, zeolites enhance the thermal stability and the mechanical strength of a polymeric membranes, and molecular sieving property, chemical stability and thermal resistance (Ridzuan and Musa, 2012: Sano et al., 1994). On the other hand, high cost of zeolites is the major draw-back (Wang, 2008:Sano, 1997).

Ciobanu et al. (2008), reported in their study that zeolite-polyurenthane membranes showed enhanced properties, such as good interaction between zeolite and the polymer at the interface. As the result, the water flux through membrane increased with increasing zeolite concentration. Jeong et al. (2007), studied the formation of mixed matrix membranes in reverse osmosis by the interfacial polymerization of thin film nanocomposite polysulfone support that

was impregnated with zeolite. In their study it was found that increasing zeolite fillers concentration resulted in smoother, more hydrophilic MMM. Consequently, the MMM showed high permeation flux, and slightly improved in salt rejection compared to membrane without zeolite fillers due to structural changes in membrane morphology.

2.6.1. Hydroxy sodalite as a filler

Sodalite is a microporous, crystalline, aluminosilicate-base, hydrophilic zeolite that has estimated pore size of 2.8 Å (Yao, 2006)**.** Sodalite are zeolite material with cubic symmetry framework structure that consists of vertex linking of $AlO_4$and SiO_4 into four- and six-membered oxygen rings (Buhl, 2017). There are different types of sodalite that can be synthesized for a specific function since they can include a wide range of cations as a result of framework flexibility (Buhl, 2017). Hydroxy sodalite zeolite, has attracted application in selective wastewater treatment due to its high adsorption capacity and very small pore sizes such that only small molecules such as water (2.65 Å), helium (2.6 Å) and ammonia (2.5 Å), can access and enter the hydroxy sodalite voids making it a potential candidate in separation of small molecules (Khajavi et al., 2007). However, occluded organic matter present in the cages of hydroxy sodalite could results in lower membrane permeation. The attempt to get rid of organic matter through dehydration of the sodalite results in destabilization and partial collapse of the framework structure (Khajavi et al., 2007). Recently, a new method called topotactic conversion has been developed to eliminate organic guest species. This method involves topotactic conversion of layered silicate RUB-15 into all-silica SOD-type zeolite with accessible micropores which allow small molecules such as hydrogen to pass through (Koike et al., 2017; Moteki et al., 2011).

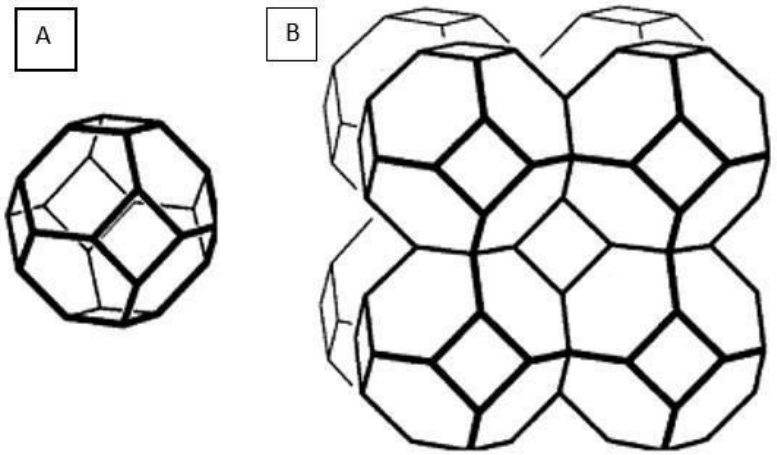

Figure 2.12: A shows β cage, B shows the sodalite structure (Adapted from Khajavi et al., 2007).

2.6.2. Sodalite-based membranes (inorganic and mixed-matrix membranes) and previous studies in water and wastewater treatment

Khajavi et al., (2010) synthesized hydroxy sodalite membrane hydrothermally and used it in pervaporation to desalinate seawater from North Sea. They desalinated sodium chloride and sodium nitrate aqueous solutions with varying concentration at 473 K and 2.2 MPa. They found that the membrane ion rejection was 99.99% and the water permeate was of a very high quality and was classified as ultrapure water. However, sodium chloride flux increased with increase in concentration while in sodium nitrate the opposite was observed. They speculated that the hydroxide groups in hydroxy sodalite cages are substituted with chloride anions of the solution resulting in higher flux. Daramola et al., (2015), investigated the application of hydroxy sodalite in polyethersulfone (PES-SOD) mixed matrix membrane for AMD treatment. They fabricated PES-SOD mixed matrix with different loadings together with pure polymeric membrane for comparison. The results showed that the performance of a pure polymeric membrane (selectivity and flux) is enhanced by loading hydroxy sodalite crystals within the matrix of PES polymer. The results of membrane performance evaluation showed that the 10% wt has higher flux whereas, 15% wt loading showed highest selectivity towards Pb^{2+} (57.44% rejection)

2.7. Concluding remarks and the contribution of this study

The use of membrane for wastewater treatment offer advantages over other technologies used for treatment of phenol in wastewater. The advantages include low cost, high selectivity and environmental friendliness. However, conventional membranes suffer from severe flux decline due to fouling, concentration polarization and mechanical deterioration. This study proposes to contribute in developing fouling resistant membranes by introducing hydrophilic sodalite fillers into the polysulfone matrix to develop a novel mixed matrix membrane. Performance of a novel organic free silica-sodalite infused membrane will be studied in comparison with hydroxy sodalite infused membrane during treatment of phenol-containing wastewater. The study further proposes to enhance hydrophilicity of the membrane through the addition of hydrophilic layer (PVA) on the surface of mixed matrix membranes. This is the sustainable approach to obtain membrane with enhanced anti-fouling property.

Chapter Three

3. Methodology

This chapter describes materials and experimental procedures used to synthesize nanoparticles (Hydroxy sodalite and silica sodalite), pure polysulfone membranes and composite membranes. The procedures and methods used to characterize nanoparticles, polysulfone membranes and mixed matrix membranes are described in this chapter, as well as the procedure used to test the separation performance of the membranes.

3.1. Materials

Sodium metasilicate nonahydrate (Na_2SiO_3), sodium hydroxide pellets (NaOH, 99%), anhydrous sodium aluminate ($NaAlO_2$, 99%), Tetra-ethoxysilane, aqueous solution tetramethylammonium hydroxide (25 wt. %: 32 mL), polysulfone (in beaded form with a molecular weight of 22,000 g/mol), N,N-dimethylacetoamide (99% or more), polyvinyl alcohol (99% or more, 44.05 g/mol), Maleic acid (MA) (Reagent plus, R; 99% or more, molecular weight 116.07 g/mol), Phenol (99% or more molecular weight 94.11g/mol) were purchased from Sigma Aldrich (Merck), South Africa and used as supplied without any further purification. The Nitrogen gas was puchased from AFROX, South Africa. The de-ionized water was prepared in the lab at the School of Chemical and Metallurgical Engineering.

3.2 Experimental

The procedure employed in this study is summarized in stages Figure 3.1

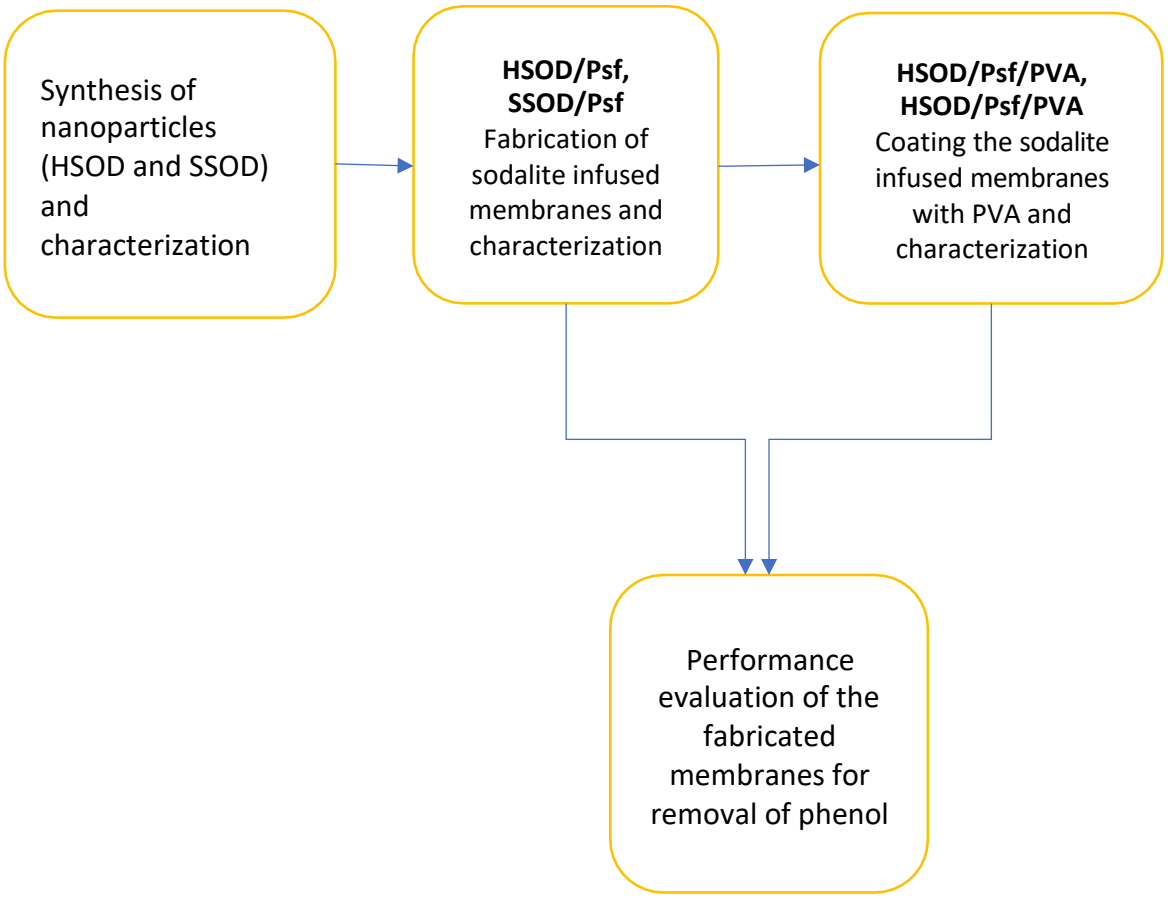

Figure 3.1: Flow diagram of four main stages involved in this study

3.2.1. Synthesis and characterization of HSOD and SSOD crystals

3.2.1.1. Synthesis of hydroxy sodalite (HSOD) crystals

Hydroxy sodalite crystals were prepared via hydrothermal synthesis method as described by (Daramola et al., 2015). Sodium metasilicate nonahydrate (1.64 g), sodium hydroxide pellets (9.44g), anhydrous sodium aluminate (0.44 g), and deionized water (44.87 g) were put in a Teflon cup. The Teflon cup was sealed with parafilm sheet, materials were mixed together and stirred for 1 h at 1000 rpm on a magnetic stirrer to yield a homogenous mixture of $5SiO_2{:}Al_2O_3{:}50NaO_2{:}1005H_2O$. During hydrothermal synthesis 45 mL (or 48 g) of the vigorously mixed precursor solution was poured into a Teflon-lined stainless-steel autoclave and subjected to hydrothermal synthesis at 413 K for 3.5 hours. After hydrothermal synthesis, hydroxy sodalite crystals were washed thoroughly with deionized water until the pH of the

water was neutral. The washed crystals were collected on filter paper and dried for 24 h at 333 K in an oven.

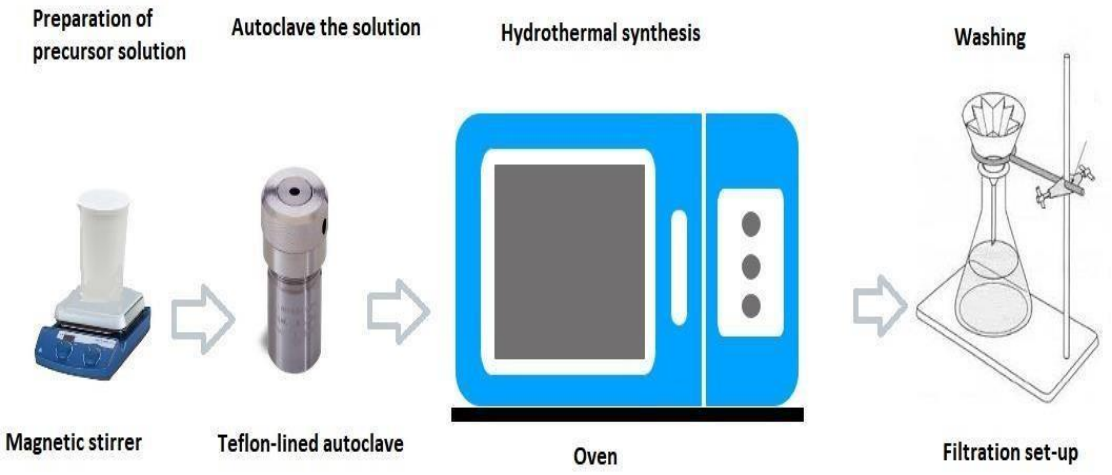

Figure 3.2: Schematic diagram for HSOD synthesis via direct hydrothermal synthesis (Adapted from Daramola et al., 2016)

3.2.1.2. Synthesis of silica sodalite (SSOD) crystals

Silica sodalite was produced through topotactic conversion using modified version of the method described by Moteki et al., (2011). Tetra-ethoxysilane (18.52 g) was slowly added to an aqueous solution tetramethylammonium hydroxide (25 wt. %: 32 mL) in a Teflon cup. The mixture was magnetically stirred for 24 h for homoginazation. The solution was poured into a Teflon-lined stainless-steel autoclave and subjected to the temperature of 413K for 7 days. The solid particles were filtered and washed with acetone. The solid particles were dried in the oven at 333K for 24 h.

Acid Pre-treatment was done by dissolving RUB-15 (0.1 g) in 30 mL of 5 M propionic acid. The solution was stirred for 3 h at room temperature. The solid particles were filtered and washed with distilled water and dried in the oven at 333 K for 24 h. The particles were calcined at 1073 K for 5 h

3.3. Fabrication and characterization of sodalite-infused polymer membranes

3.3.1 Fabrication of SSOD/PSF and HSOD/PSF membranes

Phase inversion method was used for the preparation of asymmetric membranes (Gohil and Ray, 2009) as shown in Figure 3.3. Silica sodalite nanoparticles were added to 50 mLof N,N-dimethylacetamide in different loadings (5 % wt. and 10 % wt.). The mixture was ultra-sonicated for 15 min and shook for another 15 min. Ten grams of polysulfone was added to the mixture and ultra-sonicated for 15 min thereafter, stirred on a magnetic stirrer for 24 h at 400 rpm. The solution was cast on a glass plate with the aid of a casting blade. The cast solution was left under ambient conditions for 10 s and thereafter was fully immersed in distilled water for 24 h. The membrane was dried in an oven at 60 °C for 20 min to remove the solvent. As comparison, a similar membrane was prepared using hydroxy sodalite nano-particles.

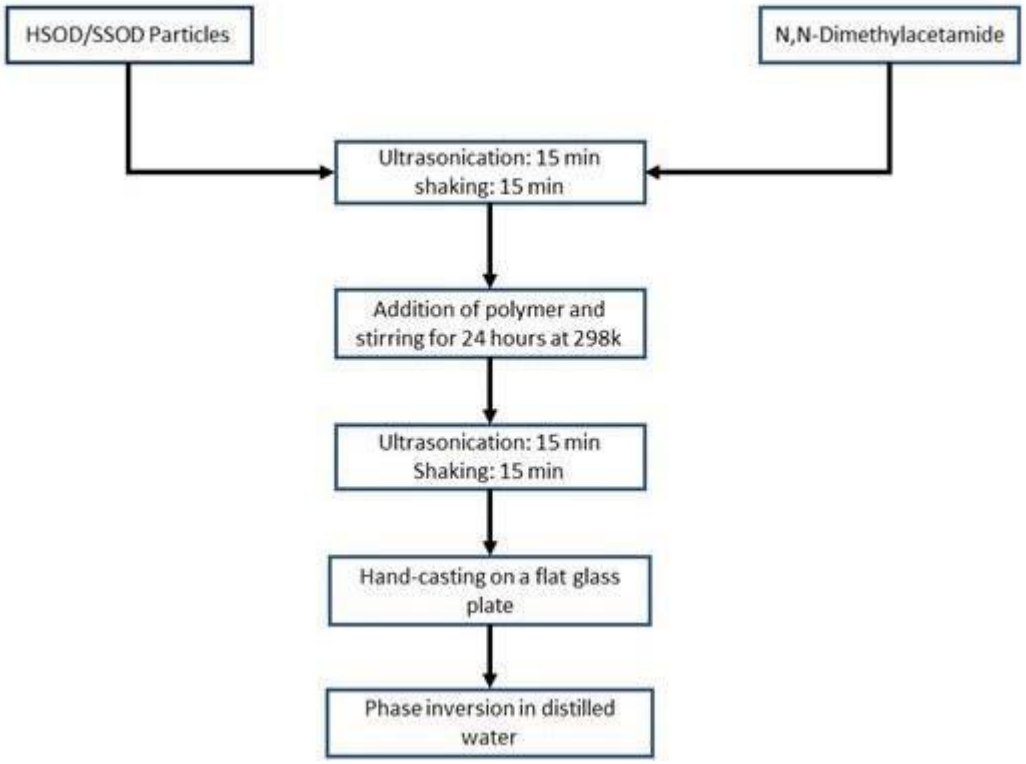

Figure 3. 3: Procedure for fabrication of composite matrix

3.4 Characterization

3.4.1. XRD to check the crystallinity of the HSOD and SSOD crystals

X-ray diffractometer (model Bruker D2 Phaser) in Figure 3.3 was used to check the crystallinity of the HSOD and SSOD particles. XRD used CoKα radiation (λ=0.179 nm) at a scan rate of 0.25 sec per step and a step size of 0.02°, respectively (Daramola et al.,2015).

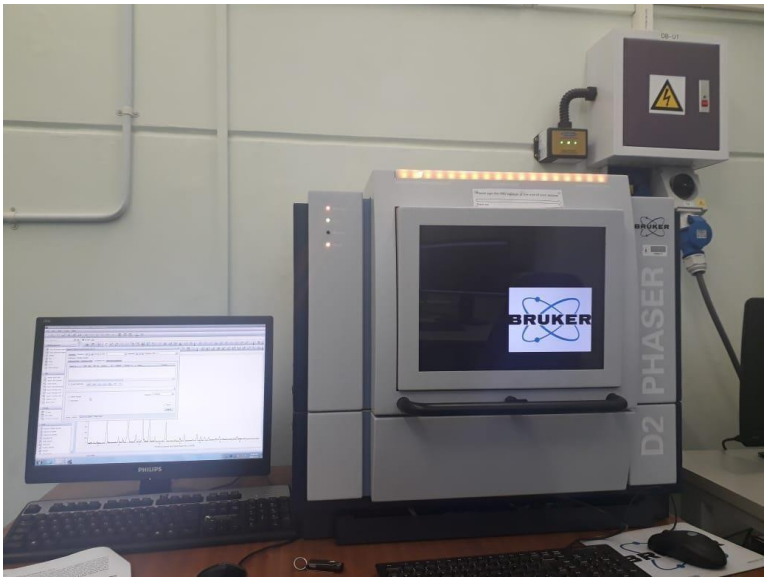

Figure 3.4: Picture of an X-ray diffraction, XRD (model Bruker D2 Phaser) analysis, Wits MMU

3.4.2. Textural properties of SSOD and HSOD crystals via Brunauer– Emmett–Teller (BET) analysis

The pore size and the surface area of HSOD and SSOD crystals were examined BET.

3.4.3. SEM for surface morphology of the synthesized HSOD and SSOD particles as well as the fabricated membranes

Scanning electron microscope produces high resolution of 3D images by scanning material focused beam of electrons (McMullan, 1988). The surface morphology of the synthesized HSOD and SSOD particles as well as the surface of fabricated membranes

were coated with gold-palladium and examined with SEM (Figure 3.4.). However, to study the cross-section of the membranes; membranes were immersed in a liquid nitrogen for 1 min, immediately after immersion they were cut open with razor blades to expose the cross-sectional area. The cross-sectional area was coated with gold-palladium and subjected to the SEM for observation.

Figure 3.5: Picture of scanning electron microscope, SEM (model Carl Zeiss Sigma), Wits, School of Chemical and Metallurgical Engineering).

3.4.4. FT-IR spectroscopy to check surface chemistry of crystals and fabricated membranes

The surface chemistry of the nanoparticles and fabricated membranes was checked with FT-IR spectroscopy using PerkinElmer spectrum two Figure 3.6. The nanoparticles and the synthesized membranes were placed on the diamond surface. The spectra were obtained inthe range 400- 4000 cm^{-1}.

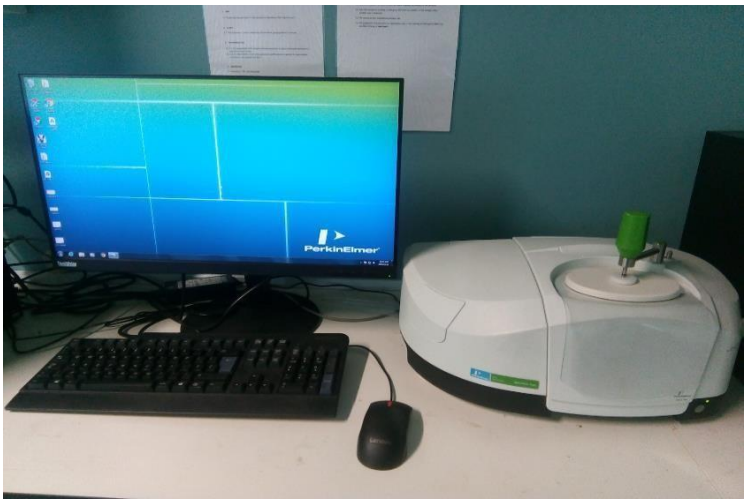

Figure 3.6: Picture of FT-IR spectroscopy (PerkinElmer spectrum two model), Wits, School of Chemical and Metallurgical Engineering).

3.4.5. Contact angle measurements for hydrophilicity/hydrophobicity of membranes

The wettability of the membranes was determined through contact angle measurements using dataphysics OCA 15 model Figure 3.6. This is the angle a liquid creates with the solid when it is deposited on it (Dwivedi et al., 2014). Contact angle was measured by placing water droplets on the outer surface of the membrane using a micro-syringe. The process was repeated 10 times at different positions after which, average value for each sample was reported and recorded for the investigation of the surface hydrophilicity of the membranes (Emadzadeh et al., 2019).

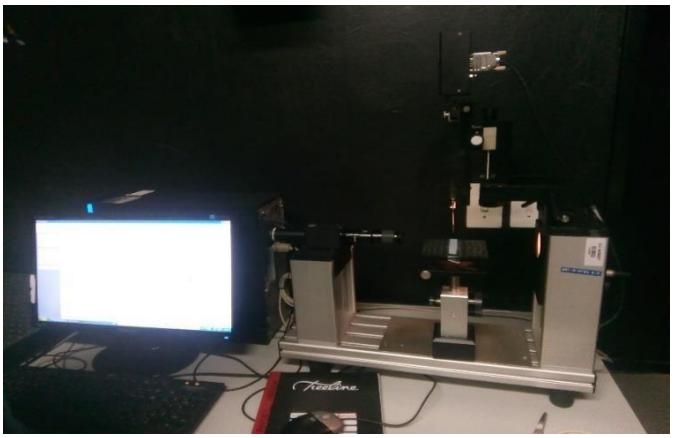

Figure 3.7: Picture of optical contact angle (dataphysics OCA 15 model), University of Johannesburg

3.4.6. Atomic force microscope (AFM) for surface roughness of the membranes

The surface roughness was determined using AFM Vi300 model as shown in Figure 3.8. Roughness values could reveal membrane's tendency to foul during operation (Tansel, 2008).

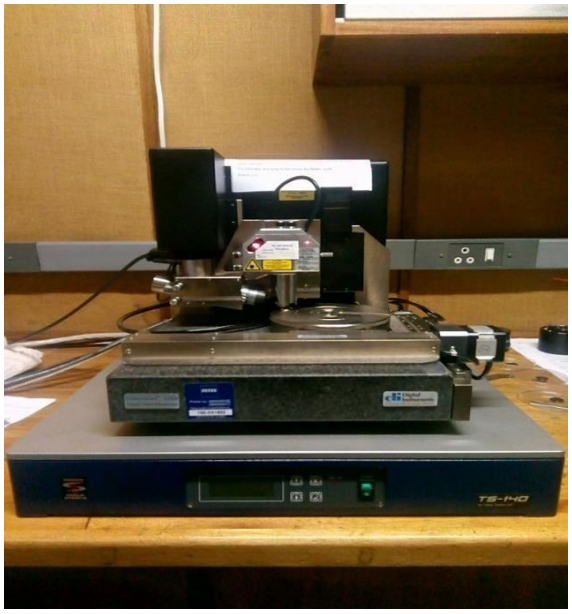

Figure 3.8: Picture of atomic force microscope (AFM Vi300 model), Wits MMU

3.4.7. Texture analyzer for mechanical Properties

The mechanical properties of the fabricated membranes were analyzed using texture analyzer, wits texture analyzer (TA.XT.plus model) (Figure 3.9). Nanotensile tests were done to measure the largest force that fabricated membranes can withstand before breaking apart (Emadzadeh et al., 2019), and characterized the ability of the membranes to resist elastic deformation under tension.

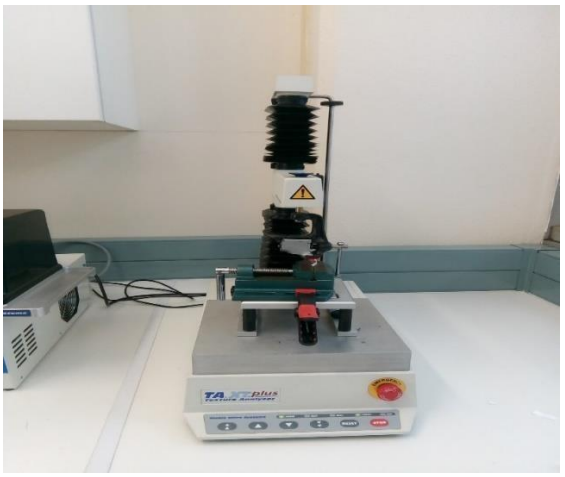

Figure 3.9: Picture of a texture analyser (TA.XT.plus model), Wits medical school

3.4. Preparation of phenol-containing wastewater and its treatment using fabricated membranes

One gram of phenol crystals was dissolved in 1 L of deionized water, the solution was gently shaken to obtain homogenous stock solution. Thereafter, 20 mL of the stock solution was diluted to 1 L with deionized water (20 mL of diluted stock solution equals 20 mg/L).

The performance of the membranes was evaluated using dead-end filtration cell (Figure 3.10). The dead-end filtration set-up consist of a filtration cell where feed was poured, inert nitrogen gas inlet pipe, stirrer bar and pressure gauge.

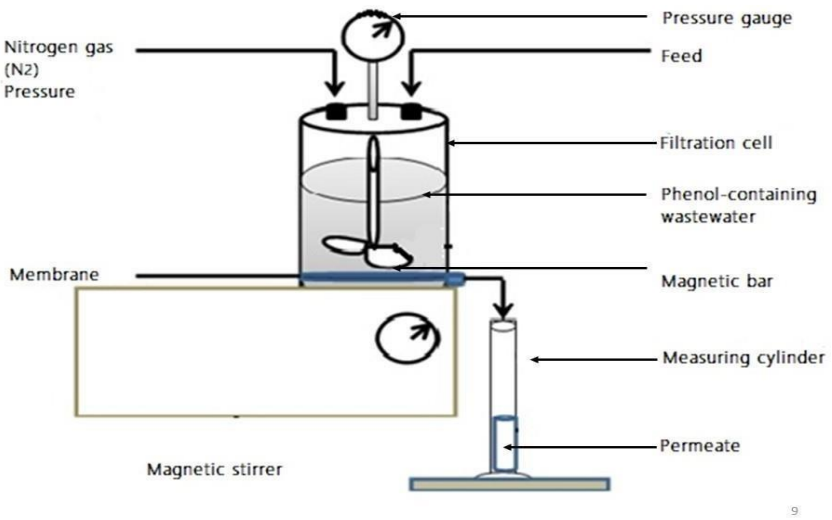

Figure 3.10: Schematic diagram of dead-end filtration cell

The set-up was fitted with one membrane at a time during the separation. Deionized water was used as pure water. Pure water permeation through the membrane was used to determine the original flux of the membrane for fouling monitoring (Daramola and Adeogun, 2011). The system was equilibrated by pressurizing pure water on the membrane placed in the cell at 4 Bar, this allows the pores to open and gives easy passage of water (Daramola et al., 2019). In this study synthetic wastewater was used whereby the concentration of phenol in water was kept constant at 20 mg/L. The nitrogen gas was used to apply pressure into the filtration cell and pressure varied from 4 to 7 bar. A stirrer plate together with magnetic bar in the filtration cell were used to maintain a homogeneous solution. Permeate from the filtration cell was collected in a measuring cylinder. The analysis of the feed and permeate was done using a pre-calibrated High-Performance Liquid Chromatography (HPLC): Agilent 1200 series model, Eclipse XDB C-18 column. Acetonitrile was used as a mobile phase; 600 mL acetonitrile was diluted with 400 mL of deionized water, 10 µL injection volume and flow rate at 1 mL/min. Pure water flux and phenol-containing flux from the membrane were calculated using equation (1). The rejection and selectivity of the membrane were obtained using Equation (3.1), and Equation (3.2), respectively:

$$J = \frac{V}{A} \qquad [3.1]$$

Where J is the permeate flux (L/m^2h); V, the volumetric flow (L/h); and A, the effective membrane area (m^2).

$$R = \frac{(C_F - C_P)}{Cf} \times 100\% \qquad [3.2]$$

R is the membrane rejection expressed in percentage; C_F is the phenol concentration in the feed stream (mg/L); and C_P is the phenol concentration in the permeate stream from dead-end cell (mg/L)

Chapter Four: Synthesis and evaluation of HSOD/PSF and SSOD/PSF membranes

4.1. Introduction

The chapter focuses on the fabrication of composite membranes whereby sodalite crystals (hydroxy sodalite (HSOD) and silica sodalite (SSOD) have been embedded into a polymer matrix (polysulfone), separately. The concentration of the sodalite crystals in the matrix has been kept at 10 % wt. This was based on the study published by Daramola and colleagues where 10 % wt. concentration of hydroxy sodalite in PES membrane gave the highest flux during the AMD treatment (Daramola et al., 2015). Therefore, 10 wt% concentration of nanoparticles has desirable flux for this study and has shown good mechanical strength as reported by Daramola et al., (2015). Sodalite crystals have desirable properties such as very small pores and high adsorption capacity which make them good candidates for wastewater treatment (Khajavi et al., 2007; Moteki et al., 2011). The performance of hydroxy sodalite and silica sodalite as fillers in polymer membranes were compared in this study. Hydroxy sodalite is formed with occluded organic matter which limit accessibility to its pores, and an attempt to remove the organic matter through dehydration leads to a partial collapse of the sodalite structure (Khajavi et al., 2007). Instead of removing organic matter in HSOD another sodalite (SSOD) has been explored, the sodalite is organic free with intact structure even after dehydration at elevated temperatures, this makes it an ideal candidate for improved permeation since it has accessible pores (Daramola et al., 2016).

4.2. Materials, methods and treatment of synthetic phenol-containing wastewater

4.2.1 Materials

Polysulfone (in beaded form with a molecular weight of 22,000 g/mol), N, N-dimethylacetoamide (99% or more), phenol-containing wastewater, hydroxy sodalite crystals synthesized via hydrothermal synthesis and silica sodalite crystals synthesized via topotactic conversion.

4.2.2. Method

Phase inversion method was used for the preparation of asymmetric membranes in this study. Silica sodalite nano-particles in 10 wt. % were added to 50 mL of N, N-dimethylacetamide. The mixture was ultrasonicated for 15 min and shook for another 15 min. Ten grams of polysulfone was added to the mixture and ultrasonicated for 15 min. Thereafter, stirred on a magnetic stirrer for 24 h at 400 rpm. The solution was cast on a glass plate with the aid of a casting blade. The cast solution was left under ambient conditions for 10 s and thereafter was fully immersed in distilled water for 24 h. The membrane was dried in an oven at 60 °C for 20 min. As for comparison, a similar membrane was prepared with the same procedure however, using hydroxy sodalite nano-particles.

The phenol-containing wastewater as prepared in Chapter 3.4 was treated through filtration in a dead-end filtration set-up (Figure 3.10). The permeate was analyzed with HPLC as described in Chapter 3.4.

4.3. Results and discussion of results

4.3.1. Membrane characterization

4.3.1.1. Crystallinity and phase of SSOD and HSOD crystals

Figure 4.1a depicts XRD patterns of the synthesized HSOD which reveal sharp peaks that are attributable to the crystallinity of the particles. The XRD patterns of the synthesized HSOD correlates the simulated XRD patterns, this confirms the successful formation of HSOD crystals and is consistent with the reported patterns (Daramola et al., 2015). The XRD patterns of the synthesized SSOD in Figure 4.1b reveal the successful formation of SSOD crystals as the patterns match the reference SSOD patterns obtained from IZA website (Iza-structure.org, 2019). However, it was noted that the intensity of the peaks for synthesized SSOD is relatively lower as compared to the reference XRD patterns, this is due that crystalline phases in the synthesized SSOD have not form completely. Furthermore, the broad hump at around $2\theta = 25$ which is a characteristic peak for amorphous silica sodalite also confirms that the SSOD is successfully synthesized, this is consistent with the XRD pattern for SSOD reported in the literature (Koike et al., 2017).

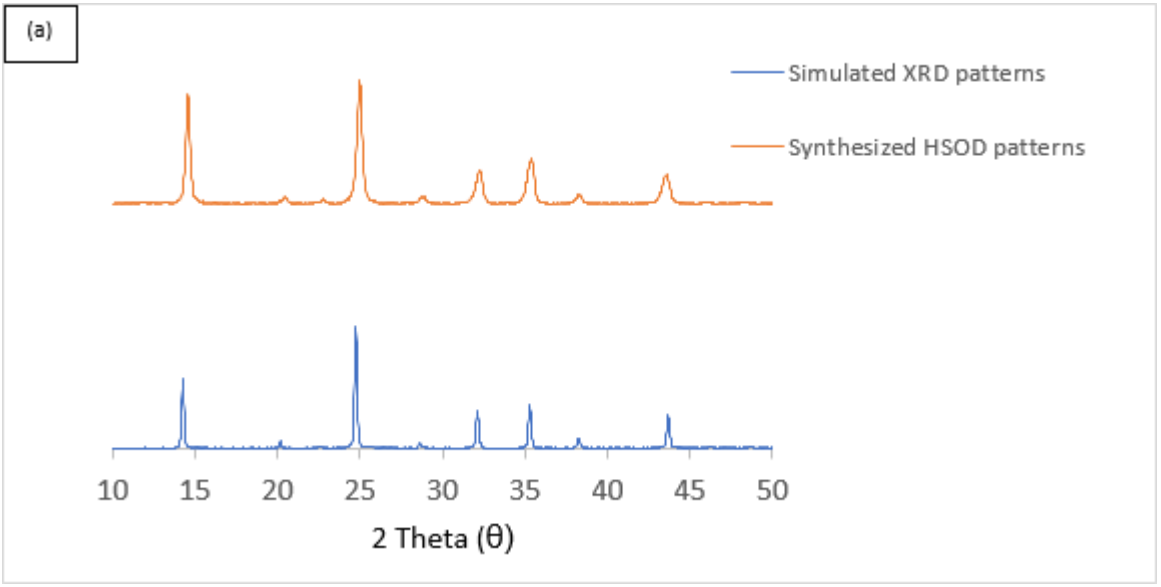

Figure 4. 1a: XRD patterns for hydroxy sodalite

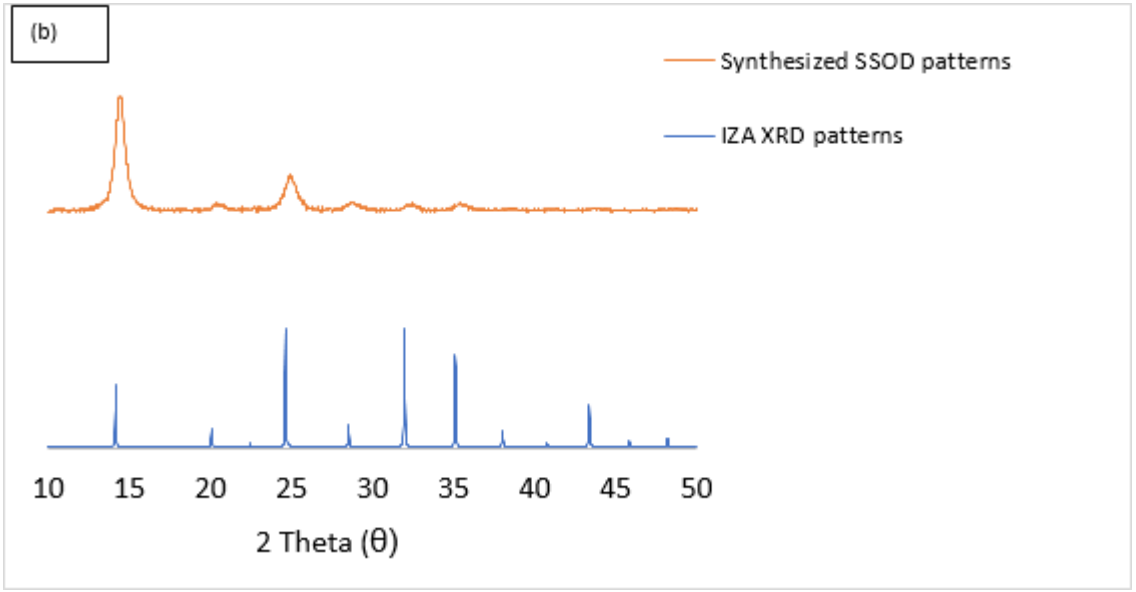

Figure 4.1b: XRD patterns for synthesized SSOD together with reference XRD patterns obtained from IZA website http://www.iza-structure.org/IZA-SC/pow_plot.php

Table 4.1 presents the BET analysis of the HSOD synthesized via hydrothermal synthesis and SSOD synthesized via topotactic conversion. The results are used to evaluate their textural properties. The results illustrate that, HSOD has a very small specific surface area 2.35 (m^2/g)

compared to the surface area of SSOD 27.29 (m^2/g), this shows that synthesis via topotactic conversion produces significantly enhanced specific surface area. The larger specific surface area implies increased adsorption capacity, hence more particles from wastewater may be trapped on the surface of the SSOD than HSOD (Pakade et al., 2016; Özsin et al., 2019). SSOD has larger pore volume than HSOD implying that SSOD has more accessible pores than HSOD. This may consequently give higher permeation flux during performance evaluation as reported by Moteki et al., (2011).

Table 4.1: BET analysis of HSOD and SSOD

Nanoparticles	BET Surface area (m^2/g)	Pore volume (cm^3/g)	Pore size (nm)
HSOD	2.3454	0.0119	20.2948
SSOD	27.2884	0.0671	9.8435

4.3.1.3. Morphology of sodalite crystals and membranes

The surface morphology of the synthesized HSOD particles was examined with scanning electron microscope (SEM). Figure 4.2a depicts SEM image of HSOD at lower magnification, thread-ball-like shapes were observed, this is consistent with the work reported by Hums, (2017). Figure 4.2b shows SEM image of HSOD at high magnification, typical cubic shapes of the crystals are visible, this further reaffirm the successful formation of HSOD. Similar observations have been reported in the literature (Daramola, et al., 2015). Figure 4.3a shows SEM image of SSOD, thin plate-like shapes stacked together are typical shapes of silica sodalite formed in a topotactic conversion manner. The observation is consistent with the work reported in the literature (Koike, et al., 2017).

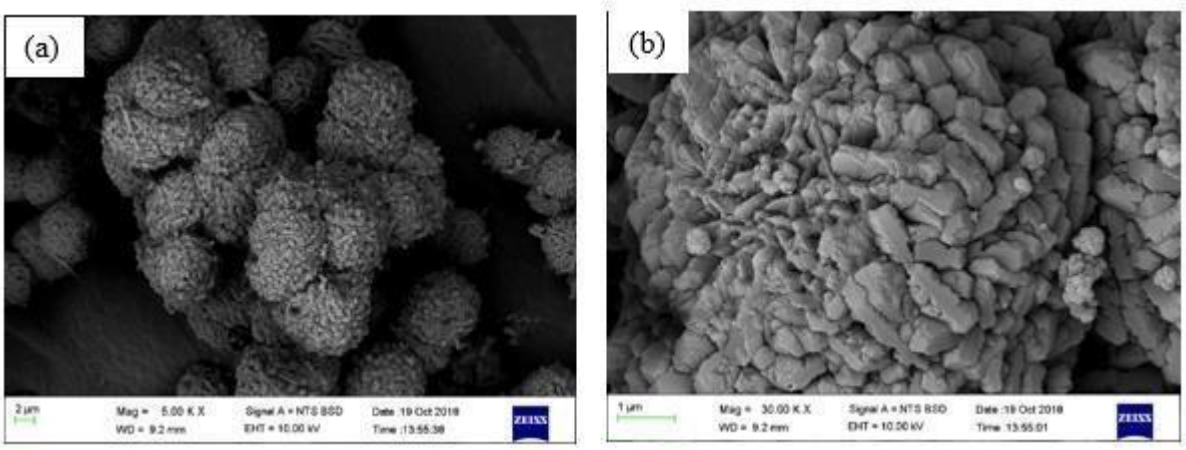

Figure 4.2: *SEM images of hydroxy sodalite (a) low magnification and (b) high magnification*

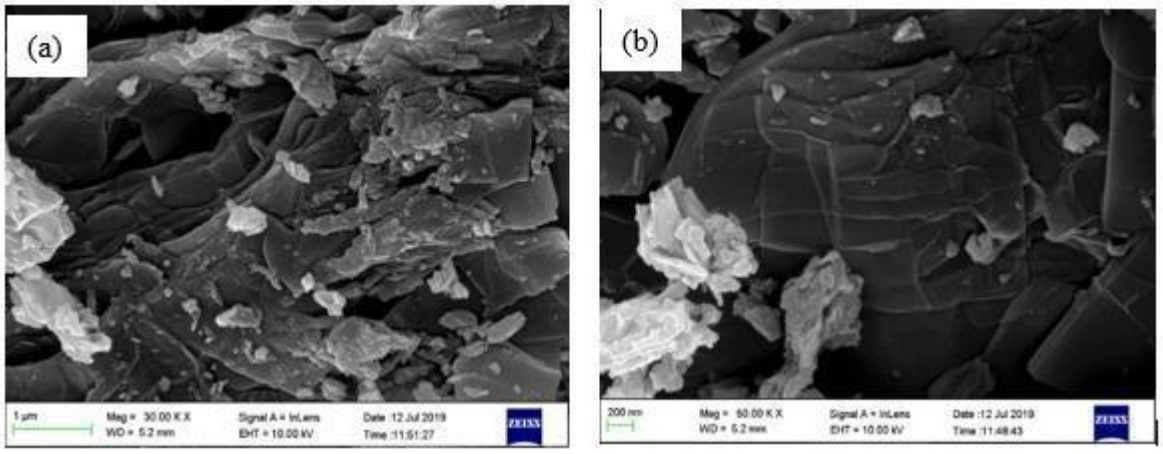

Figure 4.3: SEM images of silica sodalite (a) low magnification and (b) high magnification

Figure 4.4 (a) shows surface morphology of pure polysulfone membrane (0 wt. % HSOD/PSF), the surface is highly porous with large pores visible. Pores in PSF are also visible in the cross-section Figure 4.4b. The cross- section image in Figure 4.4 (b) shows the asymmetric nature of PSF, whereby the top is thin and dense whereas pores at the bottom are larger (Singh et al., 2014). Figure 4.4 (c) and (d) show polysufone incorporated with 10 wt. % HSOD for surface and cross-section, respectively. The surface reveals fewer pores reduced in diameter, this is due the suppression of micro-void formation at high percentage loading of nanoparticles within the polymer matrix (Unuigbe et al., 2019). The typical thread ball-like shapes of HSOD are visible in the cross-section as reported in the literature (Hums, 2017). Figure 4.4 (e) and (f) depicts the surface and cross-section of the 10 wt. % SSOD/PSF, the surface is dense with no

clearly visible pores, this is due to the suppression of micro-void formation caused by high concentration of SSOD particles, in the cross-section plate-like shapes as reported by Koike et al., (2017), are visible this reaffirms the successful embedment of SSOD particles in the PSF matrix.

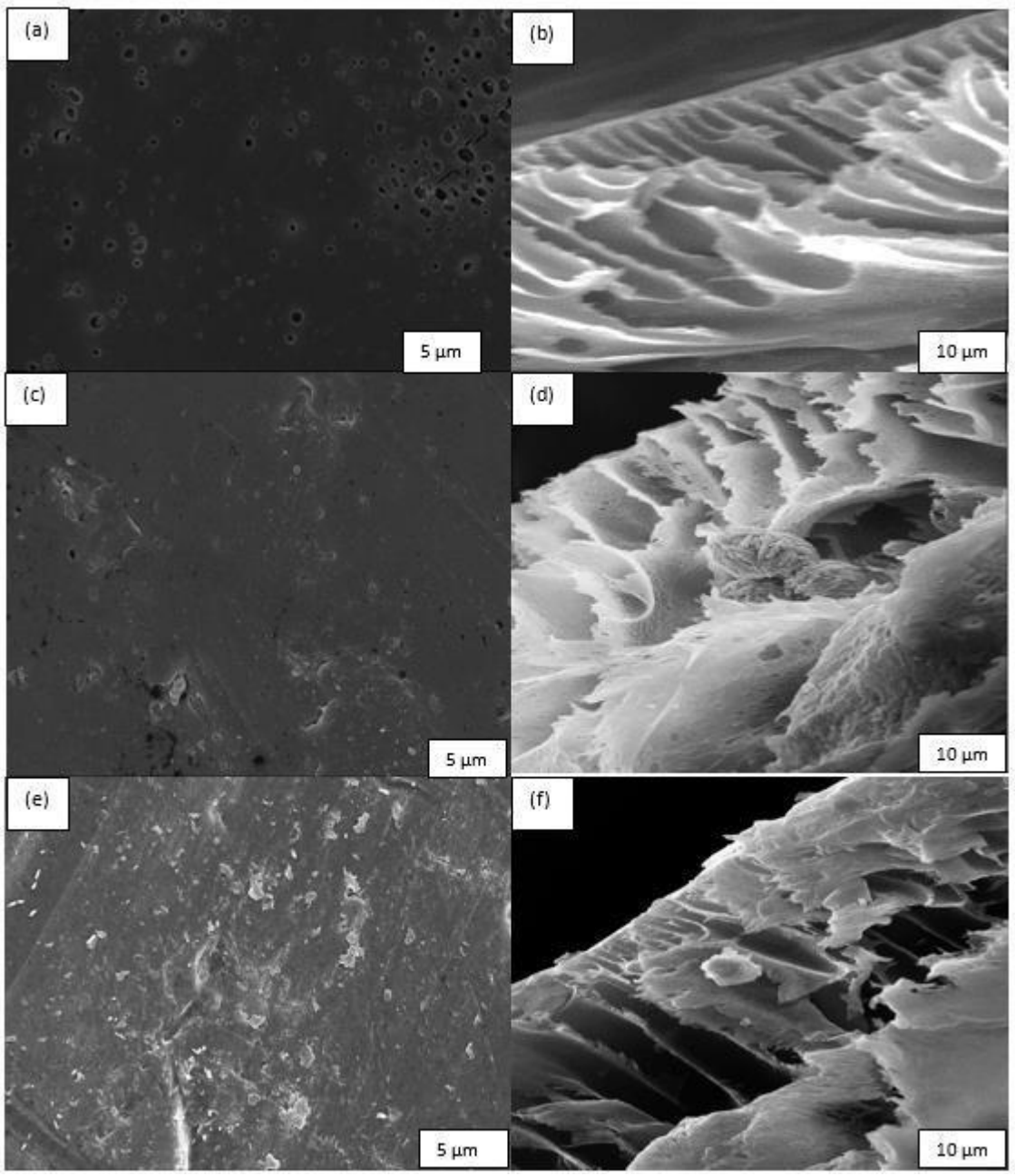

Figure 4.4: SEM images (a) and (b) show surface and cross-section of 0 wt.% SSOD/PSF, (c) and (d) show surface and cross-section of 10 wt.% HSOD/PSF and (e) and (f) show surface and cross-section of 10 wt.% SSOD/PSF, respectively.

4.3.1.4. Surface properties of sodalite crystals and membranes via FT-IR and AFM analysis

The surface chemistry of the hydroxy sodalite has been checked with FT-IR spectroscopy. Figure 4.5 shows the spectrum of HSOD, the OH-band in the range between 3000 cm^{-1} and 3300 cm^{-1} is absent. This has been observed in the literature for basic hydroxy sodalite. However, non-basic hydroxy sodalite with 2 to 8 mol water is expected to exhibit OH-band (Engelhardt et al., 1992; Günther et al., 2015). The strong broad band peak at approximately 1000 cm^{-1} could be attributed to the asymmetric stretching vibration of T−O−T (T can either be Si or Al). The symmetric stretching vibration at around 740 and 600 cm^{-1} is attributable to T−O−T. The results obtained from the FT-IR spectra of the HSOD show consistency with that of other authors literature (Yao et al., 2006; Daramola et al., 2015). Figure 4.6 depicts the spectrum of SSOD. The vibration peak at 1100 cm−1 is assignable to Si−O−S asymmetric stretching mode. There is a noticeable absence of the broad absorption band at around 3300 cm^{-1} that belongs to O–H stretching vibration of silanol groups, this is due to the dehydration that takes place during calcination (Koike, et al., 2017).

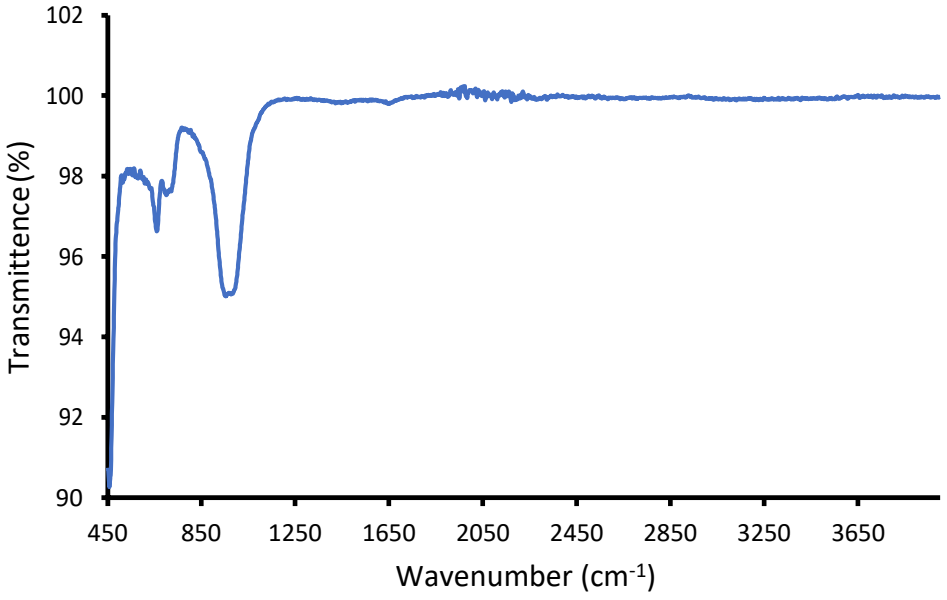

Figure 4.5: FT-IR spectrum of HSOD crystals

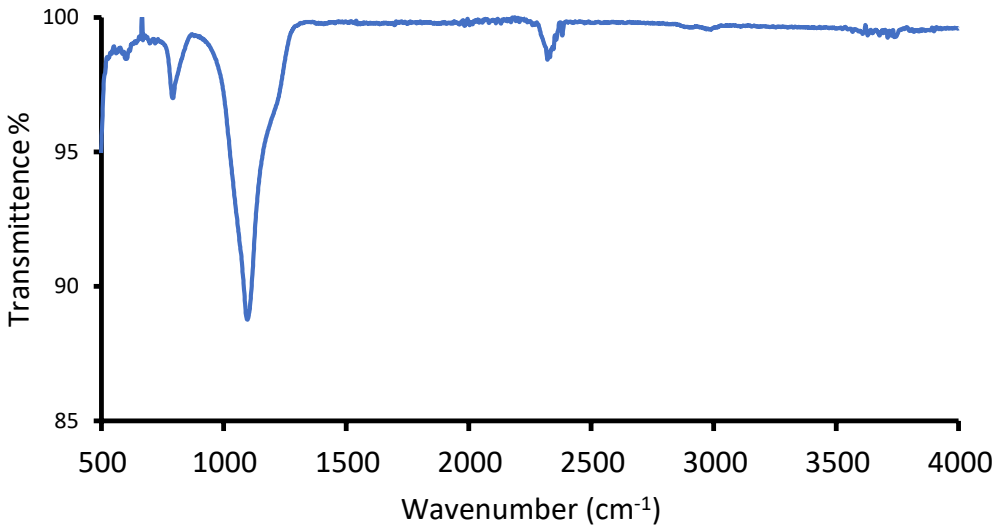

Figure 4.6: FTIR spectrum SSOD nanoparticles

4.3.1.3. FTIR for surface chemistry of membranes

The FT-IR spectra were used to analyze the functional groups and the functionalities in the membranes. Figure 4.7 shows the FT-IR spectra of PSF membranes with different nano-particles loading. It was observed that the addition of nano-particles in PSF membranes did not have significant effect on the FTIR spectra since the spectra did not show any change. All peaks present in the spectra are due to vibrational frequency of PSF membrane. The peak at $1105cm^{-1}$ belongs to a saturated C-C single bond. The $1151cm^{-1}$peak confirms the presence the stretch symmetric $C-SO_2-C$ group (Singh et al., 2006). The sharp and strong peak at $1242cm^{-1}$ is due to the presence of a stretching ether (C-O-C) group. A medium peak at $1488cm^{-1}$ corresponds to the vibrational stretch of CH_3-C-CH_3 bond. Two peaks at $1506\ cm^{-1}$ and $1587cm^{-1}$ shows a stretch of C=C bond in the aromatic ring this is consistent with the literature (Singh et al., 2006: Gohil and Ray, 2009).

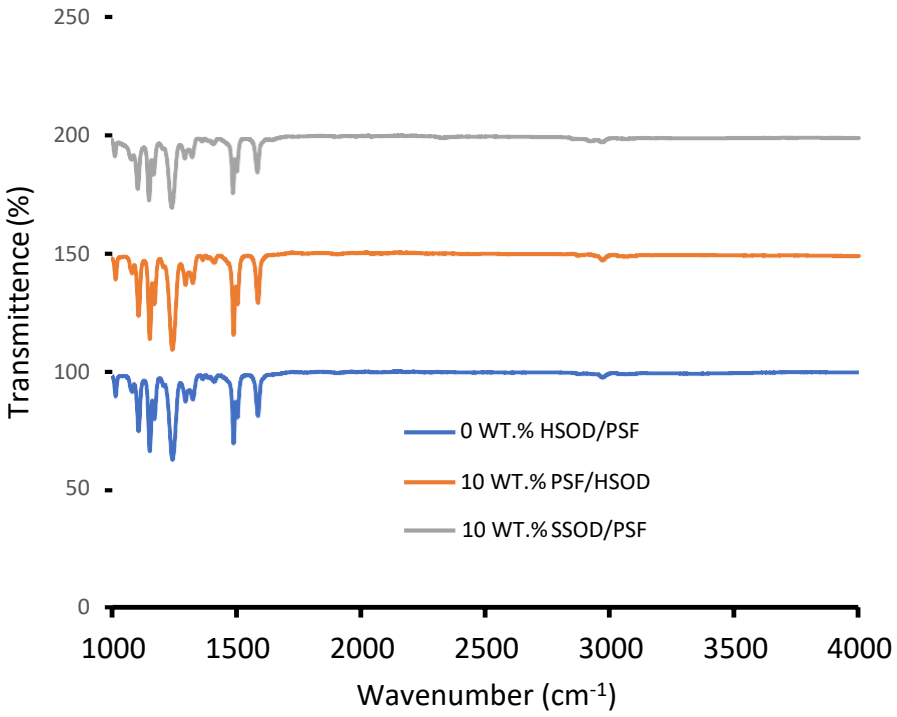

Figure 4.7: FTIR spectra of the synthesized membranes

4.3.1.4. AFM analysis

Figure 4.8 shows AFM 3D images together with roughness values. The surface roughness measurements were analyzed using AFM as shown in Chapter 3 Figure 3.8 to evaluate surface properties of the membranes. Roughness values are used as an indicator of a membrane's tendency to foul during filtration (Tansel, 2008). When roughness is high, adhesive forces on the membrane surface become larger (Bowen et al., 1998). The adhesive forces cause particles from wastewater to adhere on the membrane surface making rougher membranes highly susceptible to fouling (Caglayan, 2014). The 0 wt. % HSOD/PSF membrane has shown the highest average roughness (Ra) 163.86 nm and root mean square roughness (Rms) 130.58 nm. This could be attributed to the hydrophobic nature of pure polysulfone. The decrease in roughness has been observed when a pure PSF membrane was either loaded with 10 % wt. HSOD or 10 % wt. SSOD nanoparticles. This is due to the changing of roughness characteristics upon addition of hydrophilic nano-particles that altered the hydrophobic surface of pure PSF to the hydrophilic one, this is consistent with the study reported by (Tansel et al., 2008). The 10 % wt. SSOD has shown the least surface roughness 30.84 nm and 45.84 nm for Ra and Rms, respectively.

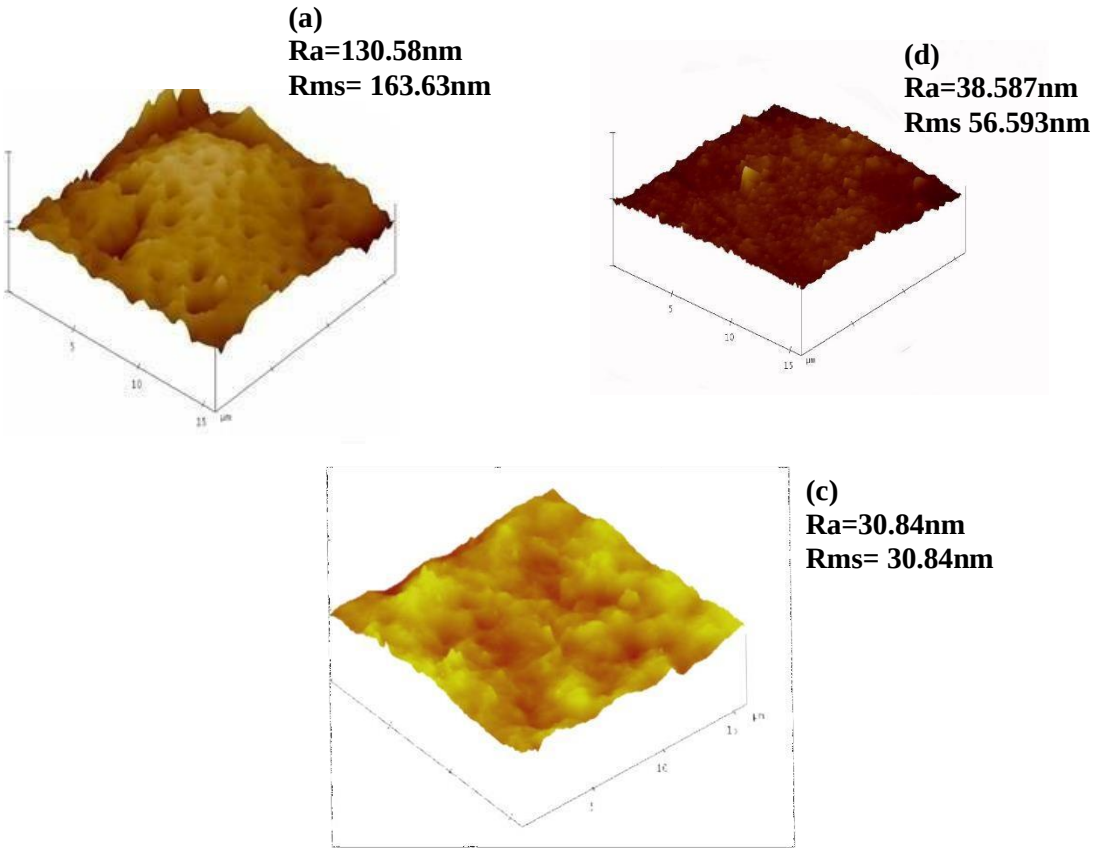

Figure 4.8: AFM images (a) 0 wt. % HSOD/PSF, (b) 10 wt. % HSOD/PSF and (C) 10 wt. % SSOD/PSF

4.3.1.5. Contact angle measurements of membranes

Figure 4.12 show contact angle measurements done to investigate the surface hydrophilicity of the membranes (wettability by water). This could be used in predicting the performance of the membranes or susceptibility to fouling (Emadzadeh et al., 2019). The hydrophobic membrane tends to have higher contact angle and hydrophilic membrane have lower contact angle (Sun et al., 2010). The pure PSF (0 wt. % HSOD/PSF) showedthe highest contact angle (83.81°) of all the membranes this is attributed to the hydrophobic nature of the membrane (Van der Bruggen et al., 2009). The incorporation of hydroxy sodalite particles into a pure PSF matrix resulted in a decrease in contact angle revealing hydrophilic enhancement. These results correspond with the trend observed in AFM roughness values.

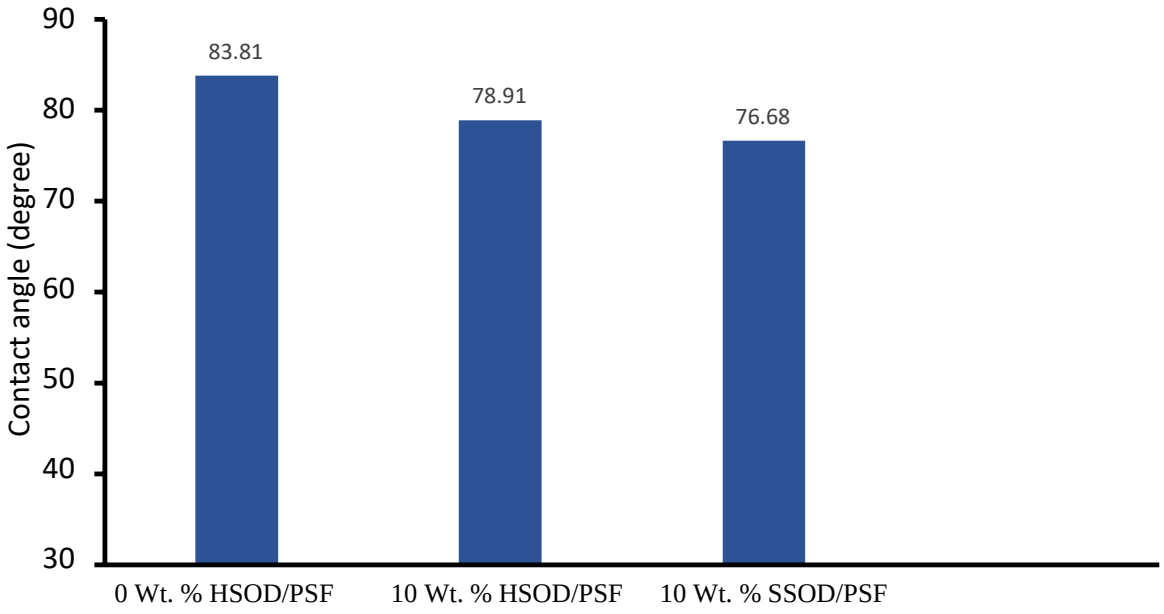

Figure 4.9: Contact angle of the fabricated membranes

4.3.1.6. Mechanical Properties of fabricated membranes

Figure 4.10 depicts the effect of nano-particles loading on the mechanical properties of the fabricated membranes. Figure 4.10 (a) illustrates the ultimate tensile strength (UTS) results which shows the largest force that fabricated membranes can withstand before breaking apart (Emadzadeh et al., 2019). Figure 4.10 (b) shows Young's modulus which evaluates theability of the membranes to resist elastic deformation. It is believed that pure polysulfone membranes with enhanced mechanical strength may have longer lifespan and less prone to mechanical deterioration (Elrasheedy et al., 2019). The increase in both UTS and young's modulus upon the addition of HSOD and SSOD particles was observed, this confirms enhancement of mechanical strength (Daramola, et al., 2015: Xu, et al., 2014). Therefore a membrane may have longer lifespan and less prone to mechanical deterioration (Elrasheedy et al., 2019).

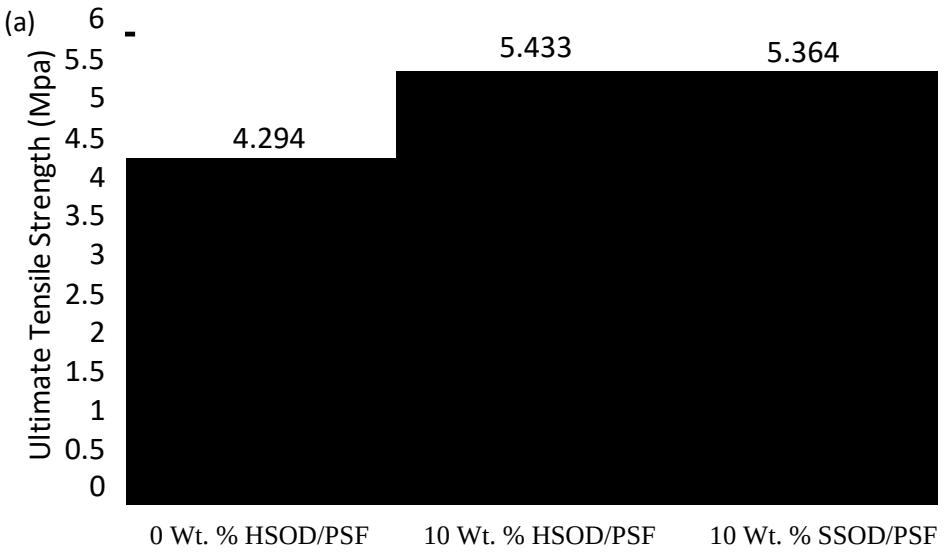

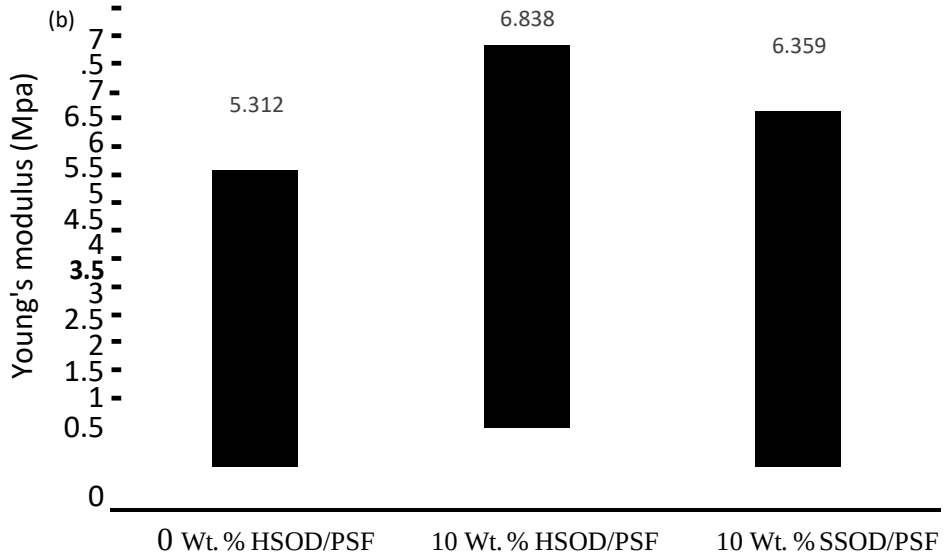

Figure 4.10: Mechanical strength of the membranes (a) UTS and (b) Young's modulus

4.4. Performance evaluation of the membranes during treatment of phenol-containing wastewater

4.4.1. Performance evaluation of HSOD/PSF membranes

Figure 4.11 (a) show the pure water flux from 0 wt. % HSOD/PSF membrane was lower than pure water flux from 10 wt. % HSOD/PSF membrane, this is due to hydrophilicity of 10 wt. % HSOD/PSF which attracts water molecules towards it resulting in higher permeation flux (Wang et al., 2010). However, when pressure is increased to 7 bar, there was an increase in flux for 0 % wt.

HSOD/PSF membrane which even surpassed the 10 wt. % HSOD/PSF membrane. This may be due to the opening of larger pores of polysulfone at high pressure (Alkhudhiri, Darwish and Hilal, 2012). The Figure 4.11b show flux during the treatment of phenol-containing wastewater, flux decreased as compared to pure water both 0 wt. % HSOD/PSF and 10 wt. % HSOD/PSF membranes this indicates fouling and competitive sorption between phenol and water molecules (Daramola et al.,2019). In the case of pure water flux membrane resistance depend only on the pore structures of the membrane (Kumar, 2017). Increasing the pressure increases the driving force for permeation flux, resulting in the higher permeation flux for both pure water and phenol- containing wastewater (Daramola et al., 2019).

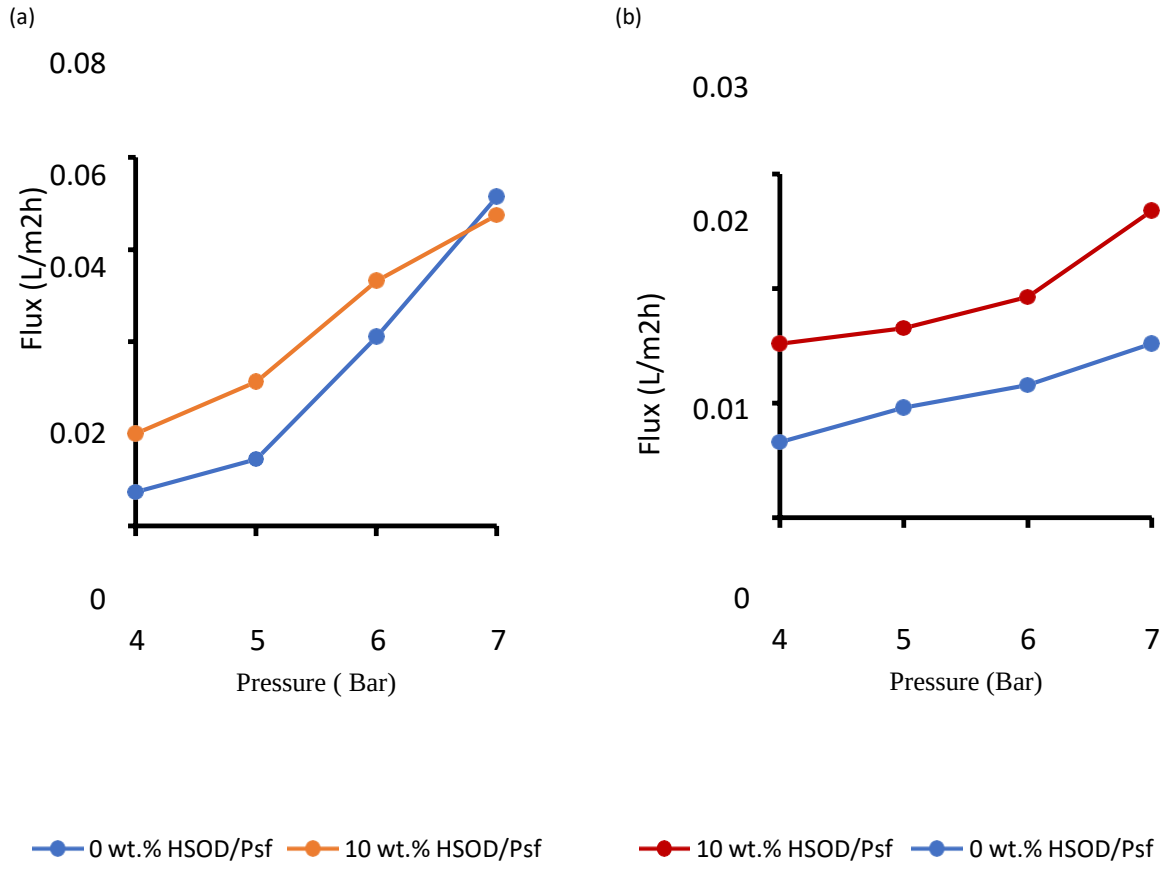

Figure 4.11: Membrane flux (a) pure water and (b) phenol-containing water

The Figure 4.12 below depicts phenol rejection from pure polysulfone (0 wt. % HSOD/PSF) and composite membrane (10 wt. % HSOD/PSF). The pure polysulfone showed the highest rejection of 93.55 % at 4 bar. Similar observation where pure polysulfone revealed higher rejection than composite membranes was made by Kumar et al, (2017) and the observation was attributed to polysulfone being synthesized with higher polymer concentration than the polymer

concentration of the composite membranes. However, at higher pressure (6 bar) there was a significant decrease in phenol rejection to 41 %, this resulted in 56.17 % rejection loss.

The 10 wt. % HSOD/PSF showed 63. 65 % phenol rejection at 4 bar. However, at 6 bar rejection decreased to 44.8%, this showed rejection loss of 29.62 %. The composite membrane sustainability at high pressure could be attributed to the incorporation of nanoparticles in the membrane matrix, which reduced the porosity of the membrane (Mukherjee and De, 2016).

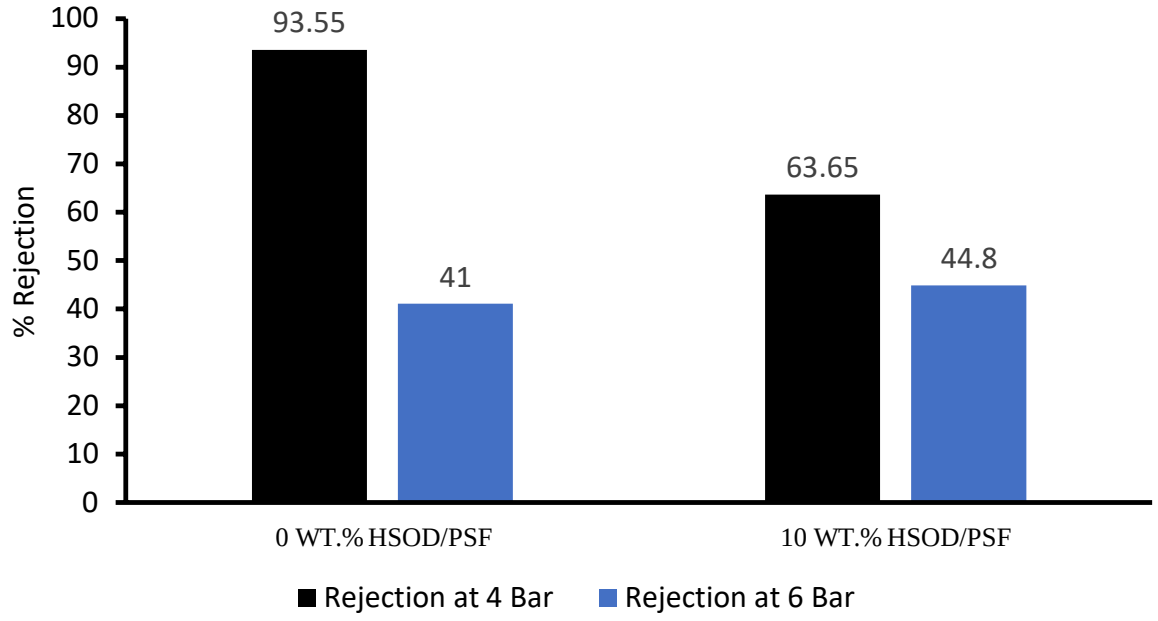

Figure 4.12: show phenol rejection from 0 % wt. HSOD/PSF and 10 % wt. HSOD.

4.4.2. Performance evaluation of SSOD/PSF membranes

Figure 4.13 (a) shows the pure water flux from pure polysulfone designated as 0 wt. % HSOD/PSF and 10 wt. % SSOD/PSF membrane. Figure 4.13 (b) depicts phenol-containing wastewater flux against applied pressure for both 0 wt. % HSOD/PSF and 10 wt. % SSOD/PSF membranes. The 10 wt. % SSOD/PSF displayed higher pure water flux than 0 wt. % HSOD/PSF membranes, this is attributable to the hydrophilicity of 10 wt. % SSOD/PSF membrane which causes attraction of water molecules towards the membrane resulting in higher permeation flux (Wang et al., 2016). The increase in filtration pressure for both membranes resulted in higher permeation flux since pressure is the driving force for permeation, hence flux increased linearly with applied pressure. In comparison with pure water flux phenol-containing wastewater showed a decrease in flux, this could be due to fouling which occurred as a result of competitive sorption between phenol and water molecules (Daramola et al., 2019).

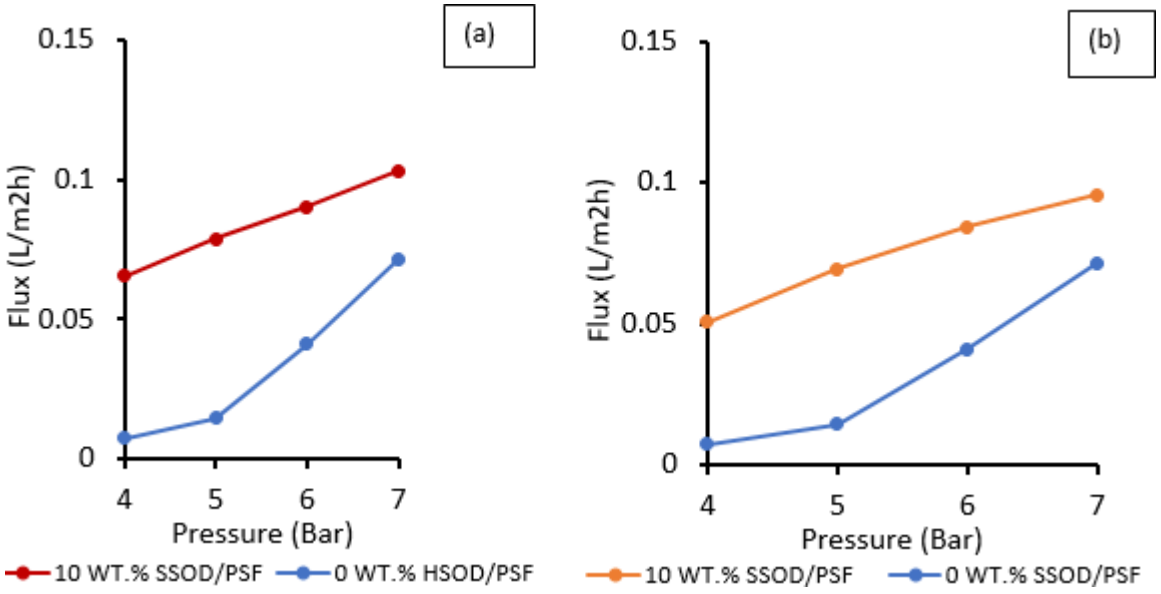

Figure 4.13: Membrane flux (a) pure water and (b) phenol-containing water

Figure 4.14 depicts phenol rejection from pure polysulfone and 10 wt. % SSOD membranes. Pure polysulfone showed the highest rejection at 4 Bar compared to the 10 % wt. SSOD loaded composite membrane. However, when the rejection is obtained at 6 Bar pure polysulfone showed decrease in rejection to 41.0 % which resulted in 56.17 % rejection loss. The 10 wt. % SSOD/PSF showed 64. 75 % phenol rejection at 4 Bar. The membrane depicts lower rejection loss of 36.29% significantly lower than pure polysufone. This higher performance at high pressure could be attributed the incorporation of SSOD nano-particles which results in reduced membrane porosity (Mukherjee and De, 2016). Hence the membrane does not severely lose its rejection capacity. Phenol molecules are only expected to enter the pores when the pressure on the filtration cell exerts a force much greater than the opposing capillary force on the surface of the membrane (Chakrabarty et al., 2010)

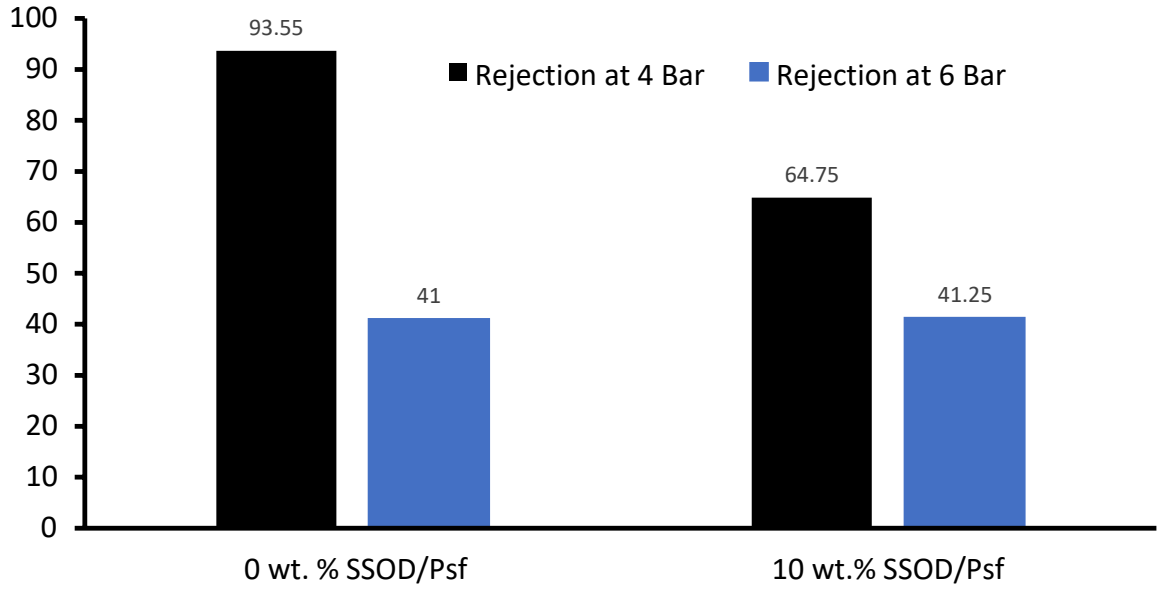

Figure 4.4: Phenol rejection of membranes at different pressure

4.4.3. Comparison of performance of HSOD/PSF and SOD/PSF membranes in this study with literature

The 10 % wt. SSOD/PSF membrane show higher permeation flux than 10 wt. % HSOD/PSF membrane this is attributed to the higher hydrophilicity in 10 wt. % SSOD/PSF as corroborated by contact angle. In addition, silica sodalite particles have higher porosity compared to HSOD particles since they are formed without organic matter (Moteki et al., 2011). This is further confirmed with BET analysis, hence explaining the higher flux.

Table 4. 2: The comparison of the performance between HSOD/PSF and SSOD/PSF and the work reported in the literature

Membrane	Permeate flux (L/m^2h)	wastewater Contaminants	% Rejection	References
1 wt.% fCNT/PSF/PVA	-	Phenol	79. 21	Daramola et al. (2019)
4 wt.% CNT/PSF	~ 12	Phenol	42.98	Mukherjee and De, (2016)
10 wt.% HSOD/PSF	0.0152	Phenol	63.65	This study
10 wt.% SSOD/PSF	0.0506	Phenol	64.75	This study

The two sodalite membranes synthesized for this study performed relatively well in comparison with sodalite infused membranes in the literature. Daramola et al., (2015), investigated the application of hydroxy sodalite in polyethersulfone (PES-SOD) mixed matrix membrane for AMD treatment. They fabricated PES membranes with different loadings hydroxy sodalite together with pure polymeric membrane for comparison. The results showed that the performance of a pure polymeric membrane (selectivity and flux) is enhanced by loading hydroxy sodalite crystals within the matrix of PES polymer. The results of membrane performance evaluation showed that the 10 wt. % has higher flux whereas, 15 wt. % loading showed highest selectivity towards Pb^{2+} (57.44 % rejection)

4.5. Concluding remarks

Mixed matrix membranes with enhanced mechanical properties and permeability were successfully developed for removal of phenol from synthetic wastewater. There is no significant difference between HSOD and SSOD infused membranes in terms of rejection. However, SSOD infused membrane showed highest permeation flux. The permeability and selectivity for SSOD/PSF membrane is slightly higher than HSOD/PSF membrane. From this study it cannot be safely concluded that SSOD has better performance than HSOD.

Chapter 5: Effect of silica sodalite loading on SOD/PSF membranes during treatment of phenol-containing wastewater.

5.1. Introduction

In Chapter 4 silica sodalite infused membrane has shown slightly higher performance in terms of flux and rejections as compared to hydroxy sodalite infused membrane. SSOD has been varied to give 5 % wt. and 10 % wt. loadings, this changes the physicochemical properties of the membranes. Furthermore, the performance of the membranes with different silica sodalite loading may differ significantly. It has been observed from previous studies that varying the concentration of nanoparticle in composite membranes affect permeability, selectivity and mechanical properties. In the study conducted by Daramola et al., 2015, it was observed that increasing sodalite concentration in PES matrix resulted in higher selectivity during AMD treatment. However, permeability decreased with increasing sodalite concentration. In another study conducted by Mukherjee and De (2016) it was found that increasing the concentration of CNTs in polysulfone matrix for the removal of toluene, benzene and phenol reached the optimum selectivity at 4 % wt., membranes with CNTs concentration higher than 4 % wt. did not show further improvement in selectivity of the composite membrane (Mukherjee and De, 2016). Therefore, in this chapter silica sodalite infused membrane was further used for investigation of the effect of varying its loading in polysulfone matrix during the treatment of phenol-containing wastewater.

5.2. Materials, methods and treatment of synthetic phenol-containing wastewater

5.2.1. Materials

Polysulfone (in beaded form with a molecular weight of 22,000 g/mol), N,N-dimethylacetoamide (99% or more), Phenol (99% or more molecular weight 94.11g/mol) were purchased from Sigma Aldrich (Merck), South Africa and used as supplied without any further purification. SSOD crystals. The Nitrogen gas was purchased from AFROX, South Africa. The de-ionized water was prepared in the lab at the School of Chemical and Metallurgical Engineering

5.2.2. Method

Phase inversion method was used for the preparation of asymmetric membranes (Gohil and Ray, 2009) as shown in Figure 3.2 below. Silica sodalite nanoparticles were added to 50 mL of N,N-dimethylacetamide in different loadings (5 wt.% and 10 wt.%). The mixture was ultra-sonicated for 15 min and shook for another 15 min. Ten grams of polysulfone was added to the mixture and ultra-sonicated for 15 min thereafter, placed on a magnetic stirrer for 24 h at 400 rpm. The solution was cast on a glass plate with the aid of a casting blade. The cast solution was left under ambient conditions for 10 s and thereafter was fully immersed in distilled water for 24 h. The membrane was dried in an oven at 60 °C for 20 min to remove the solvent.

5.3. Results and discussion of results

Here the results obtained for characterization of membranes are provided and discussed.

5.3.1. Membrane characterization

5.3.1.1. Morphology of fabricated membranes

Figure 5.1 shows SEM images (a) surface morphology of pure polysulfone (0 wt. % SSOD/PSF) membrane which is used for comparison purposes, the surface is highly porous with large visible pores. Figure 5.1 (b) presents cross-section image shows the asymmetric nature of PSF, whereby the top is thin and dense whereas pores at the bottom are larger (Singh et al., 2014). The incorporation of nano- particles in polysulfone matrix results in structural changes of the membrane surface. Figure 5.1 (c) depicts PSF loaded with 5 wt. % SSOD, fewer pores can be observed when compared with pure PSF membrane. This is caused by blocking of pores in composite membranes at increased concentration. Figure 5.1 (d) depicts the cross section of 5 wt. % SSOD/PSF, the typical plate-like shapes as reported by Koike et al., (2017) were visible on the cross-section. Figure 5.1 (e) depicts 10 wt. %SSOD/PSF as the silica sodalite loading was increased from 5 wt. % to 10 wt.% membrane pores decrease since fewer pores could be observed on the membrane surface. This is due the suppression of micro- void formation at high percentage loading of nanoparticles within the polymer matrix (Unuigbe, et al, 2019). The membrane becomes denser at higher concentration of nanoparticles this agrees with the reported literature (Mukherjee and De, 2016). Figure 5.1 (f) shows the cross-section of 10 wt. % SSOD/PSF membrane, the membrane pores on the cross-section are

blocked by the plate- like shapes which are attributable to the silica sodalite loaded on the polysulfone matrix. Furthermore, in comparison with the with cross-section of the 5 wt. % SSOD/PSF, the 10 wt. % SSOD/PSF show more plate-like shapes as expected since it was loaded with higher concentration of SSOD.

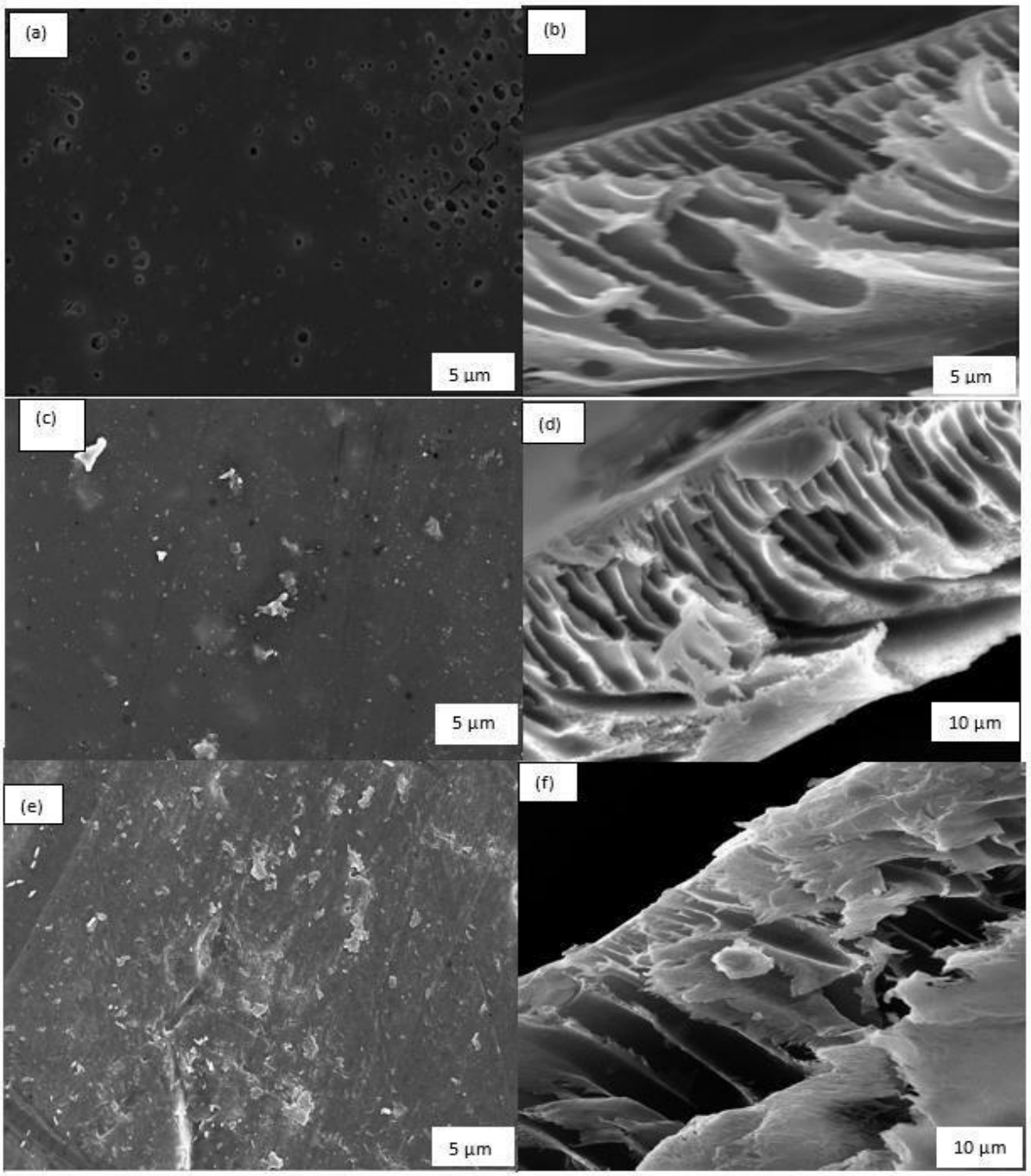

Figure 5. 1: SEM images (a) and (b) depicts surface and cross-section of 0 wt.% SSOD/PSF, (c) and (d) depicts surface and cross-section of 5 wt.% SSOD/PSF and (e) and (f) depicts surface and cross- section of 10 wt.% SSOD/PSF, respectively

5.3.1.2. Surface properties of sodalite crystals and membranes via FT-IR and AFM analysis

The FT-IR spectra were used to analyze the functional groups. Figure 5.2 depicts the FT-IR spectra of pure polysulfone membranes together with 5 % wt. and 10 % wt. SSOD loaded PSF matrix. As comparison with pure polysulfone the composite membrane (5 % wt. SSOD/PSF) doesn't show any change on the FTIR spectra, increasing nanoparticles loading to 10 wt.% also does not have effect on the spectra. The peaks present on the spectra are assignable to pure polysulfone membrane. The peak at $1105cm^{-1}$ belongs to a saturated C-C single bond. The $1151cm^{-1}$peak confirms the presence the stretch symmetric $C-SO_2-C$ group (Singh et al., 2006). The sharp and strong peak at $1242cm^{-1}$is due to the presence of a stretching ether (C-O-C) group. A medium peak at $1488cm^{-1}$ corresponds to the vibrational stretch of CH_3-C-CH_3 bond. Two peaks at $1506\ cm^{-1}$ and $1587cm^{-1}$ shows a stretch of C=C bond in the aromatic ring this is consistent with the literature (Singh et al., 2006: Gohil and Ray, 2009).

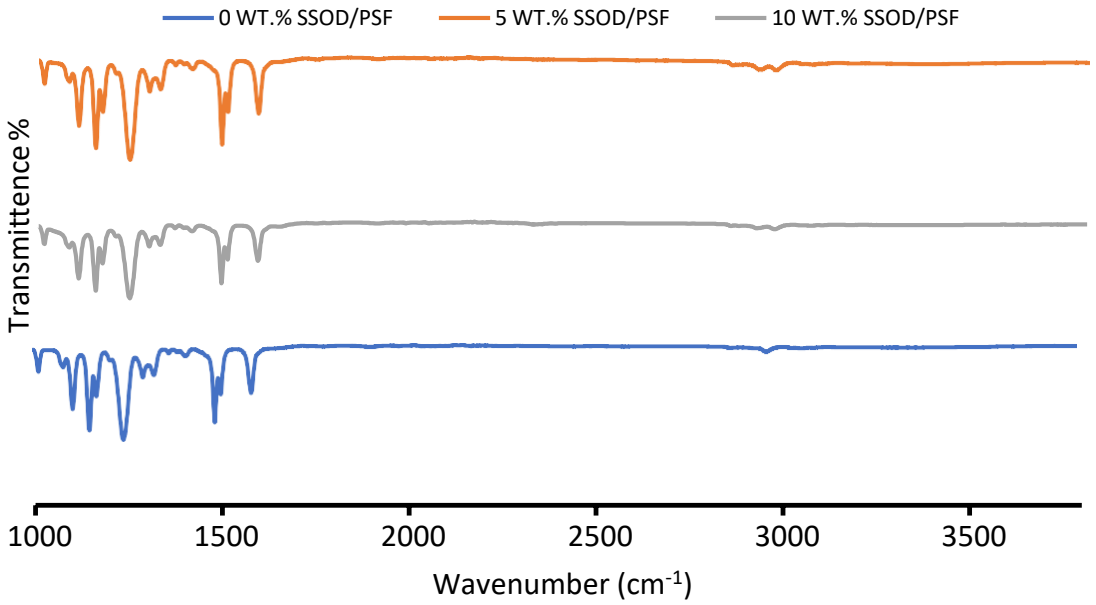

Figure 5.2: FTIR spectra for the fabricated membranes

5.3.1.3 Surface roughness of fabricated membranes

The surface roughness was measured using AFM. Figure 5.3 shows 3D AFM images together with roughness values. The roughness measurements are used to evaluate surface properties of the membranes, When roughness is high adhesive forces on the membrane surface become larger (Bowen et al.,1998). The adhesive forces are responsible for adhesion of particles on the membrane surface. This makes rougher membranes highly susceptible to fouling (Caglayan, 2014). The 0 Wt. % SSOD/PSF membrane has shown the highest average roughness (Ra) 163.86 nm and rootmean square roughness (Rms) 130.58 nm. This could be attributed to the hydrophobic nature of pure polysulfone. The decrease in roughness has been observed during the incorporation of nanoparticles. However, 10 wt. % loading show higher surface roughness than 5 wt. % loaded PSF. This may be due to slow exchange rate between solvent and polysulfone during phase inversion. The process causes membrane nodules, which results in rougher surface (Mukherjee and De, 2016)

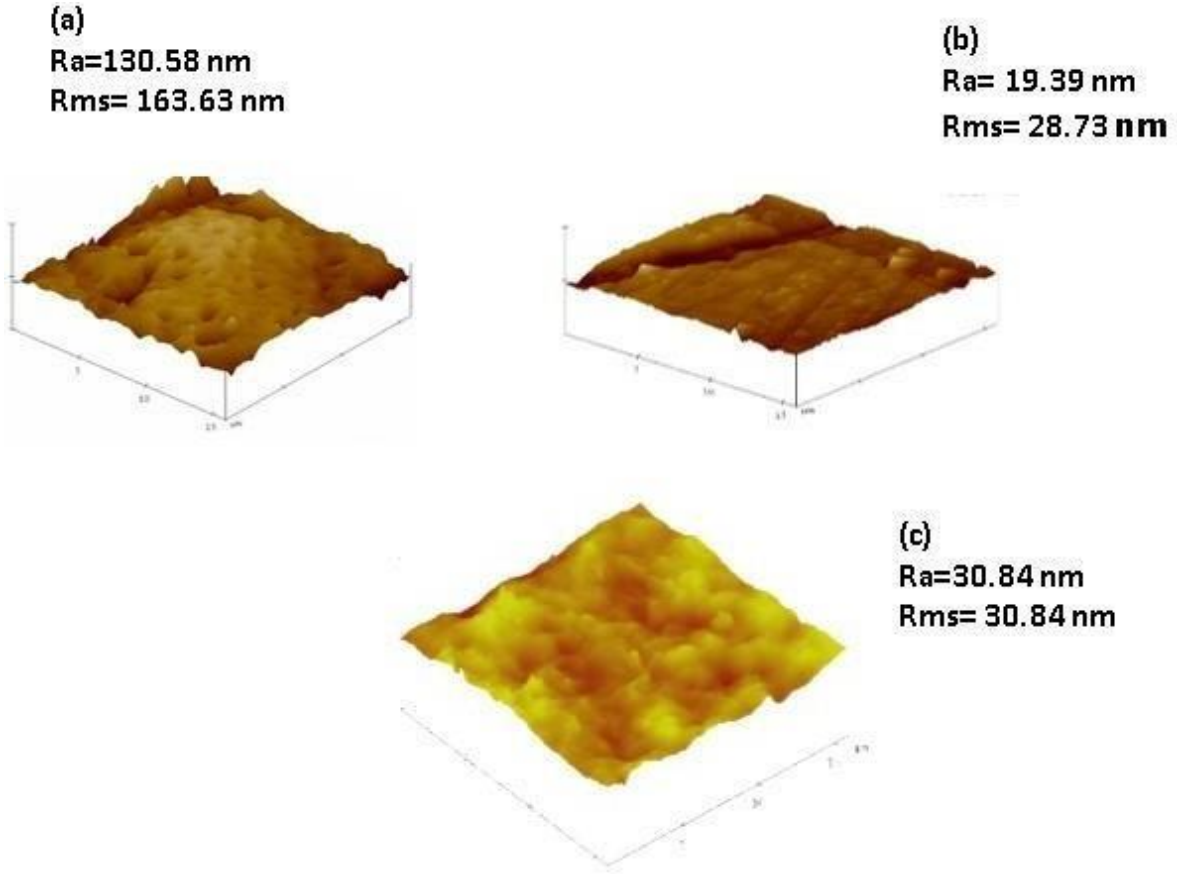

Figure 5.3: AFM images together with surface roughness values (a) 0 wt. % SSOD/PSF, (b) 5 wt. % SSOD/PSF and 10 wt. % SSOD/PSF

5.3.1.3. Hydrophilicity check via contact angle

14

The wettability of the membranes was determined through contact angle measurements, this is the angle a liquid creates when it is in contact with solid (Dwivedi et al., 2014). Figure 5.4 show contact angle measurements taken in order to investigate the hydrophilicity or hydrophobicity of the membranes (Emadzadeh et al., 2019). The wetting tendency becomes significant when the contact angle is smaller, hence the affinity between the liquid (water) and solid (membrane) becomes higher. The pure polysulfone showed the highest contact angle (83.81°) of all the membranes this is attributed to the hydrophobic nature of the membrane (Van der Bruggen et al., 2009). The incorporation of 5 wt. % SSOD nanoparticles in polysulfone matrix resulted in a decrease to 80.94° contact angle, this shows hydrophilic enhancement. Furthermore, the increase in SSOD loading to 10wt. % further enhanced the hydrophilicity of the membrane since contact angle decreased to 76.68°

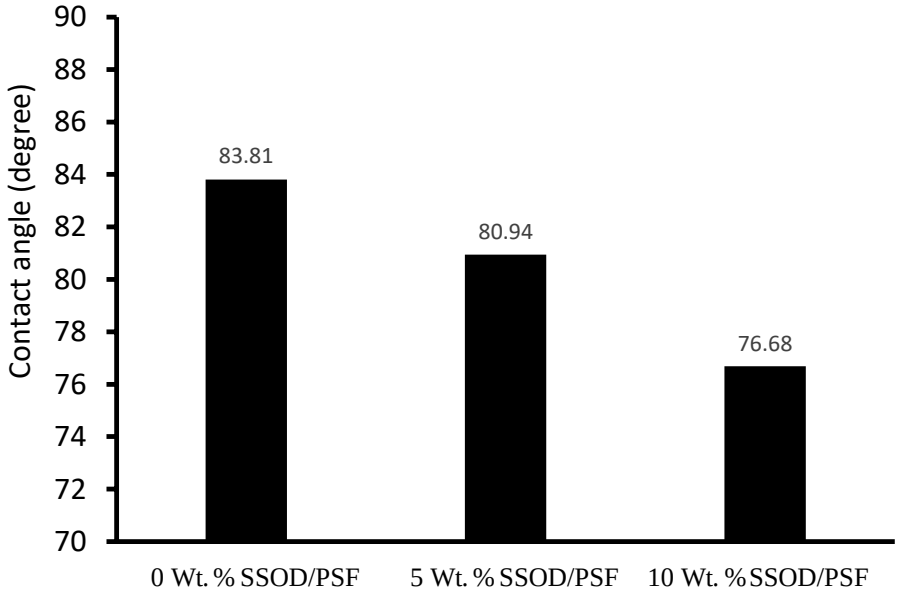

Figure 5.4: Contact angle measurements

5.3.1.4. Mechanical Properties of fabricated membranes

Figure 5.5 (a) shows Young's modulus which represent the ability of the membranes to resist elastic deformation. Figure 5.5 (b) presents Ultimate tensile strength (UTS) results which shows the largest force that fabricated membranes could withstand before breaking apart (Emadzadeh et al., 2019). The results were used for evaluation of mechanical strength for membranes with varied concentration of nanoparticles. The Young's modulus and ultimate

tensile strength (UTS) increase with SSOD concentration. The 5 wt. % SSOD/PSF showed increase in both UTS and Young's modulus as compared to the pure PSF membrane. As SSOD concentration was further increased from 5 to 10 wt. % the composite membrane showed increased in mechanical strength. The increase in both UTS and young's modulus confirm enhancement of mechanical strength upon the addition of nano- particles (Daramola, et al., 2015).

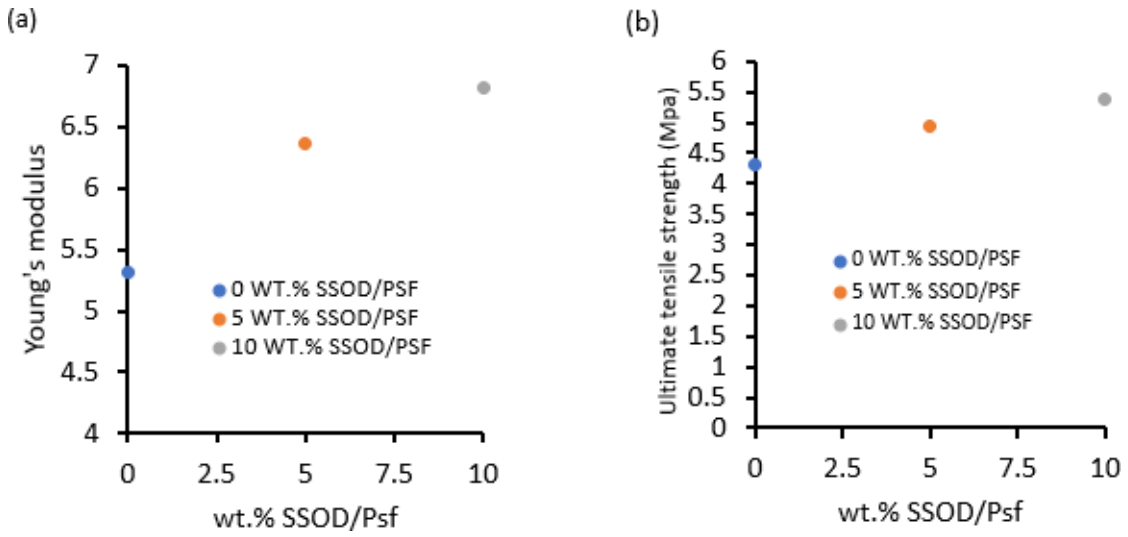

Figure 5.5: Mechanical properties (a) Young's modulus and (b) Ultimate tensile strength

5.4. Performance evaluation of the membranes during treatment ofphenol-containing wastewater

Figure 5.6 shows (a) the pure water flux and (b) the phenol-containing water flux calculated using Equation 3.1 in Chapter 3, for membranes with different SSOD loadings at the varied pressure. It has been observed that composite membranes had the highest permeation flux as compared to pure membrane. The highest flux exhibited by 10 wt. % SSOD/PSF could be linked to hydrophilic surface as revealed by contact angle value. It has been found in previous studies that hydrophilic membranes are resistant to fouling and therefore generally have higher permeate flux (Chunjin et al., 2008; Maphutha et al 2013). The pure water flux for all the membranes is higher than phenol-containing water flux, this is due to competitive sorption between phenol and water molecules (Daramola et al., 2019). Increasing pressure for both

Figure 5.6 (a) and (b) resulted in higher permeation flux since pressure is the driving force for permeation (Daramola et al., 2019).

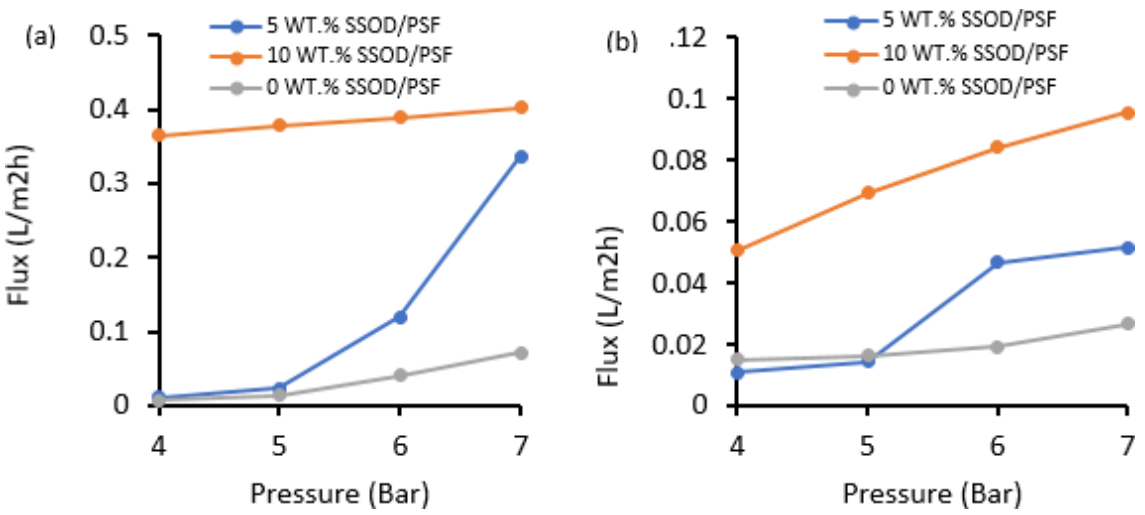

Figure 5.6: (a) pure water flux and (b) phenol containing flux

Figure 5.7 depicts the rejection performance of the membranes which were calculated using Equation 3.2. in Chapter 3. Pure polysulfone showed the highest rejection at 4 Bar compared to the composite membranes. However, the SSOD infused membranes show increase in rejection with an increase in the SSOD concentration. This is attributable to the

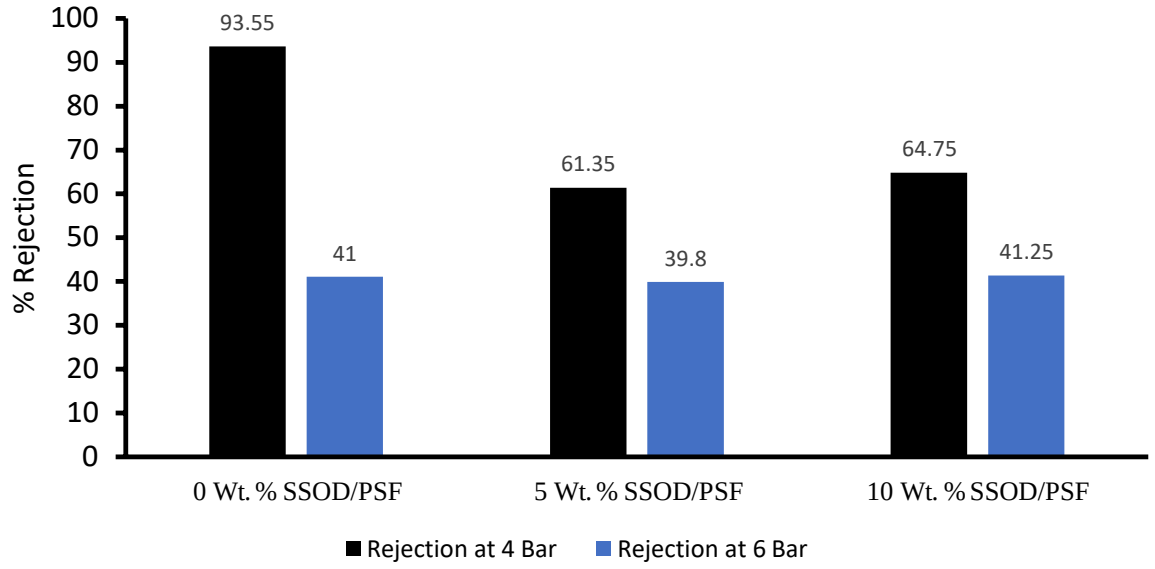

Figure 5.7: Phenol rejection of membranes at different pressure

5.5. Concluding remarks

Increasing the concentration of nanoparticles in a polymer of mixed matrix membrane in this study has enhanced; the hydrophilicity of the membrane, mechanical strength and permeation flux. The increased concentration of nanoparticles in the polymer matrix reduced the porosity of the membranes as depicted via SEM images. Nonetheless, the permeation flux was increased with increasing nanoparticles concentration implying that nanoparticles cause stronger attraction of water molecules.

Chapter 6: Effect of coating SOD/PSF and HSOD/PSF with PVA layer on performance evaluation of during treatment of phenol-containing wastewater

6.1. Introduction

Fouling and concentration polarization are the drawback when using polysulfone membranes for wastewater treatment. The two phenomena can be addressed using polyvinyl alcohol (PVA) coating on the top layer of the polysulfone membrane. PVA is a water-soluble biodegradable polymer and a good candidate for improving the hydrophilicity of polymeric membrane e.g polysufone membrane, such that the overall material becomes more hydrophilic and thus enhance anti-fouling property (Van der Bruggen, 2008; Maphutha et al., 2013). When polysulfone is coated with PVA and comes into contact with water, it creates stronger affinity for water molecules, this can significantly reduce fouling and concentration polarization (Qin et al., 2015). PVA also enhances mechanical and chemical properties of the membranes (Jayakumar et al., 2011).

In some studies, PVA has been proven to enhance the membrane selectivity and permeabilty (Huang and Rhim, 1993; Gimenez et al., 1996). The PVA that is cross-linked with maleic acid becomes quite stable in different polar and nonpolar solvents (Zulkifli et al., 2013). Therefore, in this chapter composite membranes; SSOD/PSF and HSOD/PSF are coated with PVA. For reference purposes, pure polysulfone was also coated with PVA.

6.2. Materials, methods and treatment of synthetic phenol-containing wastewater

6.2.1. Materials

polysulfone (in beaded form with a molecular weight of 22,000 g/mol), N,N-dimethylacetoamide (99 % or more), polyvinyl alcohol (99 % or more, 44.05 g/mol), Maleic acid (MA) (Reagent plus, R; 99% or more, molecular weight 116.07 g/mol), Phenol (99% or more molecular weight 94.11 g/mol) were purchased from Sigma Aldrich (Merck), South Africa and used as supplied without any further purification. The Nitrogen gas was puchased

from AFROX, South Africa. The de-ionized water was prepared in the lab at the School of Chemical and Metallurgical Engineering.

6.2.2. Methods

The SSOD/PSF and HSOD/PSF composite membranes were prepared via phase inversion as described in Chapter 3. Thereafter, 1 % wt. polyvinyl alcohol (PVA) solution was poured over the silica sodalite/PSF membrane and was kept in contact for 3 min. After which, the excess solution was drained off. Maleic acid (1 Wt. %), which acts as the cross-linker solution was poured on the PVA layer and kept in contact for 3 min (to allow enough time for cross-linking) and later drained off. The membrane was then dried in an oven at 60 °C for 20 min.

6.3. Results and discussion of results

The results obtained from membrane fabrication and characterizations are provided and discussed here.

6.3.1. Membrane fabrication and characterization

6.3.1.1. Morphology of fabricated membranes

Figure 6.1 (a) depicts SEM images of pure polysulfone membrane (0 wt. % SSOD/PSF), the surface shows the presence of pores. Figure 6.1 (b) shows pure polysulfone membrane coated with PVA (0 wt. % SSOD/PSF/PVA) the surface show no visible pores this is due to hydrophilic layer PVA that covers the membrane pores, this is consistent with the work reported by Maphutha et al., (2013). Figure 6.1 (c) and (d) depicts the surface morphology of composite membranes 10 wt. % HSOD/PSF/PVA and 10 wt. % SSOD/PSF/PVA, respectively. The surface for both composite membranes show very few tiny pores this is due to PVA that covers the membrane surface. The observation is also consistent with the reported by Maphutha et al. (2013). The addition of PVA resulted in changes of the surface structure from wider pores to almost no pores.

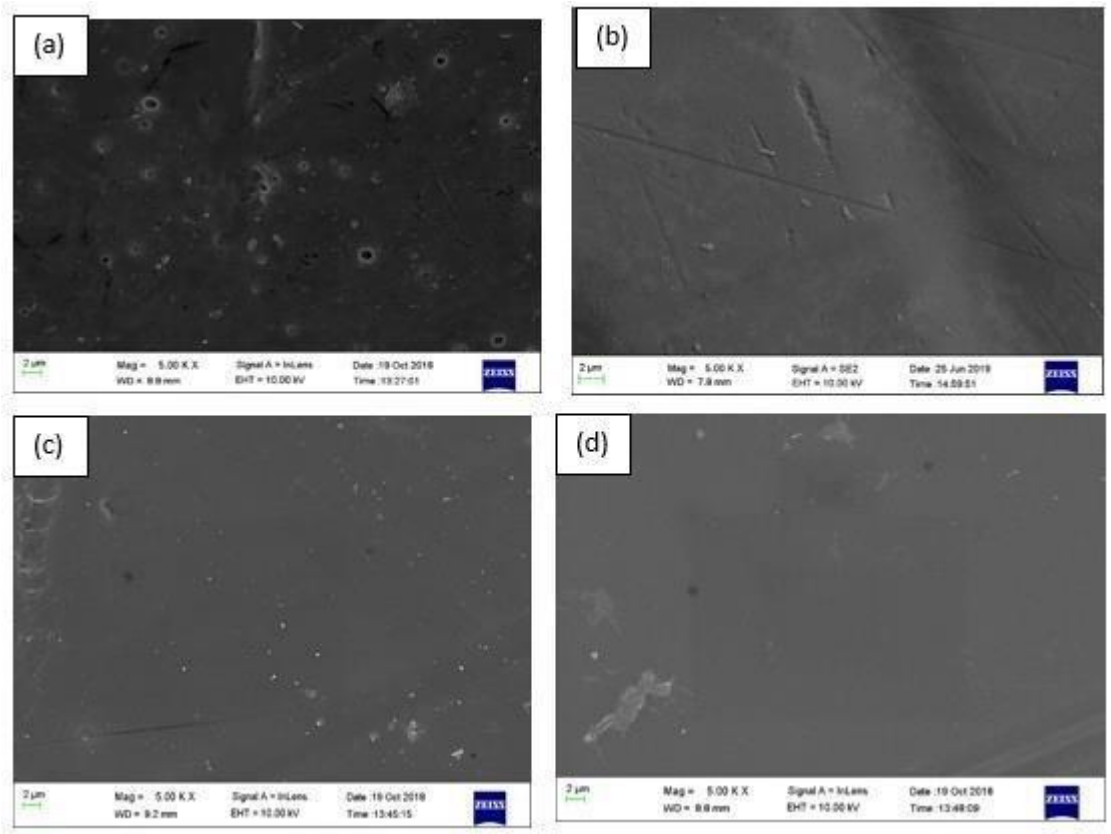

Figure 6.1: SEM images of the fabricated membranes showing surface of (a) 0 wt. % SSOD/PSF, (b) 0 wt. % SSOD/PSF/PVA, (c) 10 wt. % HSOD/PSF/PVA and (d) 10 wt. % SSOD/PVA

Figure 6.2a and (b) depicts cross-section of the membranes, pure polysulfone and polysufone coated with PVA, respectively. The cross-section for both membranes show similar structural formation whereby the asymmetric nature of the membrane is observed with thin dense structure on top and large pores at the bottom. Figure 6.2c depicts the cross-section of the 10 wt. % HSOD/PSF/PVA. The typical thread ball-like shapes are clearly visible on the sponge-like polysulfone. The thread ball-like shapes reaffirms the successful embedment of HSOD nanoparticles in polysulfone membrane (Hums, 2017). The cross-section of 10 wt. % SSOD/PSF/PVA as depicted by Figure 6.2 (d) show the spongy-like polysulfone and the presence of plate-like shapes typical for silica sodalite synthesized in a topotactic conversion manner as reported by Koike et al. (2017). It is noteworthy to mention that the image of the cross-section is not affected by the PVA layer since PVA layer is added on the surface of the membranes.

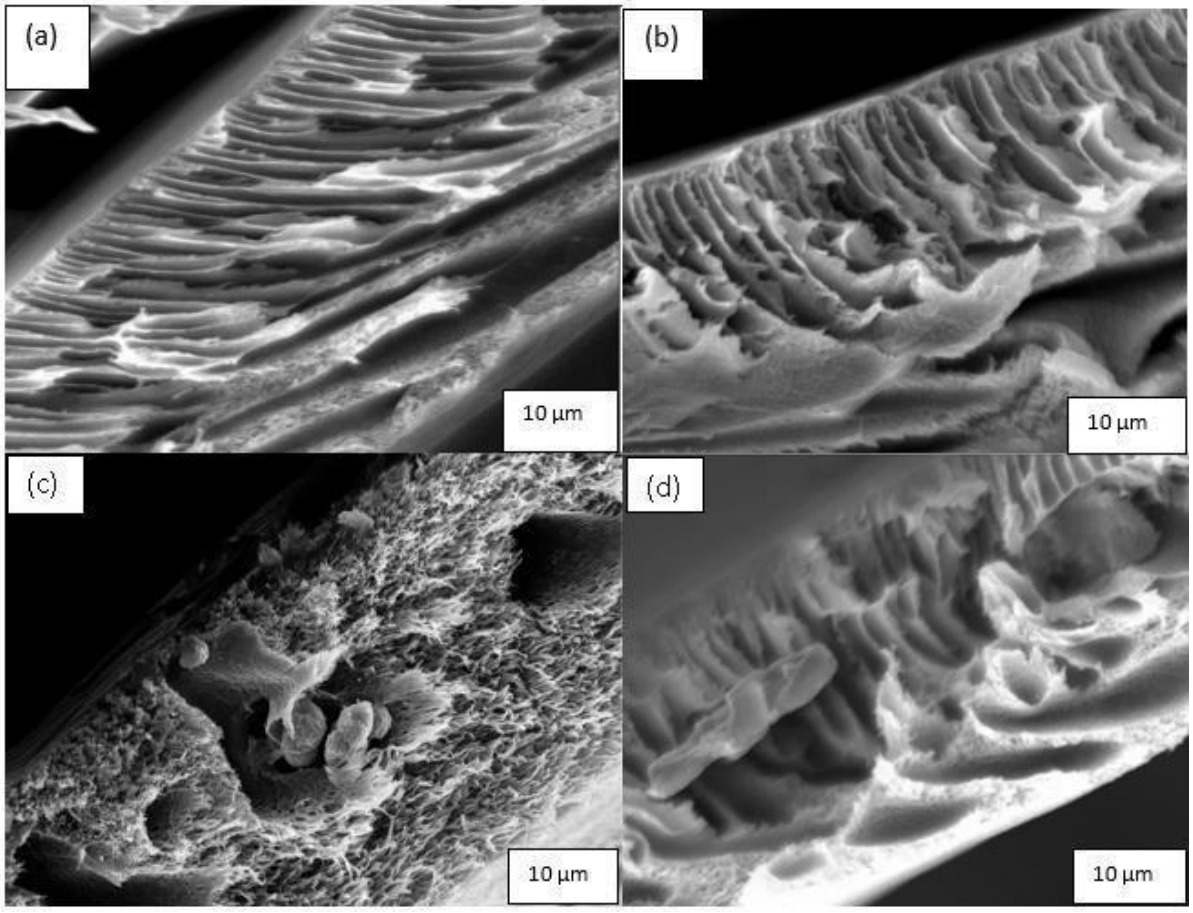

Figure 6.2: SEM images showing cross-section of (a) 0 wt.% SSOD/PSF, (b) 0 wt.% SSOD/PSF/PVA, 10 wt.% HSOD/PSF/PVA and (d) 10 wt.% SSOD/PVA

6.3.1.2. Surface properties of membranes via FT-IR and AFM analysis

FT-IR analysis

Figure 6.3 show the FTIR spectra of the polysulfone together with composite membranes coated with PVA. It was observed that PSF membranes coated with PVA show additional peak at approximately 3400 cm^{-1} this confirms successful insertion of hydrophilic group (-OH) to make the overall membrane hydrophilic. The hydrophilic membranes are less prone to fouling (Maphutha et al 2013; Kumar et al., 2016). The other peaks present in the spectra are assignable to polysulfone membrane this is consistent with the literature (Singh et al., 2006; Gohil and Ray, 2009).

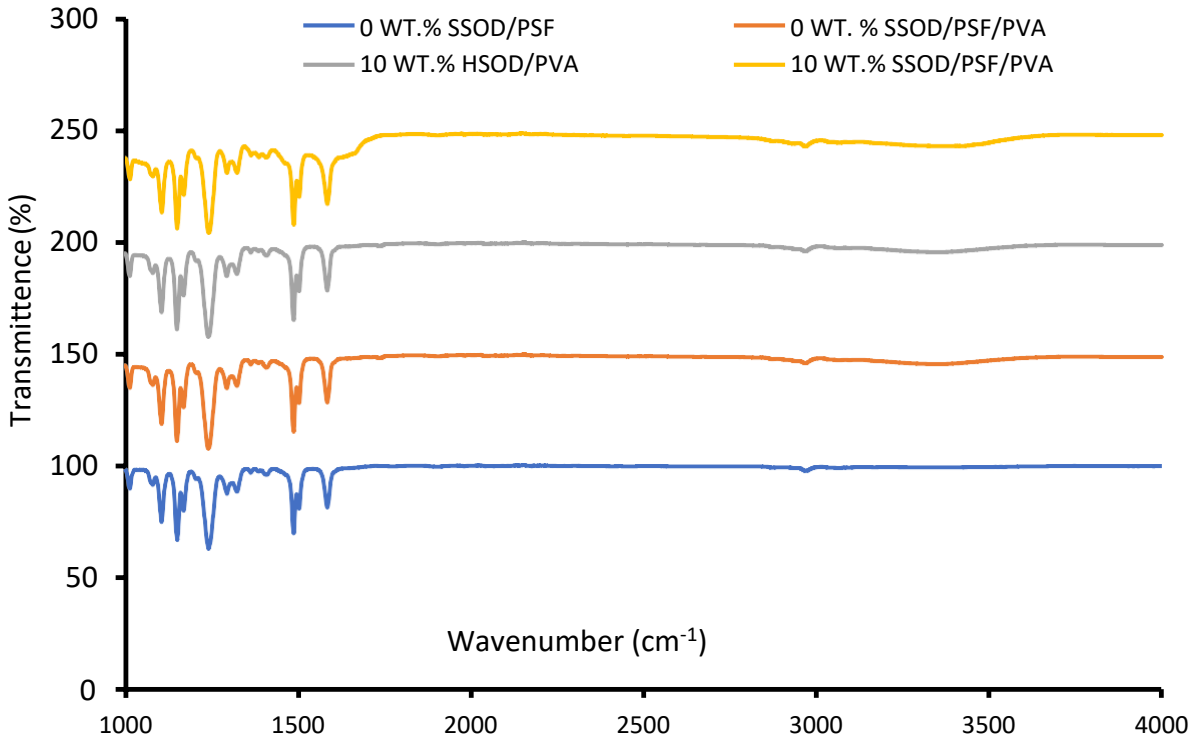

Figure 6. 3: FTIR Spectra of the fabricated membranes

AFM analysis

The surface roughness of the membranes was evaluated using AFM. Figure 6.6 depicts the 3D AFM images and roughness values. It was observed that PVA coating cause a decrease in roughness of membrane with respect to the uncoated membrane. The composite membranes coated with PVA showed the highest decrease in roughgness values. The 10 wt. % SSOD/PSF/PVA membrane showed 83.24 % and 83.35 % decrease in Ra and Rms, respectively as compared to the pure polysulfone. The composite membranes coated with PVA may be less prone to fouling since lower roughness values induces low adhesive forces on the membrane and thus less adhesion of particles on the membrane surface (Bowen et al.,1998; Caglayan, 2014).

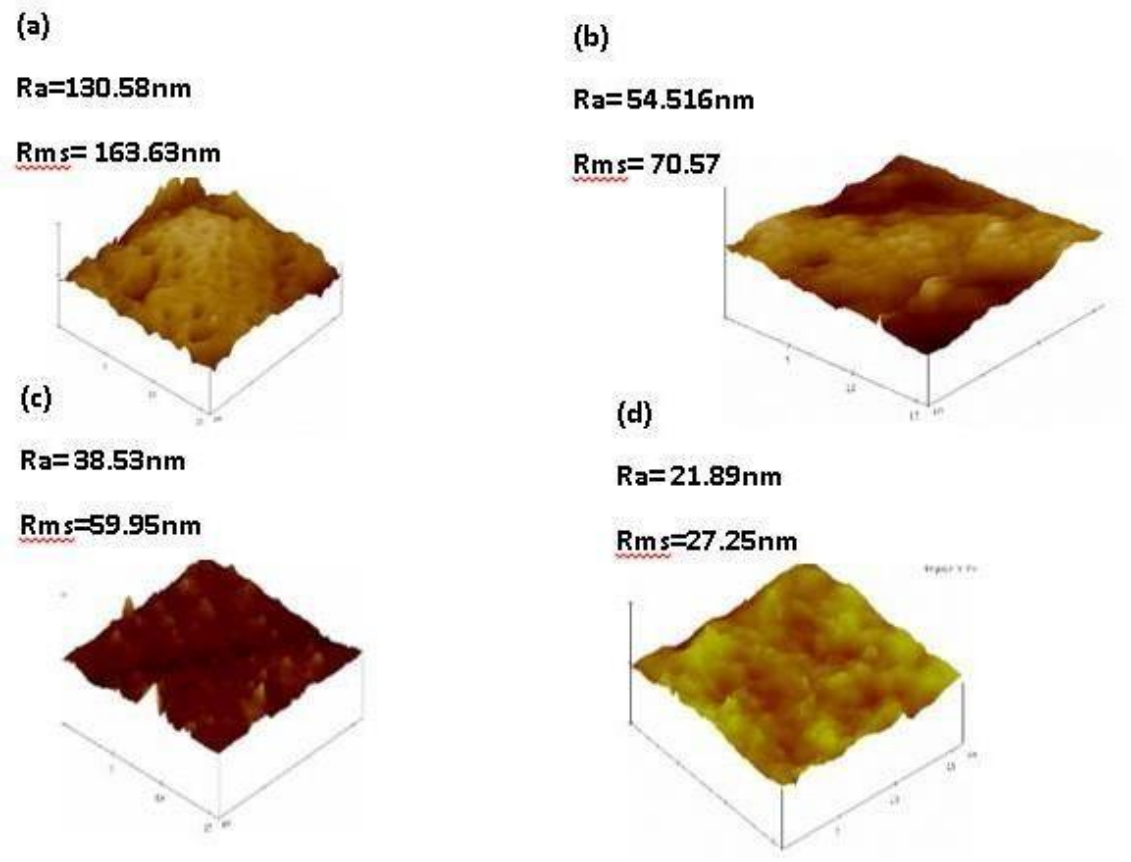

Figure 6.4: AFM 3D images together with roughness values of pure polysulfone, polysulfone and composite membranes coated with PVA (a) 0 wt.% SSOD/PSF, (b) 0 wt.% SSOD/PSF/PVA, (c) 10 wt .% HSOD/PSF/PVA and (d) 10 wt. % SSOD/PSF/PVA.

6.3.1.3. Evaluation of surface hydrophilicity analysis of fabricated the membranes

The contact angle values were used to evaluate the surface hydrophilicity of the fabricated membranes. Coating membrane surface with PVA layer resulted in a decrease in contact angle, this is due to the hydroxyl group in PVA which enhances the hydrophilicity of the overall membrane (Maphutha et al., 2013). The decrease in contact angle indicates hydrophilic enhancement, thus anti-fouling property of the membrane is enhanced. It was noticed that coating 10 wt. % HSOD/PSF and 10 wt. % SSOD/PSF with PVA reduced contact angles from 78.91° and 76.68° (uncoated) to 69.28° and 57.47°, respectively. This depicts significant hydrophilic enhancement when compared with 88.81° of the pure PSF.

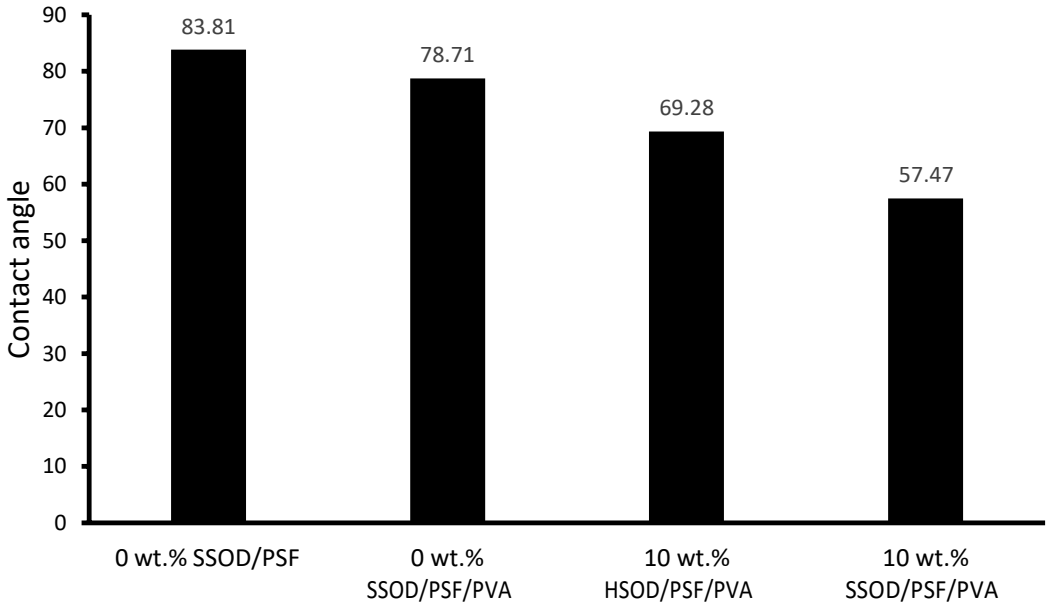

Figure 6.5: Contact angle of the fabricated membranes

6.3.1.4. Mechanical Properties of fabricated membranes

The mechanical strength of the membranes was evaluated using texture analyzer. The mechanical strength indicated by ultimate tensile strength and Young's modulus measurements from the synthesized membranes are shown in Figure 6.7 (a) and (b). Increase in both UTS and Young's modulus was observed when pure polysulfone membrane (0 wt. % SSOD/PSF) was coated with PVA. The 10 wt. % SSOD/PSF/PVA membrane showed the highest mechanical enhancement with 81.53 % and 56.14 % increase in UTS and Young's modulus, respectively compared to pure PSF. The increase in both UTS and young's modulus confirm enhancement of mechanical strength upon coating with PVA (Daramola et al., 2015).

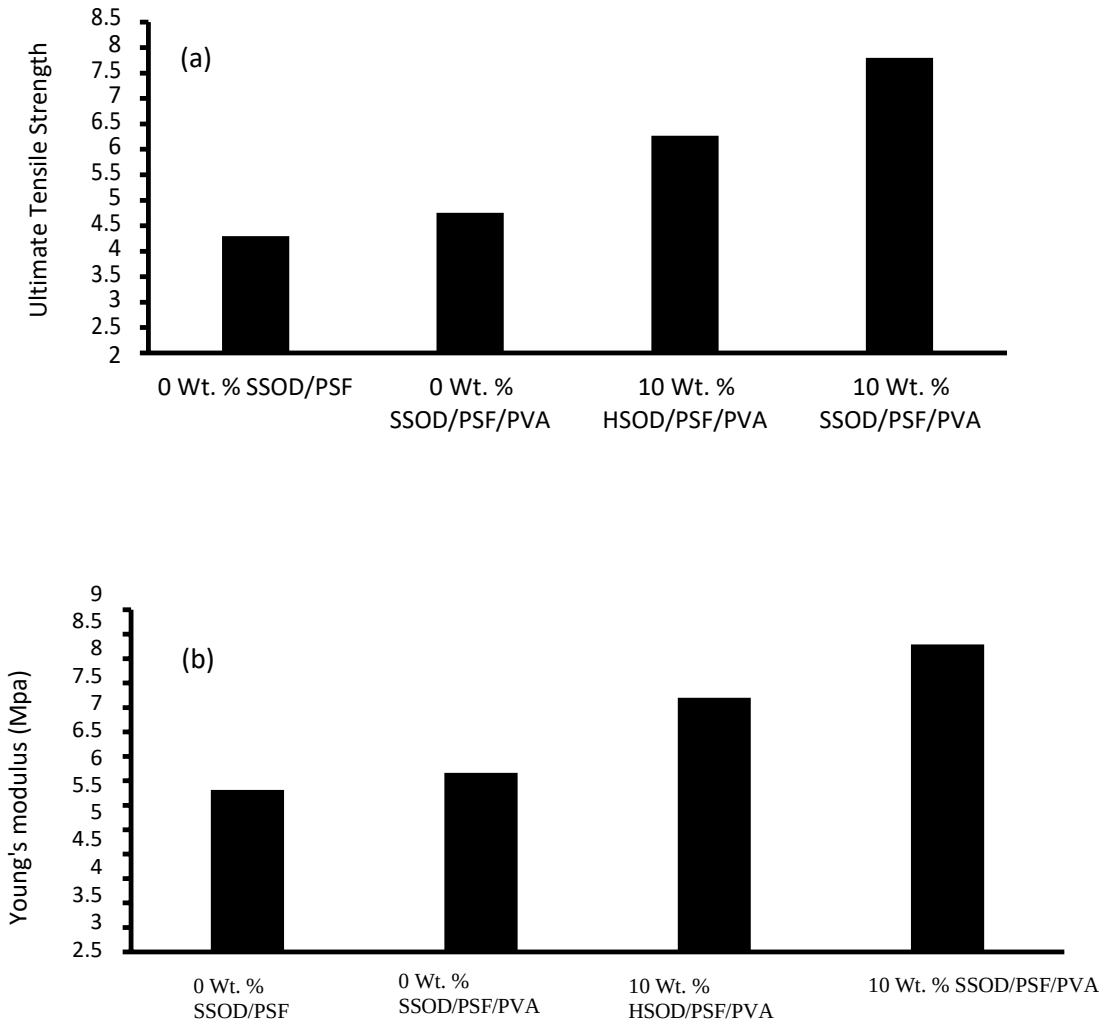

Figure 6.6: Mechanical strength (a) UTS and (b) Young's modulus

6.4. Performance evaluation of the membranes during treatment of phenol-containing wastewater

During water purification the deionized water was used as pure water. Pure water flux was used to determine the original flux of the membrane for fouling monitoring (Daramola and Adeogun, 2011). The permeate flux for pure water and phenol-containing in this study were evaluated using the dead-end filtration cell at pressure varied from 4 to 7 bar. Membrane flux was calculated using Equation 3.1. The pure water flux for all membranes is relatively higher than phenol-containing wastewater flux. The decline in flux during the treatment of phenol-containing wastewater indicates fouling and competitive sorption between the components and water (Daramola et al., 2019). In the case of pure water flux membrane resistance depend only on the pore structures of the membrane (Kumar, 2017). Pressure increment leads to higher

permeation flux, resulting in the higher permeation flux for both pure water and phenol-containing wastewater. The composite membranes namely, 10wt. % HSOD/PSF and 10 wt.

% SSOD/PSF coated with PVA showed the highest permeation flux. This is attributed to the hydrophilicity of PVA coated on the membrane (Maphutha et al., 2013) and incorporation of hydrophilic nanoparticles (Wang et al., 2012). However, 10 wt. % SSOD/PSF/PVA showed higher flux than 10wt. % SSOD/PSF/PVA, this is attributable to the accessible pores in SSOD as compared the HSOD which is formed with occluded matter on the pores (Daramola et al., 2016: Moteki et al., 2011). The results showed that pure polysulfone flux was improved from 0.07142 $Lm^{-2}h^{-1}$ to 0.625 $Lm^{-2}h^{-1}$ compared with 10 wt. % SSOD/PSF/PVA membrane phenol-containing wastewater. The 10 wt. % SSOD/PSF/PVA membrane also appeared to be the most hydrophilic membrane as confirmed by lower contact angle measurements.

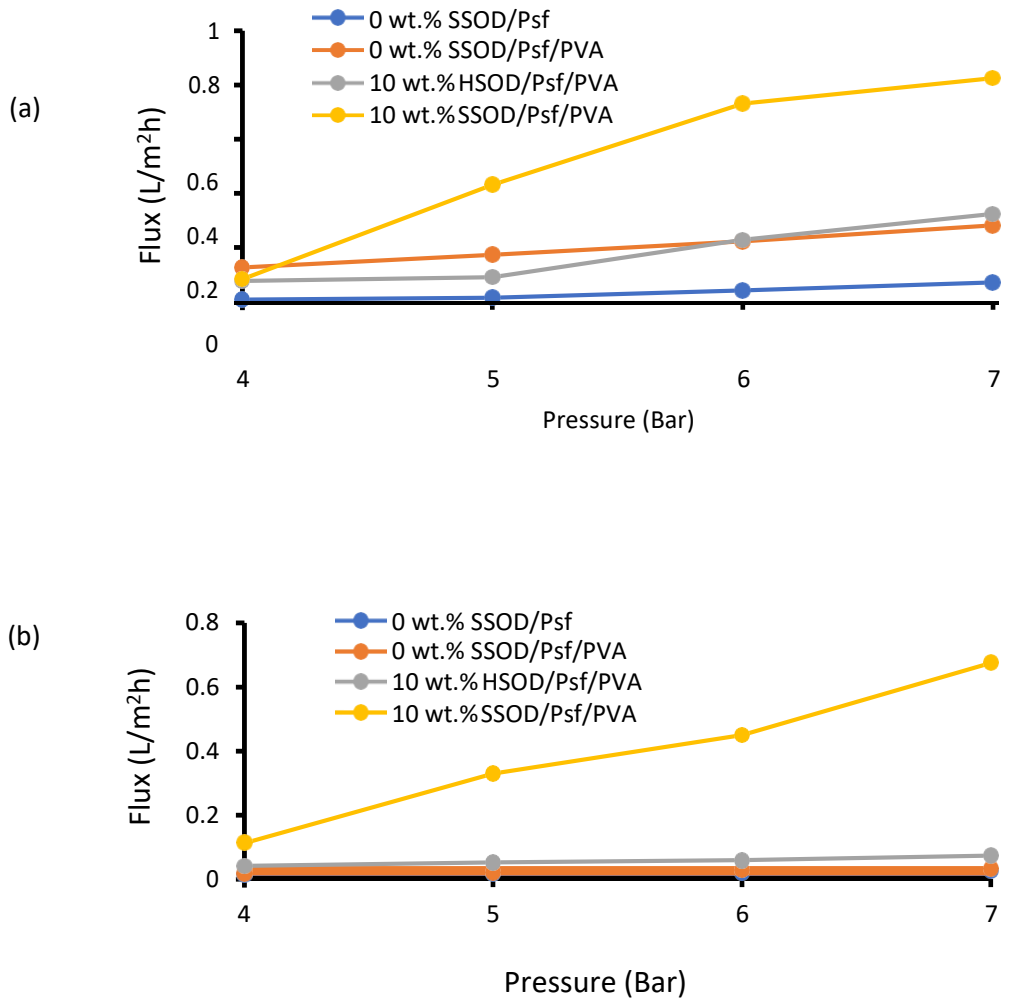

Figure 6.7: Membrane flux (a) pure water and phenol containing water

Pure PSF exhibited highest phenol rejection of 93.55 % at 4 bar this could be attributed to slightly thicker or more concentrated polymer (Kumar et al., 2017). However, when pressure was increased to 6 bar there was a significant decrease in rejection to 41 %, this may be due to the opening of pores at higher pressure. All membranes coated with PVA showed lower phenol rejections, the 10 wt. % SSOD/PSF/PVA showed lowest phenol rejections of 27.9 % and 18.05 % at 4 and 6 Bar, respectively. The phenol rejection for all the membranes decreased with increased pressure, this could be attributed to high pressure which is above the capillary pressure of the membrane that prevents the phenol from permeating, resulting in forceful permeation of phenol through the pores (Daramola et al., 2019). The lower rejection is attributable to phenol strong hydrogen bonding attraction with hydroxyl functional groups found in PVA coated membranes (Hidalgo et al., 2010). The PVA coated membranes have strong affinity towards phenol and

higher sorption capacity resulting in a very low rejection as compared to pure polysulfone (Ahmad and Tan, 2004: Xiao et al., 2017). The PVA membranes affinity towards phenol is greater than the affinity towards water, hence poor rejection (Xiao et al., 2017).

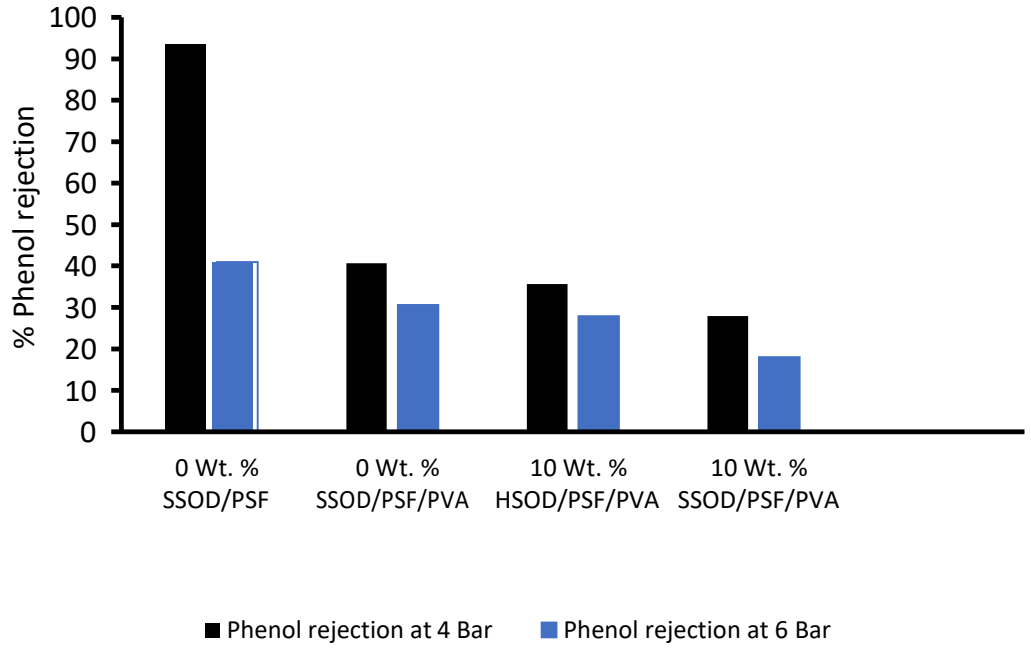

Figure 6.8: *Phenol rejection of membranes at different pressures*

6.5. Concluding remarks

The hydrophilic layer PVA, coated on the membranes has shown to enhance the permeability thus anti-fouling property of the membrane, mechanical strength of the polysulfone membrane. However, PVA coated membranes have shown great affinity towards phenol moleculeswhich resulted in poor phenol rejection. It could be concluded that there exists a trade-off between permeability and selectivity on the PVA coated membranes.

Chapter 7: General conclusions and recommendations

7.1. Conclusions

Based on the objectives highlighted Chapter 1 of this dissertation, the following studies have been carried out and reported:

- Silica sodalite nano-particles were successfully synthesized through topotactic conversion and blended in polysulfone matrix.
- The hydrophilicity and mechanical strength of pure polysulfone were enhanced with loading of SSOD, increasing loading from 5 wt. % to 10 wt. % further enhanced both hydrophilicity and mechanical strength of pure polysulfone.
- Coating the fabricated membranes with PVA layer resulted in enhanced hydrophilicity of the pure polysufone and composite membranes.
- The fabricated membranes were evaluated for the removal of phenol from wastewater. Results showed that pure PSF flux was improved from 0.07142 Lm^2h^{-1} to 0.625 Lm^2h^{-1} with 10% wt. SSOD/PSF/PVA membrane phenol-containing wastewater. Pure PSF membrane performed well rejecting 93.55 % phenol at 4 Bar. However, the 10 Wt. % SSOD/PSF/PVA, 0 Wt. % SSOD/PSF/PVA, and 10 Wt. % HSOD/PSF/PVA all coated with PVA displayed lower rejection of 27.9 %, 40.65 % and 35.6 %, respectively.
- The 10 wt. % SSOD/PSF membrane performed relatively well with 64.75 % rejection compared to 27.9 % achieved with 10 wt. % SSOD/PSF/PVA.
- Therefore, a novel mixed matrix membrane with enhance mechanical properties and anti-fouling property was successfully developed for removal of phenol from industrial wastewater.

7.2. Recommendations

- The concentration of polysulfone used in this study was kept at 20 wt. %, this resulted in lower permeation flux, and in order to achieve higher permeation flux lower polymer concentration should be used in future.
- The cross-sectional morphology of the polymer matrices incorporated with HSOD and SSOD nanoparticles depicts agglomeration of the particles. It is advisable that in future functionalization of nanoparticles be done to enhance the dispersion of nanoparticles.

- Degassing a casting solution is an alternative way other than sonication to get rid of air bubbles completely before casting a membrane. Air bubbles in a casting solution cause defects on the membrane so a careful removal of the air bubbles after stirring the solution is required. It is recommended that in future studies the stirred solution should be allowed to chill in a vacuum desiccator overnight before casting.
- Membranes used in this study were susceptible to breaking during performance evaluation at high pressure such 6 to 7 Bar. To alleviate this in future, membranes should be cast on a nonwoven membrane support such as polyethylene terephthalate (PET). The support enhances the mechanical strength of the membranes for operation at very high pressure.
- The future studies should consider using cross-flow filtration mode to check the stability of the membranes during the performance evaluation. In addition, cross-flow filtration mode is less prone to fouling due to shear rates of the passing flow, hence improved permeation flux is expected (Haldenwang et al., 2019).

References

Abadi S.R.H., Sebzari M.R., Hemati M., Rekabdar F., Mohammadi T. (2010). Ceramic performance in microfiltration of oily wastewater. Desalination, 265, pp.222–228.

Adamsons, K. (2000). Chemical surface characterization and depth profiling of automotive coating systems. Prog Polym Sci:1363-1409

Adeleye, A.S., Conway, J.R., Garner, K., Huang, Y., Su, Y., Keller, A.A., 2016. Engineered nanomaterials for water treatment and remediation: costs, benefits, and applicability. Chem. Eng. J. 286, pp.640–662.

Ahmad, A. and Tan, K. (2004). Reverse osmosis of binary organic solute mixtures in the presence of strong solute-membrane affinity. *Desalination*, 165, pp.193-199

Ahmadiannamini, S., Eswaranandam, P., Wickramasinghe, S and Qian, X. (2017). Mixed-matrix membranes for efficient ammonium removal from wastewaters. *Journal of Membrane Science, 526*, 147-155.

Ahmaruzzaman, M. and Sharma, D. (2005). Jute Fiber Composites from Coal, Super Clean Coal, and Petroleum Vacuum Residue–Modified Phenolic Resin. *Polymer-Plastics Technology and Engineering*, 44(8-9), pp.1607-1629.

Alavi, S. and Thompson, D. (2004). A molecular-dynamics study of structural and physical properties of nitromethane nanoparticles. *The Journal of Chemical Physics*, 120(21), pp.10231-10239.

Altaee, Ali and Al-Rawajfeh, Aiman and Baek, Y.J.. (2010). Application of Vibratory System to Improve the Critical Flux in Submerged Hollow Fiber MF Process. Separation Science and Technology. 45. 28-34.

Armanet, L. and Hunkeler, D. (2006). Phase inversion of polyacrylamide-based inverse-emulsions: Influence of inverting-surfactant type and concentration. *Journal of Applied Polymer Science*, 103(6), pp.3567-3584.

Aroon, M., Ismail, A., Matsuura, T. and Montazer-Rahmati, M. (2010). Performance studies of mixed matrix membranes for gas separation: A review. *Separation and Purification Technology*, 75(3), pp.229-242.

Atadashi, I. (2015). Purification of crude biodiesel using dry washing and membrane technologies. *Alexandria Engineering Journal*, 54(4), pp.1265-1272

Bachman, J., Smith, Z., Li, T., Xu, T., and Long, J. (2016). Enhanced ethylene separation and plasticization resistance in polymer membranes incorporating metal–organic framework nanocrystals. *Nature Materials*, *15*(8), 845-849.

Baker, R. 2012. Membrane technology and applications, Menlo Park, California, John Wiley and Sons.

Baransi, K., Dubowski, Y. and Sabbah, I. (2012). Synergetic effect between photocatalytic degradation and adsorption processes on the removal of phenolic compounds from olive mill wastewater. *Water Research*, 46(3), pp.789-798.

Baumgartinger, J., Strasser, S., Starlinger, R., and Groesswang, R. (2009). Technology review: RFF – membrane free backwash microfiltration. *Filtration and Separation,46* (2), 13-14.

Bergeson, L. (2016). The EPA Proposes Changes to RCRA Hazardous Waste Export and Import Regulations. *Environmental Quality Management*, 25(3), pp.107-109.

Bolong, N., Ismail, A., Salim, M. and Matsuura, T. (2009). A review of the effects of emerging contaminants in wastewater and options for their removal. *Desalination*, 239(1-3), pp.229-246.

Boributh, S., Chanachai, A. and Jiraratananon, R. (2009). Modification of PVDF membrane by chitosan solution for reducing protein fouling. *Journal of Membrane Science*, 342(1-2), pp.97-104.

Bowen, W. R. and Welfoot, J. S. (2002): Modelling the performance of membrane nanofiltration critical assessment and model development, *Chem. Eng. Sci.*, 57, 1121–1137.

Bowen, W. R., Calvo, J. I., Hernández, A. (1995). Steps of membrane blocking in flux decline during protein microfiltration. *Journal Membrane Science*, 101, 153-165

Bowen, W., Lovitt, R., and Wright, C. (2000). Journal search results - Cite This For Me. *Biotechnology Letters*, *22*(11), 893-903.

Bowen, W. R., Welfoot, J. S., and Williams, P. M. (2002: Linearized transport model for nanofiltration: development and assessment, *AIChE J.*, 48, 760–772.

Bowen, W.R., Hilal, N., Lovitt, R.W. and Wright, C.J. 1998, A new technique for membrane characterisation: Direct measurement of the force of adhesion of a single particle using an atomic force microscope. Journal Membrane Science 139: 269-274.

Bruce R. M., Santodonato J. and Neal M. W. (1987). Summary review of the health effects associated with phenol. *Toxicology and Industrial Health* 3, pp. 535–568.

Bubert H, Jenett H (2002) Surface and thin film analysis: Principles, instrumentation, applications. Wiley-VCH Verlag GmbH, Weinheim

Cadotte, J., Forester, R., Kim, M., Petersen, R., and Stocker, T., (1988). Nanofiltration membranes broaden the use of membrane separation technology, *Desalination,* 70, 77–88.

Caglayan, M. (2014). Atomic Force Microscopy as a Characterization Tool for Contact Lenses: Indentation Tests and Grain Analysis. International Journal of Polymeric Materials and Polymeric Biomaterials, 63(13), pp.680-684.

Chakrabarty, B., Ghoshal, A. and Purkait, M. (2010). Ultrafiltration of oil-in-water emulsion: Analysis of fouling mechanism. *Membrane Water Treatment*, 1(4), pp.297-316.

Choi, H. and Spengler, J., 2014. Source attribution of personal exposure to airborne polycyclic aromatic hydrocarbon mixture using concurrent personal, indoor, and outdoor measurements. *Environment International*, 63, pp.173-181.

Cheng, S., Yuan, Z., Leitch, M., Anderson, M. and Xu, C. (2013). Highly efficient de-polymerization of organosolv lignin using a catalytic hydrothermal process and production of phenolic resins/adhesives with the depolymerized lignin as a substitute for phenol at a high substitution ratio. *Industrial Crops and Products*, 44, pp.315-322.

Chinh, V., Hung, L., Di Palma, L., Hanh, V. and Vilardi, G. (2018). Effect of Carbon Nanotubes and Carbon Nanotubes/Gold Nanoparticles Composite on the Photocatalytic Activity of TiO2 and TiO2-SiO2. *Chemical Engineering and Technology*, 42(2), pp.308-315.

Chuang, W.Y., Young, T.H., Chiu, W.Y., Lin, C.Y. (2000). The effect of polymeric additives on the structure and permeability of poly(vinyl alcohol) asymmetric membranes. Polymer, 41, pp. 5633–5641.

Chun, Y., Mulcahy, D., Zou, L. and Kim, I. (2017). A Short Review of Membrane Fouling in Forward Osmosis Processes. *Membranes*, 7(2), p.30.

Chung, T. S., Jian, L. Y., Li, Y. and Kulprathipanja, S. (2007). Mixed matrix membranes (MMMs) comprising organic polymers with dispersed inorganic fillers for gas separation, *Prog. Polym. Sci.*, 32, 483 —507.

Chunjin W. *et al* (2008). Treatment of oily water by a poly(vinyl alcohol) ultrafiltration membrane. Desalination 225, 312–321.

Ciobanu, G., Carja, G. and Ciobanu, O. (2008). Structure of mixed matrix membranes made with SAPO-5 zeolite in polyurethane matrix. *Microporous and Mesoporous Materials*, 115(1-2), pp.61-66.

Conidi, C. and Cassano, A. (2014). Recovery of phenolic compounds from bergamot juice by nanofiltration membranes. *Desalination and Water Treatment*, 56(13), pp.3510-3518.

Dai, Z., Ansaloni, L. and Deng, L. (2016). Recent advances in multi-layer composite polymeric membranes for CO2 separation: A review. *Green Energy and Environment*, 1(2), pp.102-128.

Damjanovica L., Rakic V., Rac V., Stosic D., Aurouxc A. (2010). The investigation of phenol removal from aqueous solutions by zeolite as solid adsorbents. J. Hazard. Mater; 18, pp: 477–484.

Daramola, M. O., Oloye, O., and Yaya, A. (2016). Nanocomposite sodalite/ceramic membrane for pre-combustion CO2 capture: Synthesis and morphological characterization. *International Journal of Coal Science and Technology, 4*(1), 60-66.

Daramola, M., Sadare, O., Oluwasina, O., Iyuke, S. (2019). Synthesis and Application of Functionalized Carbon Nanotube Infused Polymer Membrane (fCNT/PSF/PVA) for Treatment of Phenol-Containing Wastewater. *Journal of Membrane Science and Research*, 5(4), 310-316

Daramola, M., Silinda, B., Masondo, S., and Oluwasina, O. (2015). Polyethersulphone-sodalite (PES-SOD) mixed-matrix membranes: Prospects for acid mine drainage (AMD) treatment. *Journal of the Southern African Institute of Mining and Metallurgy, 115*(12), 1221-1228.

Daramola, M.O.; Adeogun, A.G. (2011). Empirical modelling of chemically enhanced backwash during ultrafiltration process. *Membr. Water Treat. 2*, 225–237.

Donald, D. (1980). Special Report: Standard Practice of Liquid Size-Exclusion Chromatography - SEC (GEL Permeation Chromatography - GPC. *Journal of Liquid Chromatography*, 3(3), pp.465-470.

Dwivedi, M., Harishchandra, R., Koshkina, O., Maskos, M., and Galla, H. (2014). Size Influences the Effect of Hydrophobic Nanoparticles on Lung Surfactant Model Systems. *Biophysical Journal*, *106*(1), 289-298.

Ebnesajjad, S. (2011). *Handbook of adhesives and surface preparation: Technology, applications and manufacturing*. Amsterdam: William Andrew/Elsevier

El-Ashtoukhy ESZ, El-Taweel YA, Abdelwahab O, Nassef EM (2013). Treatment of petrochemical wastewater containing phenolic compounds byelectrocoagulation using a fixed bed electrochemical reactor. Int J Electrochem Sci;8: pp.1534–50.

Elrasheedy, A., Nady, N., Bassyouni, M., and El-Shazly, A. (2019). Metal Organic Framework Based Polymer Mixed Matrix Membranes: Review on Applications in Water Purification. *Membranes, 9*(7), 88.

Emadzadeh, D., Matsuura, T., Ghanbari, M. and Ismail, A. (2019). Hybrid forward osmosis/ultrafiltration membrane bag for water purification. *Desalination*, 468, p.114071.

Engelhardt, G., Felsche, J. and Sieger, P. (1992). The hydrosodalite system Na6+x[SiAlO4]6(OH)x.cntdot.nH2O: formation, phase composition, and de- and rehydration studied by 1H, 23Na, and 29Si MAS-NMR spectroscopy in tandem with thermal analysis, x-ray diffraction, and IR spectroscopy. *Journal of the American Chemical Society*, 114(4), pp.1173-1182.

Fauzan, N., Mannan, H., Nasir, R., Mohshim, D. and Mukhtar, H. (2019). Various Techniques for Preparation of Thin-Film Composite Mixed-Matrix Membranes for CO2 Separation. *Chemical Engineering and Technology*, 42(12), pp.2608-2620.

Feng L, Zhang ZY, Mai ZH, Ma YM, Liu BQ, and Jiang L., 2004. A super-hydrophobic and super-oleophilic coating mesh film for the separation of oil and water. Angewandte Chemie International Edition, 43, pp. 2012-2014.

Gimenez, V., Mantecon, A. and Cadiz, V., 1996, 'Crosslinking of poly (viny1 alcohol) using acid and its application to the separation of acetic acid-water mixtures by the pervaporation technique', Polymer International 30, 129-135.

Gohil, J. M. and Ray, P. (2009). Polyvinyl alcohol as the barrier layer in thin film composite nanofiltration membranes: Preparation, characterization, and performance evaluation. J. Colloid Interface Sci. 338, 121–127

Goosen, M., Sablani, S., AlHinai, H., Al Obeidani, S., Al Belushi, R. and Jackson, D. (2005). Fouling of Reverse Osmosis and Ultrafiltration Membranes: A Critical Review. Separation Science and Technology, 39(10), pp.2261-2297.

Gordano, A and Buonomenna, M.G. 2012.New materials, new devices, newsolutions: How to prepare a membrane. In Membrane technologies and applications. 1-14. CRS Press.

Gozalvez, J. M., Lora, J., Mendoza, J. A., and Sancho, M. (2002). Modelling of a low-pressure reverse osmosis system with concentrate recirculation to obtain high recovery levels, Desalination, 144, 341–345.

Greenlee, L., Lawler, D., Freeman, B., Marrot, B. and Moulin, P. (2007). *Reverse osmosis desalination: Water sources, technology, and today's challenges*: Water Research, vol. 43, no. 9, pp. 2317–2348

Grey, D., Garrick, D., Blackmore, D., Kelman, J., Muller, M., Sadoff, C., 2013. Water security in one blue planet: twenty-first century policy challenges for science. Philos. Trans. Roy. Soc. London A: Math., Phys. Eng. Sci. 371, 20120406.

Günther, C., Richter, H., Voigt, I., Michaelis, A., Tzscheutschler, H., Krause-Rehberg, R. and Serra, J. (2015). Synthesis and characterization of a sulfur containing hydroxy sodalite without sulfur radicals. *Microporous and Mesoporous Materials*, 214, pp.1-7.

Haldenwang, P., Bernales, B., Guichardon, P. and Ibaseta, N. (2019). Simple Theoretical Results on Reversible Fouling in Cross-Flow Membrane Filtration. *Membranes*, 9(4), p.48.
Hellegers, P. and Leflaive, X. (2015). Water allocation reform: what makes it so difficult? *Water International*, 40(2), pp.273-285.

Hidalgo M, Sánches-Moreno C, Pascual-Teresa S 2010. Flavonoid-flavonoid interaction and its effect on their antioxidante activity. *Food Chem 121*: 691-696.

Hobbs, R., Arico, S., Aronson, J., Baron, J., Bridgewater, P., and Cramer, V. et al. (2006). Novel ecosystems: theoretical and management aspects of the new ecological world order. *Global Ecology And Biogeography*, *15*(1), 1-7.

Hoffmann, C., Silau, H., Pinelo, M., Woodley, J. and Daugaard, A. (2018). Surface modification of polysulfone membranes applied for a membrane reactor with immobilized alcohol dehydrogenase. *Materials Today Communications*, 14, pp.160-168.

Huang, R.Y.M. and Rhim, J.W., 1993, 'Modification of poly (viny1 alcohol) using maleic dianhydrides as hardeners', Journal of Applied Polymer Science 59, 425-431.

Hums, E. (2017). Synthesis of Phase-Pure Zeolite Sodalite from Clear Solution Extracted from Coal Fly Ash. *Journal Of Thermodynamics and Catalysis*, *08*(02). 2157-7544

Iritani, E., Mukai, Y., Tanaka, Y. and Murase, T. (1995). Flux decline behaviour in deadend microfiltration of protein solutions. Journal of Membrane Science, 103, pp.181-191.

Ismail A.F., David L. (2001). A review on the latest development of carbon membranes for gas separation. J. Membr. Sci. ;193, pp 1–18

Iza-structure.org. (2019). *: XPD Plot*. [online] Available at:http://www.iza-structure.org/IZA-SC/pow_plot.php [Accessed 11 Sep. 2019].

Jayakumar, R., Prabaharan, M., Sudheesh Kumar, P., Nair, S. and Tamura, H. (2011). Biomaterials based on chitin and chitosan in wound dressing applications. *Biotechnology Advances*, 29(3), pp.322-337.

Jeong, B., Hoek, E., Yan, Y., Subramani, A., Huang, X., Hurwitz, G., Ghosh, A. and Jawor, A. (2007). Interfacial polymerization of thin film nanocomposites: A new concept for reverse osmosis membranes. *Journal of Membrane Science*, 294(1-2), pp.1-7.

Jie, G., Kongyin, Z., Xinxin, Z., Zhijiang, C., Min, C., Tian, C., Junfu, W., 2015. Preparation and characterization of carboxyl multi-walled carbon nanotubes/calcium alginate composite hydrogel nano-filtration membrane. Mater. Lett. 157, 112–115.

Judd, S. 2006. Principles and applications of membrane bioreactors in water and wastewater treatment, Cranfield University, UK.

Kamble S.P., Mangrulkar P.A., Bansiwal A.K. and Rayalu S.S. (2008). Adsorption of phenol and o-chlorophenol on surface altered fly ash based molecular sieves, Chemical Engineering Journal, 138, pp.73-83.

Kasongo, G., Steenberg, C., Morris, B., Kapenda, G., Jacobs, N. and Aziz, M. (2019). Surface grafting of polyvinyl alcohol (PVA) cross-linked with glutaraldehyde (GA) to improve resistance to fouling of aromatic polyamide thin film composite reverse osmosis membranes using municipal membrane bioreactor effluent. *Water Practice and Technology*, 14(3), pp.614-624.

Kayvani Fard, A., McKay, G., Buekenhoudt, A., Al Sulaiti, H., Motmans, F., Khraisheh, M. and Atieh, M. (2018). Inorganic Membranes: Preparation and Application for Water Treatment and Desalination. *Materials*, 11(1), pp.74.

Khajavi, S., Jansen, J. C., and Kapteijn, F. (2010). Production of ultrapure water by desalination of seawater using a hydroxy sodalite membrane. *Journal of Membrane Science, 356* (1-2),52-57.

Khajavi, S., Kapteijn, F. and Jansen, J. (2007). Synthesis of thin defect-free hydroxy sodalite membranes: New candidate for activated water permeation. Journal of Membrane Science, 299(1-2), pp.63-72.

Khazaali, F., Kargari, A. and Rokhsaran, M. (2014). Application of low-pressure reverse osmosis for effective recovery of Bisphenol A from aqueous wastes. Desalin Water Treat;52(40–42):pp.7543–51

Khulbe, K. C., and Matsuura, T. (2018). Removal of heavy metals and pollutants by membrane adsorption techniques. *Applied Water Science,* 8:19,

Kim, S., Lee, S., Lee, E., Sarper, S., Kim, C. and Cho, J. (2009). Enhanced or reduced concentration polarization by membrane fouling in seawater reverse osmosis (SWRO) processes. *Desalination*, 247(1-3), pp.162-168.

Kim, T., Park, C. and Kim, S. (2005). Water recycling from desalination and purification process of reactive dye manufacturing industry by combined membrane filtration. *Journal of Cleaner Production*, 13(8), pp.779-786.

Koike, M., Asakura, Y., Sugihara, M., Kuroda, Y., Tsuzura, H., Wada, H., Shimojima, A. and Kuroda, K. (2017). Topotactic conversion of layered silicate RUB-15 to silica sodalite through interlayer condensation in N-methylformamide. *Dalton Transactions*, 46(31), pp.10232-10239.

Kota AK, Kwon G, Choi W, Mabry JM, Tuteja A. 2012. Hygro-responsive membranes for effective oil-water separation. Nature Communications, 3, pp. 1025.

Kuilla, T., Bhadra, S., Yao, D., Kim, N., Bose, S. and Lee, J. (2010). Recent advances in graphene based polymer composites. *Progress in Polymer Science*, 35(11), pp.1350-1375.

Kulkarni, S. J., and Kaware, J. P. (2015). Phenol removal from effluent by rice husk carbon: Batch and column studies. *International Journal of Environmental Engineering, 7*(2), 131.

Kumar, M., Gholamvand, Z., Morrissey, A., Nolan, K., Ulbricht, M., and Lawler, J. (2016). Preparation and characterization of low fouling novel hybrid ultrafiltration membranes based on the blends of GO−TiO2 nanocomposite and polysulfone for humic acid removal. *Journal of Membrane Science, 506*, 38-49.

Kumar, R., Al-Jabli, H., Al-Haddad, S., Al-Rughaib, M. and Samuel, J. (2017). Modified titanate nanotubes incorporated polyamide layer for the fabrication of fouling control thin film nanocomposite forward osmosis membranes, Desalination and Water Treatment, 69, pp.56-64.

Kumar, R., Basumatary, A., Ghoshal, A. and Pugazhenthi, G. (2015). Performance assessment of an analcime-C zeolite–ceramic composite membrane by removal of Cr (vi) from aqueous solution. *RSC Advances*, 5(9), pp.6246-6254.

Kumar, Y., Brahmbhatt, H., Trivedi, G., and Bhattacharya, A. (2011). Surfactant enhanced filtration performances of monochlorophenol isomers through low-pressure membrane. *Membrane Water Treatment*, *2*(3), 137-145.

Kwon, b., Molek, j. and Zydney, A. (2008). Ultrafiltration of PEGylated proteins: Fouling and concentration polarization effects. *Journal of Membrane Science*, 319(1-2), pp.206-213.

Laval, A. (2007). Beer filtration: Top end beer from cross-flow filters. *Filtration and Separation*, 44(2), pp.40-41.

Lee, A., Elam, J. and Darling, S. (2016). *Membrane materials for water purification: design, development, and application*, 2, 17-42

Lin, J., Lee, D. and Huang, C. (2010). Membrane Fouling Mitigation: Membrane Cleaning. *Separation Science and Technology*, 45(7), pp.858-872.

Liu, J., Lu, X. and Wu, C. (2013). Effect of Preparation Methods on Crystallization Behavior and Tensile Strength of Poly (vinylidene fluoride) Membranes. *Membranes*, 3(4),pp.389-405.

Liu, Y., Hu, H., Yang, X., Lv, J., Zhou, L. and Luo, Z. (2019). Hydrophilic modification on polyvinyl alcohol membrane by hyaluronic acid. *Biomedical Materials*, 14(5), p.055009.

Loeb, S. and Sourirajan S. (1961). Sea water demineralization by means of a semipermeable membrane. Report no. pp.60-60

Loh, C., Zhang, Y., Goh, S., Wang, R. and Fane, A. (2016). Composite hollow fiber membranes with different poly(dimethylsiloxane) intrusions into substrate for phenol removal via extractive membrane bioreactor. *Journal of Membrane Science*, 500, pp.236-244.

Ma, N., Wei, J., Liao, R., and Tang, C. (2012). Zeolite-polyamide thin film nanocomposite membranes: Towards enhanced performance for forward osmosis. *Journal of Membrane Science, 405-406,* 149-157.

Mahugo-Santana C, Sosa Ferrera Z, Torres Padrón EM, Santana Rodríguez JJ (2009). Methodologies for the extraction of phenolic compounds from environmental samples: new approaches. Molecules; 14(1): 298–320.

Maphutha, S., Moothi, K., Meyyappan, M. and Iyuke, S. (2013). A carbon nanotube-infused polysulfone membrane with polyvinyl alcohol layer for treating oil-containing waste water. *Scientific Reports*, 3(1). 1509-1515

Martinez-Huitle CA, Ferro S (2006). Electrochemical oxidation of organic pollutants for the wastewater treatment: direct and indirect processes. Chem Soc Rev; 35(12): 1324–40.

Masomi M, Ghoreyshi AA, Najafpour GD, Mohamed ARB (2014). Adsorption of phenolic compounds onto the activated carbon synthesized from pulp and paper mill sludge: equilibrium isotherm, kinetics, thermodynamics and mechanism studies. Int J Eng Trans A Basics, 27(10):1485–94.

Mathioulakis, E., Belessiotis, V. and Delyannis, E. (2007). Desalination by using alternative energy: review and state-of-the-art," Desalination, vol. 203, no. 1–3, pp. 346–365.

Mazinani, S., Darvishmanesh, S., Ehsanzadeh, A. and Van der Bruggen, B. (2017). Phase separation analysis of Extem/solvent/non-solvent systems and relation with membrane morphology. *Journal of Membrane Science*, 526, pp.301-314.

McMullan, D. (1988). "Von Ardenne and the scanning electron microscope". Proc Roy Microsc Soc. 23: 283–288.

Mofradi, M., Karimi, H. and Ghaedi, M. (2019). Hydrophilic polymeric membrane supported on silver nanoparticles surface decorated polyester textile: Toward enhancement of water flux and dye removal. *Chinese Journal of Chemical Engineering* (in press) https://doi.org/10.1016/j.cjche.2019.09.011

Mohammadi, S., Kargari, A., Sanaeepur, H., Abbassian, K., Najafi, A., and Mofarrah, E. (2014). Phenol removal from industrial wastewaters: A short review. *Desalination and Water Treatment, 53*(8), 2215-2234.

Moteki, T., Chaikittisilp, W., Sakamoto, Y., Shimojima, A. and Okubo, T. (2011). Role of Acidic Pretreatment of Layered Silicate RUB-15 in Its Topotactic Conversion into Pure Silica Sodalite. *Chemistry of Materials*, 23(15), pp.3564-3570.

Mukherjee, R., and De, S. (2016). Novel carbon-nanoparticle polysulfone hollow fiber mixed matrix ultrafiltration membrane: Adsorptive removal of benzene, phenol and toluene from aqueous solution. *Separation and Purification Technology*, *157*, 229-240.

Mukherjee, R., Sharma, R., Saini, P., and De, S. (2015). Nanostructured polyaniline incorporated ultrafiltration membrane for desalination of brackish water. *Environ. Sci.: Water Res. Technol*., 1: 893–904.

Mulder, M. (1996). Basic Principles of Membrane Technology, Kluwer, Dordrecht
Murali, R., Sridhar, S., Sankarshana, T. and Ravikumar, Y. (2010). Gas Permeation Behavior of Pebax-1657 Nanocomposite Membrane Incorporated with Multiwalled Carbon Nanotubes. *Industrial and Engineering Chemistry Research*, 49(14), pp.6530-6538.

Murray, T. and Sasnett, S. (2000). A Multimedia Strategy from the USEPA for Priority Persistent, Bioaccumulative, and Toxic Pollutants. *Environmental Practice*, 2(1), pp.56-59.

Nafees, M. and Waseem, A. (2014). Organoclays as Sorbent Material for Phenolic Compounds: A Review. *CLEAN - Soil, Air, Water*, 42(11), pp.1500-1508.

Ngo, H. and Guo, W. (2009). Membrane fouling control and enhanced phosphorus removal in an aerated submerged membrane bioreactor using modified green bioflocculant. *Bioresource Technology*, 100(18), pp.4289-4291.

Ni, G., Zhao, G., Jiang, Y., Li, J., Meng, Y. and Wang, X. (2013). Steam plasma jet treatment of phenol in aqueous solution at atmospheric pressure. Plasma Process Polym, 10, pp.353–63.
Ouma, J., Septien, S., Velkushanova, K., Pocock, J. and Buckley, C. (2016). Characterization of ultrafiltration of undiluted and diluted stored urine. *Water Science and Technology*, 74(9), pp.2105-2114.

Özsin, G., Kılıç, M., Apaydın-Varol, E., and Pütün, A. (2019). Chemically activated carbon production from agricultural waste of chickpea and its application for heavy metal adsorption: equilibrium, kinetic, and thermodynamic studies. *Applied Water Science*, *9*, 56. https://doi.org/10.1007/s13201-019-0942-8.

Park, H., Koduru, J., Choo, K. and Lee, B. (2015). Activated carbons impregnated with iron oxide nanoparticles for enhanced removal of bisphenol A and natural organic matter. *Journal of Hazardous Materials*, 286, pp.315-324.

Percival, S. L., Yates, M. V., Williams, D. W., Chalmers, R., and Gray, N. F. (2014). *Microbiology of waterborne diseases microbiological aspects and risks*. Amsterdam: Elsevier/Academic Press.

Qadir, D., Mukhtar, H., and Keong, L.K. (2016) Mixed Matrix Membranes for Water Purification Applications. *Sep. Purif. Rev.*, 46:62–80.

Qin, D., Liu, Z., Delai Sun, D., Song, X., and Bai, H. (2015). A new nanocomposite forward osmosis membrane custom-designed for treating shale gas wastewater. *Scientific Reports, 5*(1). doi: 10.1038/srep14530

Qu, X., Brame, J., Li, Q., Alvarez, P.J., 2012. Nanotechnology for a safe and sustainable water supply: enabling integrated water treatment and reuse. Acc. Chem. Res. 46 (3), pp834–843.

Oliveira, C., and Rubio, J. (2007). Adsorption of ions onto treated natural zeolite. *Materials Research*, *10*(4), 407-412.

Ouma, J., Septien, S., Velkushanova, K., Pocock, J., and Buckley, C. (2016). Characterization of ultrafiltration of undiluted and diluted stored urine. *Water Science And Technology*, *74*(9), 2105-2114.

Pakade, V., Nchoe, O., Hlungwane, L. and Tavengwa, N. (2016). Sequestration of hexavalent chromium from aqueous solutions by activated carbon derived from Macadamia nutshells. Water Science and Technology, 75(1), pp.196-206.

Rana, d., Matsuura, t. and Narbaitz, R. (2006). Novel hydrophilic surface modifying macromolecules for polymeric membranes: Polyurethane ends capped by hydroxy group. *Journal of Membrane Science*, 282(1-2), pp.205-216.

Rana, D., Matsuura, T., Narbaitz, R. and Feng, C. (2005). Development and characterization of novel hydrophilic surface modifying macromolecule for polymeric membranes. *Journal of Membrane Science*, 249(1-2), pp.103-112.

Raza, W., Lee, J., Raza, N., Luo, Y., Kim, K-H., and Yang, J. (2019). Removal of phenolic compounds from industrial waste water based on membrane-based technologies. *Journal of Industrial and Engineering Chemistry, 71*, 1-18.

Ridzuan, N., and Musa, M. (2012). Comparison between Treated and Untreated Zeolite towards the Performance of Polyethersulfone Mixed Matrix Membranes (MMMs) for O2/N2 Gas Separation. *Advanced Materials Research, 550-553*, 728-735.

Rossignol, N., et al. 1999 "Membrane Technology for the Continuous Separation Microalgae/Culture Medium: Compared Performances of Cross-Flow Microfiltration and Ultrafiltration." *Aquacultural Engineering*, vol. 20, no. 3, 1999, pp. 191–208.

Rudra, R., Kumar, V. and Kundu, P. (2015). Acid catalysed cross-linking of poly vinyl alcohol (PVA) by glutaraldehyde: effect of crosslink density on the characteristics of PVA membranes used in single chambered microbial fuel cells. *RSC Advances*, 5(101), pp.83436-83447.

Rushton, A., and Matsis, V. (1994). Studies of constant rate filtration in dead-end and crossflow modes. *Filtration and Separation*, *31*(6), 643-630.

Ruutenhuch, R. (1992). Membrane Separation Systems - Recent Developments and Future Directions. VonR. W. Baker u.a. Noyes Data Corp., Park Ridge 1991. XV, 451 S., zahlr.Abb. u. Tab., geb., US-$64,-. *Chemie Ingenieur Technik*, 64(6), pp.584-584.

Salame I. I. and Bandosz T. J. (2003). Role of surface chemistry in adsorption of phenol on activated carbons, Journal of Colloid and Interface Science, 264, pp.307–312.

Sano, T. (1997). Separation of acetic acid-water mixtures by pervaporation through silicalite membrane. *Journal of Membrane Science*, 123(2), pp.225-233.

Sano, T., Yanagishita, H., Kiyozumi, Y., Mizukami, F. and Haraya, K. (1994). Separation of ethanol/water mixture by silicalite membrane on pervaporation. *Journal of Membrane Science*, 95(3), pp.221-228.

Seader, J.D., Henley, E.J., Roper, D.K., 2013. Separation Process Principles, third ed. (978-0-470-48183-7).

Shirazi, M., Kargari, A. and Shirazi, M. (2012). Direct contact membrane distillation for seawater desalination. *Desalination and Water Treatment*, 49(1-3), pp.368-375.

Shon, H., Phuntsho, S., Chaudhary, D., Vigneswaran, S. and Cho, J. (2013). Nanofiltration for water and wastewater treatment – a mini review. *Drinking Water Engineering and Science*, 6(1), pp.47-53.

Shugman, E., Aldrich, C., Sanderson, R., and Mclachlan, D. (2013). Infrasonic backpulsed membrane cleaning of micro- and ultrafiltration membranes fouled with alumina and yeast. *Water SA,39*(1). doi:10.4314/wsa.v39i1.2

Singh, K., Devi, S., Bajaj, H., Ingole, P., Choudhari, J. and Bhrambhatt, H. (2014). Optical Resolution of Racemic Mixtures of Amino Acids through Nanofiltration Membrane Process. *Separation Science and Technology*, 49(17), pp.2630-2641.

Singh, P.S., Joshi, S.V., Trivedi, J.J., Devmurari, C.V., Rao, A.P., Ghosh, P.K. (2006). Probing the structural variations of thin film composite RO membranes obtained by coatingpolyamide over polysulfone membranes of different pore dimensions. *Journal Membrane Science*, 278, 19–25.

Sioutopoulos, D. and Karabelas, A. (2012). Correlation of organic fouling resistances in RO and UF membrane filtration under constant flux and constant pressure. Journal of Membrane Science, 407(408), pp.34-46.

Sioutopoulos, D., Karabelas, A. and Mappas, V. (2019). Membrane Fouling Due to Protein—Polysaccharide Mixtures in Dead-End Ultrafiltration; the Effect of Permeation Flux on Fouling Resistance. *Membranes*, 9(2), p.21.

Suda, H., Wenzel, A., Yanagishita, H. and Haraya, K. (2000). Gas Permeation Properties of Carbon Molecular Sieve Membranes Prepared in Alkali Metal-Organic Solvent Systems. *Molecular Crystals and Liquid Crystals Science and Technology. Section A. Molecular Crystals and Liquid Crystals*, 341(2), pp.567-572.

Sun, W., Liu, J., Chu, H. and Dong, B. (2013). Pretreatment and Membrane Hydrophilic Modification to Reduce Membrane Fouling. *Membranes*, 3(3), pp.226-241.

Sun, X., Wang, C., Li, Y., Wang, W. and Wei, J. (2015). Treatment of phenolic wastewater by combined UF and NF/RO processes. *Desalination*, 355, pp.68-74.

Sun, M., Su, Y., Mu, C. and Jiang, Z. (2010) Improved antifouling property of PESultrafiltration membranes using additive of silica−PVP nanocomposite. Industrial and Engineering Chemistry Research, 49(2), pp 790–796

Sun, X.f., et al. 2012 "Comparison of Microfiltration and Ultrafiltration for Algae Harvesting." *Procedia Engineering*, vol. 44, 2012, pp. 2108–2111.

Suresh, S., Srivastava, V. C., and Mishra, I. M. (2011). Adsorptive removal of phenol from binary aqueous solution with aniline and 4-nitrophenol by granular activated carbon. *Chemical Engineering Journal*, *171*(3), 997–1003.

Takewaki, T. (2019). Outline of Artificial Photosynthetic Chemical Process Project and Hydrogen Separation by Surface Modified Zeolite Membrane. *MEMBRANE*, 44(4), pp.148-152.

Tang, H., and Goldman, D. (2002). Myocyte Enhancer Factor 2C (MEF-2C). *Wiley Encyclopedia of Molecular Medicine*.

Tansel, B. (2008). Extracellular Polymeric Substances and Membrane Fouling: Microtopographical Characterization of Fouling Phenomana by Atomic Force Microscopy. *Proceedings of the Water Environment Federation*, 2008(1), pp.432-437.

Tasic Z, Gupta VK, Antonijevic MM (2014). The mechanism and kinetics of degradation of phenolics in wastewaters using electrochemical oxidation. Int J Electrochem Sci; 9: pp.3473–90.

Tay, M., Liu, C., Cornelissen, E., Wu, B. and Chong, T. (2018). The feasibility of nanofiltration membrane bioreactor (NF-MBR) +reverse osmosis (RO) process for water reclamation:

Comparison with ultrafiltration membrane bioreactor (UF-MBR)+RO process. *Water Research*, 129, pp.180-189.

Tran VS, Ngo HH, Guo W, Zhang J, Liang S, Ton-That C (2005). Typical low cost biosorbents for adsorptive removal of specific organic pollutants from water. Bioresour Technol, 182, pp.353–63.

Tsapuik, E. and Bryk, M. (1993). An interpretation of the separation of low and high molecular weight solutes by ultrafiltration. *Journal of Membrane Science*, 79(2-3), pp.227-240.

U.S. Environmental Protection Agency (1998). Hazardous waste management system; identification and listing of hazardous waste; solvents; final rule. Federal Register 63 FR 64371- 402.

Unesco.org. (2019). *Water for a Sustainable World | United Nations Educational, Scientific and Cultural Organization*. [online] Available at: http://www.unesco.org/new/en/natural-sciences/environment/water/wwap/wwdr/ 015-water- for-a-sustainable-world [Accessed 26 Oct. 2019].

Unuigbe, C., Fayemiwo, O., and Daramola, M. (2019). Performance evaluation of iron nanoparticles infused polyethersulphone (Fe-NPs/PES) membrane during treatment ofBTEX-contaminated wastewater. *Water And Environment Journal*.

Van der Bruggen, B. (2009). Chemical modification of polyethersulfone nanofiltration membranes: A review. Journal of Applied Polymer Science, 114(1), pp.630-642.

Van der Bruggen, B., Manttari, M. and Nystromb, M. (2008). Drawbacks of applying nanofiltration and how to avoid them: a review. Sep. Purif. Technol. 63, 251–263

Vazquez G., Gonzalez A., lvarez J., Garcia A.I., Freire M.S. and Antorrena v. (2007). Adsorption of phenol on formaldehyde-pretreated Pinus pinaster bark: Equilibrium and kinetics, Journal of Bioresource Technology, 98, pp.1535–1540.

Verma, A. (2008). Applications of Advanced Oxidation Processes in Wastewater Treatment.

Water Research, 42(18), p.4589

Villegas, L., Mashhadi, N., Chen, M., Mukherjee, D., Taylor, K. and Biswas, N. (2016). A Short Review of Techniques for Phenol Removal from Wastewater, *Current Pollution Reports*, 2, pp.157–167.

Vinoth Kumar, R., Kumar Ghoshal, A. and Pugazhenthi, G. (2015). Elaboration of novel tubular ceramic membrane from inexpensive raw materials by extrusion method and its performance in microfiltration of synthetic oily wastewater treatment. *Journal of Membrane Science*, 490, pp.92-102.

Wang C., Zhou, J., Wang, Y., Yang, M., Li, Y., Menga, C., J (2013). Chem Technol Biotechnol. 88, pp. 1350

Wang, H., Wang, T., Yang, S. and Fan, L. (2013). Preparation of thermal stable porous polyimide membranes by phase inversion process for lithium-ion battery. *Polymer*, 54(23), pp.6339-6348.

Wang, K., Abdala, A. A., Hilal, N., and Khraisheh, M. K. (2017). Mechanical Characterization of Membranes. In *Membrane Characterization* (pp. 259-306).

Wang, S., Peng, Y., 2010. Natural zeolites as effective adsorbents in water and wastewater treatment. Chem. Eng. J. 156, 11–24.

Wang, X. (2008). Synthesis of Sn-Substituted ZSM-5/Carbon Zeolite Membrane and Application in Separation of Acetic Acid/water Mixtures by Pervaporation. *Journal of Inorganic Materials*, 23(6), pp.1225-1230.

White, M. (2016). Consider Microfiltration and Ultrafiltration Membranes for Water Treatment. *Opflow*, *42*(7), 22–25.

WHO (World Health Organization), 2015. Drinking-water: Fact sheet No. 391 <http://www.who.int/mediacentre/factsheets/fs391/en/>

WHO-UNICEF, Progress in drinking water and sanitation 2012 update, Joint Monitoring Programme for Water Supply and Sanitation. (2018). WHO, p.58.

Xiao, T., Nghiem, L., Song, J., Bao, R., Li, X. and He, T. (2017). Phenol rejection by cellulose triacetate and thin film composite forward osmosis membranes. *Separation and Purification Technology*, 186, pp.45-54.

Xue, Z.; Li, Z.; Ma, J.; Bai, X.; Kang, Y.; Hao, W.; Li, R. (2014). Effective removal of Mg2+ and Ca2+ ions by mesoporous LTA zeolite. Desalination, 341, 10–18.

Yanagishita, H., Kitamoto, D., Haraya, K., Nakane, T., Okada, T., Matsuda, H., Idemoto, Y. and Koura, N. (2001). Separation performance of polyimide composite membrane prepared by dip coating process. *Journal of Membrane Science*, 188(2), pp.165-172.

Yao, J. Wang, H. Ratinac, K.R. Ringer, S.P (2006). Formation of colloidal hydroxy-sodalite nanocrystals by the direct transformation of silicalite nanocrystals Chem. Mater., 18, pp. 1394-1396.

Yi Suen, S. (2015). Mixed Matrix Membranes for Adsorption Application. *Journal of Chemical Engineering and Process Technology*, 06(01).

Yu, J., Liu, Y., Song, S., Gao, G. and Liu, F. (2017). Phase behavior of a high-concentration sulfobetaine zwitterionic polymer solution. *Polymer Journal*, 49(11), pp.767-774.

Yurekli, Y., 2016. Removal of heavy metals in wastewater by using zeolite nano-particles impregnated polysulfone membranes. J.Hazard. Mater. 309, pp. 53–64.

Zhang, X. and Minear, R. (2006). Removal of low-molecular weight DBPs and inorganic ions for characterization of high-molecular weight DBPs in drinking water. *Water Research*, 40(5), pp.1043-1051.

Zhao, S., Wang, Z., Wang, J., Yang, S., and Wang, S. (2011) PSF/PANI nanocomposite membrane prepared by in situ blending of PSF and PANI/NMP. *J. Membr. Sci*., 376: 83–95.

Zhao, S., Wang, Z., Wei, X., Tian, X., Wang, J., Yang, S.and Wang, S. (2011) Comparison study of the effect of PVP and PANI nanofibers additives on membrane formation mechanism, structure and performance. *J. Membr. Sci*., 385: 110–122.

Zhu, J., Guo, N., Zhang, Y., Yu, L., and Liu, J. (2014) Preparation and characterization of negatively charged PES nanofiltration membrane by blending with halloysite nanotubes grafted with poly (sodium 4-styrenesulfonate) via surface-initiated ATRP. *J. Membr. Sci*., 465: 91–99.

Zhu, J., Tian, M., Zhang, Y., Zhang, H., and Liu, J. (2015) Fabrication of a novel "loose" nanofiltration membrane by facile blending with Chitosan–Montmorillonite nanosheets for dyes purification. *Chem. Eng. J*., 265: 184–193.

Zularisam, A., Ismail, A., and Salim, R. (2006). Behaviours of natural organic matter in membrane filtration for surface water treatment — a review. *Desalination, 194*(1-3), 211-231.

Zulkifli, F., Shahitha, F., Yusuff, M., Hamidon, N. and Chahal, S. (2013). Cross-Linking Effect on Electrospun Hydroxyethyl Cellulose/Poly(Vinyl Alcohol) Nanofibrous Scaffolds. *Procedia Engineering*, 53, pp.689-695.

Appendix

This section contains the supporting data for Chapter Four, Five and Six

A. HPLC Data

These results were obtained using high-performance liquid chromatography described in chapter 3

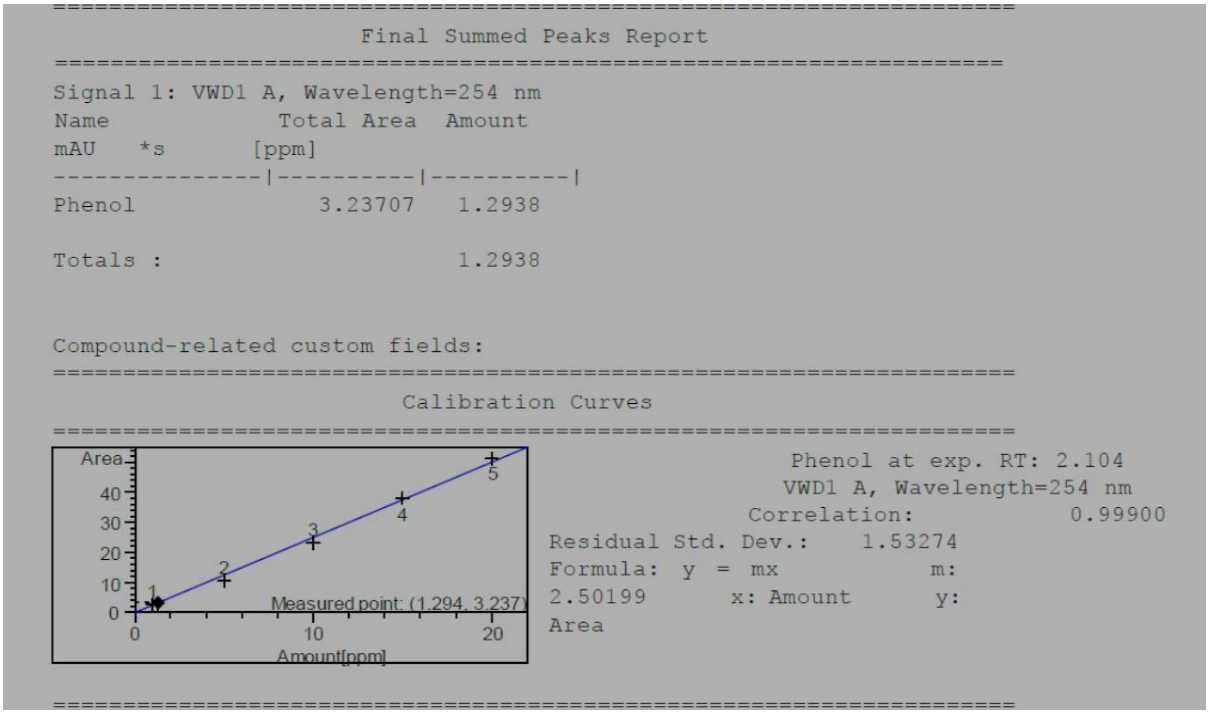

Figure A.1: *HPLC report for phenol rejection at 4 Bar for 0 wt% SSOD/PSF membrane*

Final Summed Peaks Report

Signal 1: VWD1 A, Wavelength=254 nm

Name	Total Area mAU *s	Amount [ppm]
Phenol	29.52782	11.8017
Totals :		11.8017

Compound-related custom fields:

Calibration Curves

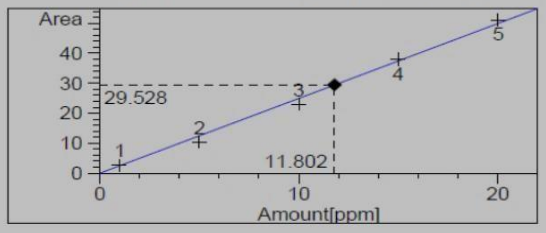

Phenol at exp. RT: 2.104
VWD1 A, Wavelength=254 nm
Correlation: 0.99900
Residual Std. Dev.: 1.53274
Formula: y = mx
m: 2.50199
x: Amount
y: Area

*** End of Report ***

Figure A.2: *HPLC report for phenol rejection at 6 Bar for 0 wt% SSOD/PSF membrane*

Final Summed Peaks Report

Signal 1: VWD1 A, Wavelength=254 nm

Name	Total Area mAU *s	Amount [ppm]
Phenol	18.17765	7.2653
Totals :		7.2653

Compound-related custom fields:

Calibration Curves

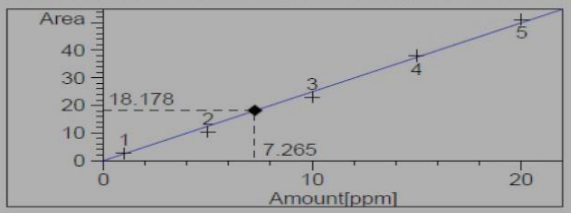

Phenol at exp. RT: 2.104
VWD1 A, Wavelength=254 nm
Correlation: 0.99900
Residual Std. Dev.: 1.53274
Formula: y = mx
m: 2.50199
x: Amount
y: Area

*** End of Report ***

Figure A.3*: HPLC report for phenol rejection at 4 Bar for 10 wt% HSOD/PSF membrane*

Final Summed Peaks Report

Signal 1: VWD1 A, Wavelength=254 nm

Name	Total Area mAU *s	Amount [ppm]
Phenol	27.61001	11.0352
Totals :		11.0352

Compound-related custom fields:

Calibration Curves

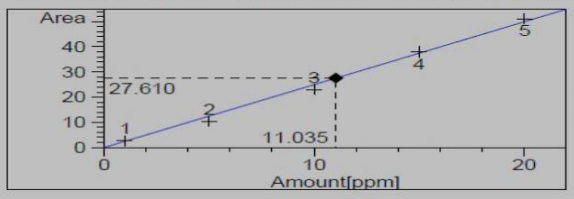

Phenol at exp. RT: 2.104
VWD1 A, Wavelength=254 nm
Correlation: 0.99900
Residual Std. Dev.: 1.53274
Formula: y = mx
m: 2.50199
x: Amount
y: Area

*** End of Report ***

Figure A.4: *HPLC report for phenol rejection at 6 Bar for 10 wt% HSOD/PSF membrane*

Final Summed Peaks Report

Signal 1: VWD1 A, Wavelength=254 nm

Name	Total Area mAU *s	Amount [ppm]
Phenol	17.64550	7.0530
Totals :		7.0530

Compound-related custom fields:

Calibration Curves

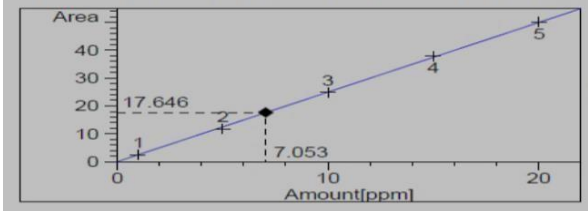

Phenol at exp. RT: 2.010
VWD1 A, Wavelength=254 nm
Correlation: 0.99992
Residual Std. Dev.: 0.43381
Formula: y = mx
m: 2.50185
x: Amount
y: Area

*** End of Report ***

Figure A.5: *HPLC report for phenol rejection at 4 Bar for 10 wt% SSOD/PSF membrane*

Final Summed Peaks Report

Signal 1: VWD1 A, Wavelength=254 nm

Name	Total Area mAU *s	Amount [ppm]
Phenol	29.38427	11.7450
Totals :		11.7450

Compound-related custom fields:

Calibration Curves

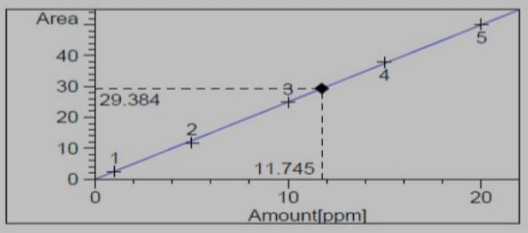

Phenol at exp. RT: 2.010
VWD1 A, Wavelength=254 nm
Correlation: 0.99992
Residual Std. Dev.: 0.43381
Formula: y = mx
m: 2.50185
x: Amount
y: Area

*** End of Report ***

Figure 4.6: *HPLC report for phenol rejection at 6 Bar for 10 wt% SSOD/PSF membrane*

Final Summed Peaks Report

Signal 1: VWD1 A, Wavelength=254 nm

Name	Total Area mAU *s	Amount [ppm]
Phenol	19.33071	7.7266
Totals :		7.7266

Compound-related custom fields:

Calibration Curves

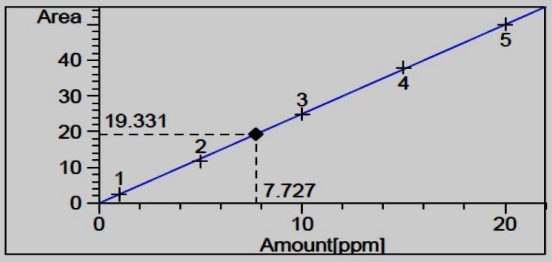

Phenol at exp. RT: 2.010
VWD1 A, Wavelength=254 nm
Correlation: 0.99992
Residual Std. Dev.: 0.43381
Formula: y = mx
m: 2.50185
x: Amount
y: Area

*** End of Report ***

Figure A.6*: HPLC report for phenol rejection at 4 Bar for 5 wt% SSOD/PSF membrane*

Final Summed Peaks Report

Signal 1: VWD1 A, Wavelength=254 nm

Name	Total Area mAU *s	Amount [ppm]
Phenol	30.13011	12.0431
Totals :		12.0431

Compound-related custom fields:

Calibration Curves

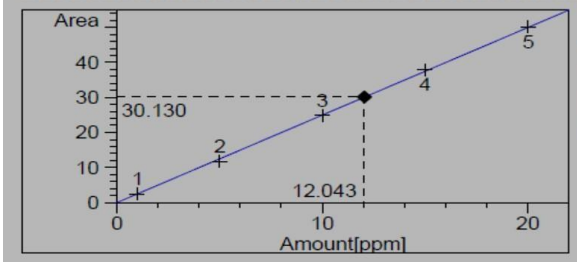

Phenol at exp. RT: 2.010
VWD1 A, Wavelength=254 nm
Correlation: 0.99992
Residual Std. Dev.: 0.43381
Formula: y = mx
m: 2.50185
x: Amount
y: Area

*** End of Report ***

***Figure A.7**: HPLC report for phenol rejection at 6 Bar for 5 wt% SSOD/PSF membrane*

Final Summed Peaks Report

Signal 1: VWD1 A, Wavelength=254 nm

Name	Total Area mAU *s	Amount [ppm]
Phenol	29.70934	11.8750
Totals :		11.8750

Compound-related custom fields:

Calibration Curves

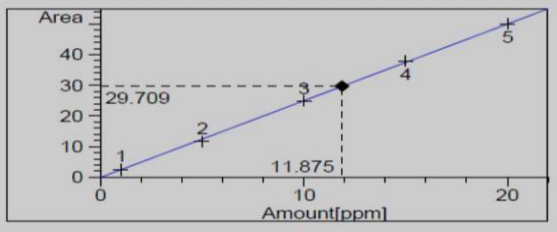

Phenol at exp. RT: 2.010
VWD1 A, Wavelength=254 nm
Correlation: 0.99992
Residual Std. Dev.: 0.43381
Formula: y = mx
m: 2.50185
x: Amount
y: Area

*** End of Report ***

***Figure A.8**: HPLC report for phenol rejection at 4 Bar for 0 wt.% SSOD/PSF/PVA membrane*

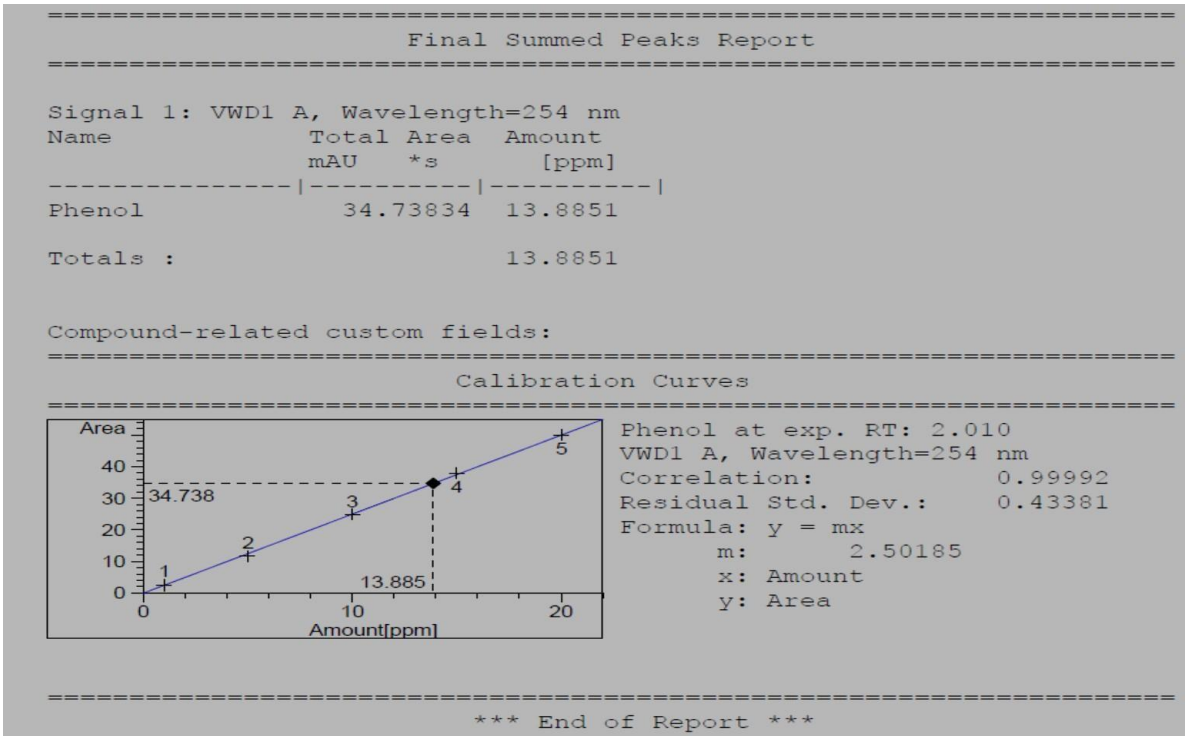

Figure A.9: *HPLC report for phenol rejection at 6 Bar for 0 wt.% SSOD/PSF/PVA membrane*

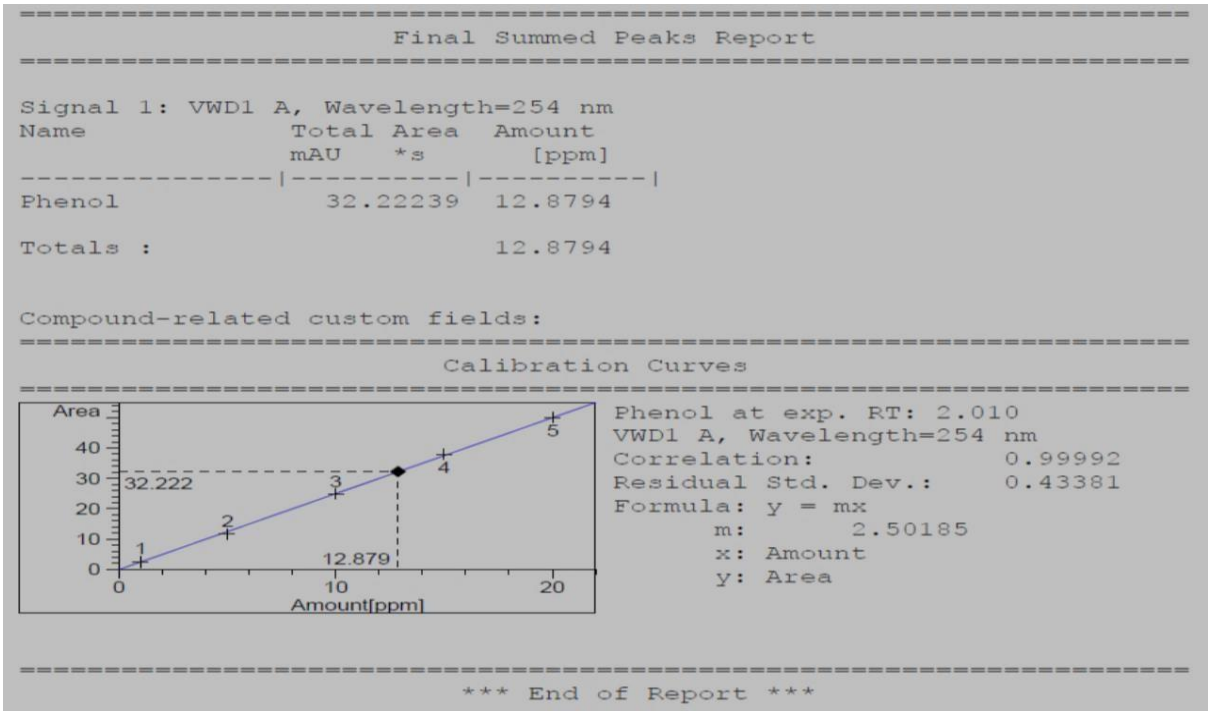

Figure A.10: *HPLC report for phenol rejection at 4 Bar for 10 wt.% HSOD/PSF/PVA*

Final Summed Peaks Report

Signal 1: VWD1 A, Wavelength=254 nm

Name	Total Area mAU *s	Amount [ppm]
Phenol	36.07526	14.4194
Totals :		14.4194

Compound-related custom fields:

Calibration Curves

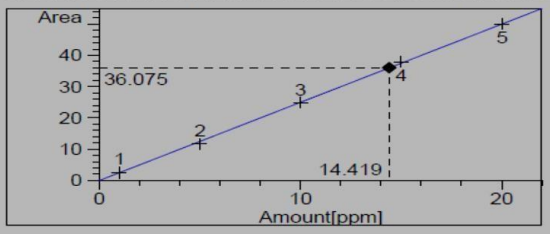

Phenol at exp. RT: 2.010
VWD1 A, Wavelength=254 nm
Correlation: 0.99992
Residual Std. Dev.: 0.43381
Formula: y = mx
m: 2.50185
x: Amount
y: Area

*** End of Report ***

Figure A.11: *HPLC report for phenol rejection at 6 Bar for 10 wt.% HSOD/PSF/PVA membrane*

Final Summed Peaks Report

Signal 1: VWD1 A, Wavelength=254 nm

Name	Total Area mAU *s	Amount [ppm]
Phenol	40.99759	16.3869
Totals :		16.3869

Compound-related custom fields:

Calibration Curves

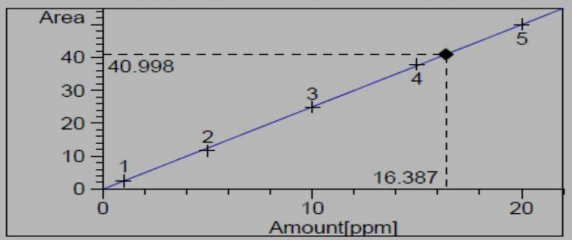

Phenol at exp. RT: 2.010
VWD1 A, Wavelength=254 nm
Correlation: 0.99992
Residual Std. Dev.: 0.43381
Formula: y = mx
m: 2.50185
x: Amount
y: Area

*** End of Report ***

Figure A.12: *HPLC report for phenol rejection at 4 Bar for 10 wt.% SSOD/PSF/PVA*

```
================================================================================
                        Final Summed Peaks Report
================================================================================

Signal 1: VWD1 A, Wavelength=254 nm
Name             Total Area   Amount
                 mAU   *s       [ppm]
---------------|----------|----------|
Phenol             41.77685   16.6984

Totals :                      16.6984


Compound-related custom fields:
================================================================================
                           Calibration Curves
================================================================================
```

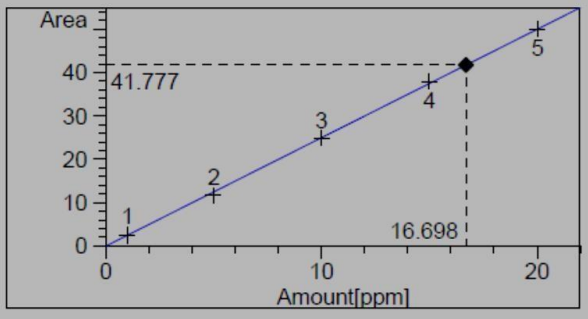


```
Phenol at exp. RT: 2.010
VWD1 A, Wavelength=254 nm
Correlation:                0.99992
Residual Std. Dev.:         0.43381
Formula: y = mx
      m:          2.50185
      x: Amount
      y: Area


================================================================================
                        *** End of Report ***
```

Figure A:13: *HPLC report for phenol rejection at 6 Bar for 10 wt.% SSOD/PSF/PVA membrane*